LIGAND SUBSTITUTION STUDIES IN THE TETRACOBALT CLUSTER $Co_4(CO)_{10}(\mu_4\text{-}PPh_2)$ AND SYNTHESIS AND REACTIVITY STUDIES IN THE Fe_2Pt AND $FeCo_2$ MIXED-METAL CLUSTERS

DISSERTATION

Presented to the Graduate Council of the
University of North Texas in Partial
Fulfillment of the Requirements

For the Degree of

DOCTOR OF PHILOSOPHY

BY

Ming-jaw Don, B.S.
Denton, Texas
August, 1991

LIGAND SUBSTITUTION STUDIES IN THE TETRACOBALT CLUSTER $Co_4(CO)_{10}(\mu_4\text{-}PPh_2)$ AND SYNTHESIS AND REACTIVITY STUDIES IN THE Fe_2Pt AND $FeCo_2$ MIXED-METAL CLUSTERS

DISSERTATION

Presented to the Graduate Council of the
University of North Texas in Partial
Fulfillment of the Requirements

For the Degree of

DOCTOR OF PHILOSOPHY

BY

Ming-jaw Don, B.S.
Denton, Texas
August, 1991

Don, Ming-jaw, Ligand Substitution Studies in the Tetracobalt Cluster $Co_4(CO)_{10}(\mu_4\text{-}PPh_2)$ and Synthesis and Reactivity Studies in the Fe_2Pt and $FeCo_2$ Mixed-Metal Clusters. Doctor of Philosophy (Chemistry), August, 1991, 167 pp., 34 tables, 15 figures, reference list, 272 titles.

The kinetics of ligand substitution for CO in $Co_4(CO)_{10}(\mu_4\text{-}PPh_2)$, **1**, have been investigated for the ligands $P(OMe)_3$, $P(OEt)_3$, PPh_2H, $P(O\text{-}i\text{-}Pr)_3$, $P(n\text{-}Bu)_3$, PPh_3, $P(i\text{-}Pr)_3$, and PCy_3 over a wide temperature range. Ligand substitution is observed under mild conditions to yield $Co_4(CO)_9(L)(\mu_4\text{-}PPh_2)$, [**2a-h**]. The kinetics for substitution step reveal a two-term rate law: $(k_1 + k_2[Ligand])[Cluster]$. The k_2 term corresponds to a ligand-dependent attack on **1**. For large cone angle ligands ($\geq 145^\circ$), the k_1 term involves CO dissociation. However, for small cone angle ligands ($< 145^\circ$), the k_1 term is inconsistent with a dissociative loss of CO, but rather with a unimolecular closo→nido cluster rearrangement.

The reaction of $[Fe_2(CO)_6(\mu\text{-}S)_2]^{-2}$ with various $(L\frown L)PtCl_2$ (where L⌒L = 1,5-cod, bpy, 1,10-phen, diphos, dppf) affords the corresponding mixed-metal arachno cluster $Fe_2(CO)_6(\mu_3\text{-}S)_2Pt(L\frown L)$, [**5a-e**], in high yield. The reaction of **5a-c** with reducing agents (H^- and R^-) at -78 °C yields the corresponding radical anion without the spectroscopic

observation of any intermediates. All of the new clusters may be oxidized to corresponding radical cation by known one-electron oxidizing agents.

The reaction of the mixed-metal tetrahedrane cluster $FeCo_2(CO)_9(\mu_3\text{-}PPh)$, **3**, with various reducing agents has been examined in THF. $[Et_3BH][Li]$ and $[(sec\text{-}Bu)_3BH][K]$ react with **3** at -78 °C to give the thermally unstable cluster $[FeCo_2(CO)_9(\mu_2\text{-}PPhH)^-]$, $[\mathbf{8}^-]$, as a result of hydride attack at the μ_3-phosphinidene capping ligand and heterolytic scission of a Co-P bond. Reduction of **3** with MeLi is suggested to proceed at a cobalt-bound CO group, giving the acyl cluster $[FeCo_2(CO)_8\{C(O)Me\}(\mu_3\text{-}PPh)^-]$, $[\mathbf{9}^-]$. Use of the Grignard reagents t-BuMgCl or MeMgBr gives the 49-electron cluster $[FeCo_2(CO)_9(\mu_3\text{-}PPh)^{-\bullet}]$, $[\mathbf{10}^{-\bullet}]$. [MeO][Li] reacts with **3** at a cobalt-bound CO group at -78 °C to furnish the methoxycarbonyl cluster $[FeCo_2(CO)_8\{C(O)OMe\}(\mu_3\text{-}PPh)^-]$, $[\mathbf{11}^-]$. Treatment of **3** with methanolic $[Et_4N][OH]$ in THF at -70 °C gives the corresponding methoxycarbonyl and hydroxycarbonyl clusters in a 55:45 ratio, respectively, as determined by IR band-shape analysis.

ACKNOWLEDGMENTS

The author thanks Dr. Michael G. Richmond for his kind guidance, encouragement, and assistance in directing the described research. I thank Dr. W. H. Watson for his assistance with all of the X-ray crystallographic structures. I appreciate Dr. M. Schwartz and Mr. George DeLong for the use of the line-shape program and NMR assistance, respectively. Drs. P. S. Braterman, R. T. Conlin, P. R. Jones, D. A. Kunz, and R. D. Thomas are thanked for serving on my advisory committee.

I am very grateful to my parents, Yuan-pi and Li-chun, and to my wife, Shui-tsai, for their support and encouragement throughout the years.

Finally, I thank the University of North Texas for support in the form of a teaching assistantship and the Robert A. Welch Foundation for financial support in the form of a research assistantship.

TABLE OF CONTENTS

LIST OF TABLES

LIST OF FIGURES

Page

CHAPTER I

INTRODUCTION

Transition metal organometallic chemistry has developed to be an exciting and rapidly growing interdisciplinary subject in the last several years. Much interest has been expressed in the preparation and study of new organometallic compounds which pose significant questions of structure and bonding, or which are designed to exhibit unusual reactivity towards chemical transformations, or which may function as potential catalysts in the transformation of small molecules to commodity chemicals.[1] Three areas of organometallic chemistry are presented in this dissertation. They encompass the area of ligand substitution reactions involving the tetracobalt cluster, $Co_4(CO)_{10}(\mu_4\text{-PPh})_2$, the synthesis and reactivity of Fe_2/Pt chalcogenide arachno clusters, and CO reactivity studies in the mixed-metal phosphinidene-capped cluster, $FeCo_2(CO)_9(\mu_3\text{-PPh})$.

A. Metal Cluster Ligand Substitution Studies

The ligand substitution behavior of multinuclear metal carbonyl complexes with metal-metal bonds has been an important topic of transition metal organometallic chemistry. Ligand substitution studies at multinuclear metal complexes are not only of academic interest but are of

significance in providing a detailed analysis of homogeneous catalytic processes.[2-7] For example, the $H_4Ru_4(CO)_{12}$ catalyzed hydrogenation of alkenes or alkynes,[2-4] the $HRu_3(CO)_{11}^-$ catalyzed water gas shift reaction,[5] and the tricobalt or tetracobalt cluster catalyzed hydroformylation of pent-1- and -2-ene[6,7] have all been suggested to proceed through polynuclear species. In addition, kinetic measurements of ligand substitutional processes are also useful in defining the reactivity of reaction intermediates which result from ligand dissociation.[8] Hence, the kinetic parameters governing ligand substitution reactions in metal clusters may provide invaluable information necessary for designing new and selective homogeneous catalysts.

The three possible intimate mechanisms for ligand substitution processes in mononuclear metal complexes have been classified as (a) dissociative (D), (b) associative (A), and (c) interchange (I).[9] The interchange mechanism is further divided into I_a and I_b, depending on binding strength of both the entering and leaving ligands to the metal in the transition state. In addition to these substitution pathways, Darensbourg has classified that the polynuclear metal compounds have other mechanisms which include metal-metal bond dissociation without cluster fragmentation and with cluster fragmentation.[10]

The dissociation mechanism is one of the most common

pathways for ligand substitution reactions, with many examples been reported in the current literature.[8,11] For example, the ligand substitution reaction of $Os_3(CO)_{11}(NCMe)$ with phosphines has been shown to be quantitative, resulting in replacement of the CH_3CN ligand.[11] The rate constants were found to be independent of both the nature and concentration of the entering phosphine ligand. The trinuclear ruthenium hydride anion, $HRu_3(CO)_{11}^-$, undergoes facile CO substitution with PPh_3 in tetrahydrofuran. At a given $[PPh_3]$, k_{obsd} decreased with increasing [CO], suggesting a reaction pathway proceeding by CO dissociation.[8]

The association mechanism is not common but may hold for electron-poor metal clusters. For example, the triplatinum clusters $Pt_3(CO)_3L_3$ (L = phosphine) have been found to undergo a facile ligand substitution reaction with phosphines.[12] In these clusters each metal center formally contains 16 electrons. The reaction rate was found to be dependent on both the nature and concentration of incoming phosphine ligand. Basolo has stated the following rule: Substitution reactions involving 18-electron transition metal organometallic compounds may proceed by an associative mechanism provided the metal complex can delocalize a pair of electrons onto one of its ligands like NO, cyclopentadienyl, or arenes.[13]

Recent examples from the literature, including

$Ru_3(CO)_{12}$[14] and $Ir_4(CO)_{12}$,[15] showed that the rate-constant expression observed for ligand substitution reactions is comprised of a ligand-independent and ligand-dependent terms, represented in equation 1. The ligand-dependent term may be accounted for by several reaction pathways, including an associative process, an interchange (I_d or I_a) process, or a heterolytic fission of the metal-metal bond.

$$k_{obsd} = k_1 + k_2[L] \qquad (1)$$

The kinetics and mechanism of CO substitution reactions of $M_3(CO)_{12}$ (M = Fe, Ru, Os) in the presence of trimethylamine N-oxide in protic solvents was observed to undergo the interchange mechanism.[16] The rates of formation of $M_3(CO)_{11}L$ were found to be first-order in the concentration of $M_3(CO)_{12}$ and Me_3NO but zero-order in the concentration of L. This suggests that the reaction pathway involves nucleophilic attack of Me_3NO on the C atom of a CO ligand, resulting in oxidation of CO to CO_2 and the

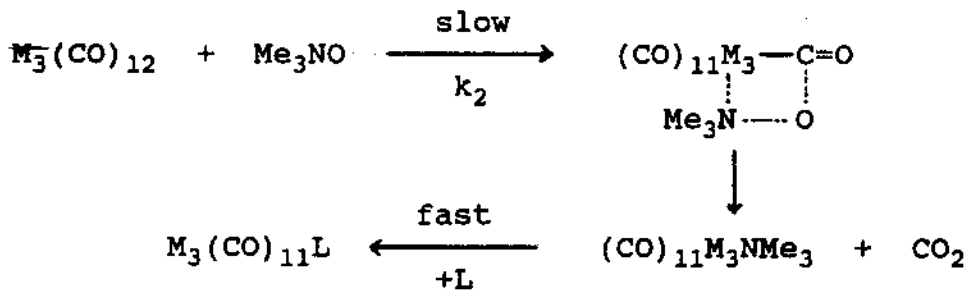

Scheme 1

concomitant production of a reactive metal cluster species (Scheme 1). From the second-order rate constants, the order of reactivity, $Fe_3(CO)_{12} > Ru_3(CO)_{12} > Os_3(CO)_{12}$, is noted.

The reaction of $Ru_3(CO)_{12}$ with $P(n\text{-}Bu)_3$ was found to undergo bimolecular nucleophilic fragmentation to give the products $Ru(CO)_4[P(n\text{-}Bu)_3]$ and $Ru(CO)_3[P(n\text{-}Bu)_3]_2$ in a mole ratio of 2 : 1.[17] It was concluded from these studies that $Ru_3(CO)_{11}[P(n\text{-}Bu)_3]$ was the initially formed product and that this species subsequently led to the formation of mononuclear derivatives upon spontaneous cluster fragmentation. This mechanism is depicted in Scheme 2. Kinetic studies showed that the fragmentation is induced by nucleophilic attack in the cluster. Similar observations were noted for the reaction of $Os_3(CO)_{11}[P(n\text{-}Bu)_3]$ with $P(n\text{-}Bu)_3$.[18]

In addition to previous examples, there are some ligand substitution reactions of trinuclear and tetranuclear

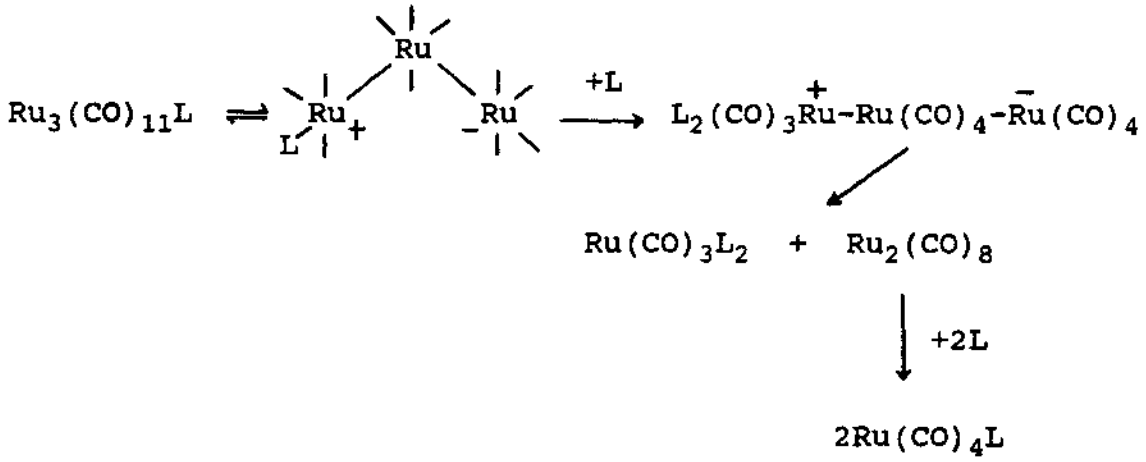

Scheme 2

carbonyl clusters which have appeared in the literature.[19,20] Presently there are few mechanistic studies of ligand substitutional processes involving higher nuclearity metal clusters.[21,22]

Many investigations of ligand substitution reactions involving transition metal carbonyl compound have used phosphines (PR_3) as ligands because they constitute one of the few series of ligands in which electronic and steric properties can be altered in a systematic and predictable way over a very wide range of varying R. Like NH_3, phosphines have a lone pair on the central atom which can be donated to metal. Unlike NH_3, they are also π acceptors. In the case of CO, it has long been recognized that it is the π^* orbital which accepts electrons from the metal. In the case of PR_3, the σ^* orbitals of the P-R bonds have been recognized as playing the role of acceptor.[23,24] Figure 1 shows the appropriate molecular orbital picture for such an interaction. Figure 1 shows that as the R group becomes more electronegative, the orbital that the R fragment uses to bond to phosphorus becomes more stable, which implies that σ^* orbital of the P-R bond also becomes more stable. At the same time the phosphorus contribution to σ^* increases, so does the size of σ^* lob that points toward the metal increases. Both of these factors make the σ^* more accessible for back donation. The final order of increasing π-acceptor character is:

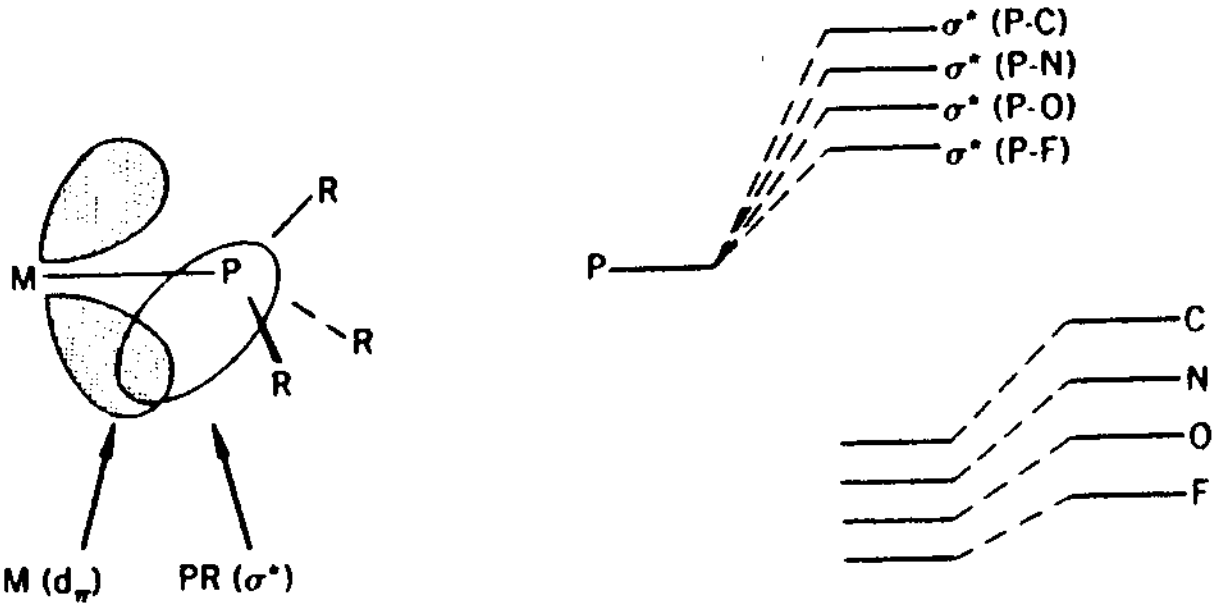

Figure 1. The σ^* orbitals of the P-R bonds play the acceptor role in metal complexes of phosphorus ligands. As the atom attached to phosphorus becomes more electronegative, the empty σ^* orbital of the P-X bond moves to lower energy and becomes more accessible; the PX_3 ligand therefore becomes a better acceptor from the metal

$$PMe_3 < PAr_3 < P(OMe)_3 < P(OAr)_3 < P(NR_2)_3 < PCl_3 < CO \approx PF_3$$

The dependence of the electronic effect of various PR_3 ligands on the nature of the R group has been quantified by Tolman,[25] who compared the ν(CO) frequencies of a series of complexes of the type $LNi(CO)_3$, containing different PR_3 ligands. The stronger donor phosphines increase the electron density on Ni, which passes some of this increase along to the CO's by π back donation. This in turn lowers ν(CO), as shown in fig. 2. The second important feature of PR_3 as a ligand is the variable steric size, which can be adjusted by changing R. Tolman has also quantified the steric effects of phosphines with his cone angle. This is obtained by taking a space-filling model of the $M(PR_3)$ group, folding back the R substituents away from the metal as far as they will go, and measuring the angle of a cone that will just contain all of the ligand, when the apex of the cone is at the metal. The results of these studies also appear on fig. 2 with the electronic parameters.

Interest in the tetracobalt cluster $Co_4(CO)_{10}(\mu_4\text{-PPh})_2$, **1**, and its phosphinated derivatives stems from their reported catalytic activity in the hydroformylation of 1-pentene[6,26] along with the varied regiochemistry and stereochemistry attendant upon ligand substitution.[27,28] This tetracobalt carbonyl cluster, which possesses a pair of μ_4-phosphinidene caps, has been observed to undergo

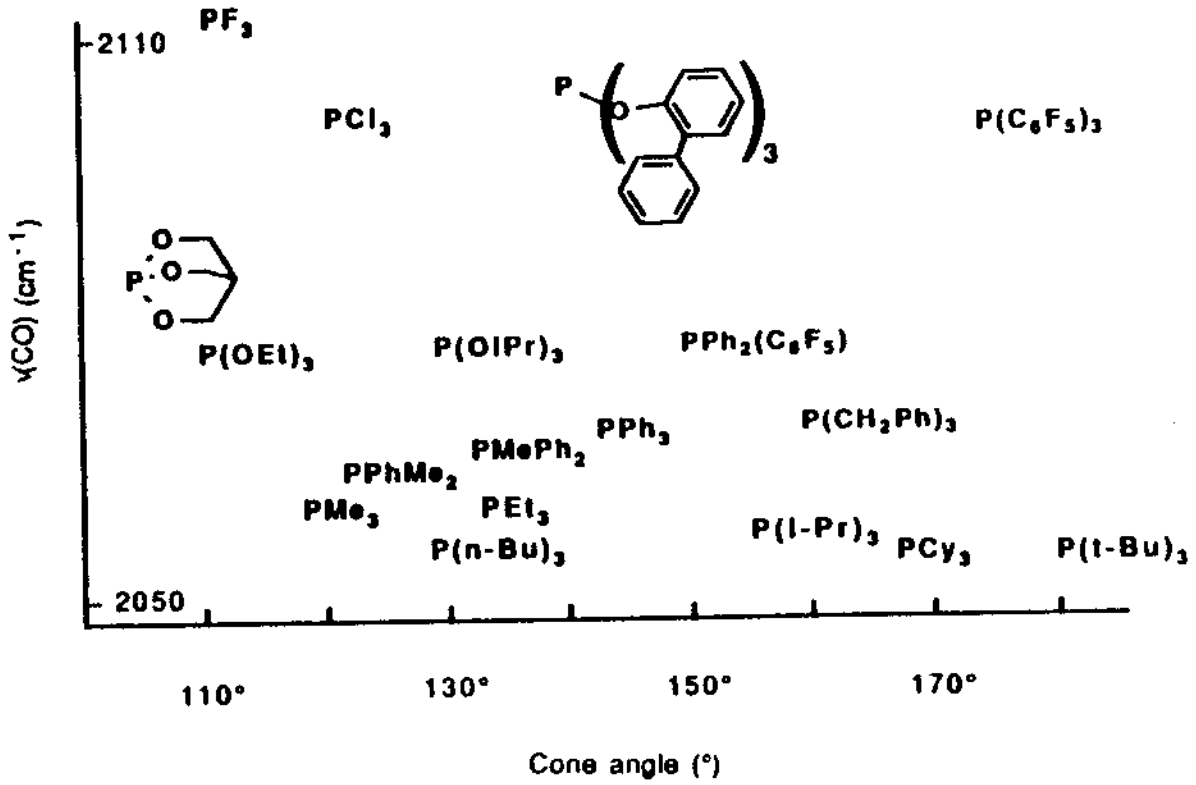

Figure 2. The Tolman electronic parameter and cone angels for a variety of phosphines

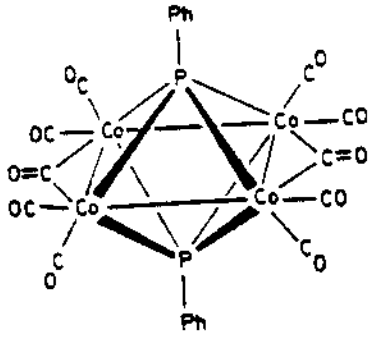

1

sequential CO ligand substitution with trimethyl phosphite thermally to afford the mono, bis, tris, and tetrakis derivatives, where the phosphite ligands are bound to a separate cobalt centers as demonstrated by X-ray crystallography.[20] The kinetics and activation parameters indicate that the mono- and bis-substitutions occur primarily via an associative mechanism, whereas a dissociative process is dominant in the tris- and tetrakis-substitutions. This tetracobalt cluster was also observed to undergo electron-transfer chain or ETC catalysis, thus allowing for the selective synthesis of a variety of monosubstituted derivatives.[29] A dissociative mechanism was proposed for the electrocatalytic substitution process, Scheme 3, where E_i represents the electrode of chemical potential necessary to reduce a portion of the tetracobalt cluster to the anion radical. Furthermore, there are very few kinetic or mechanistic studies on tetranuclear transition-metal clusters with a series of phosphorus donor

ligands of varying electronic and steric properties.[30,31] Accordingly, the study of the kinetics associated with the mono ligand substitution in the tetracobalt cluster, $Co_4(CO)_{10}(\mu_4\text{-}PPh)_2$, using various phosphine and phosphite ligands has been examined.

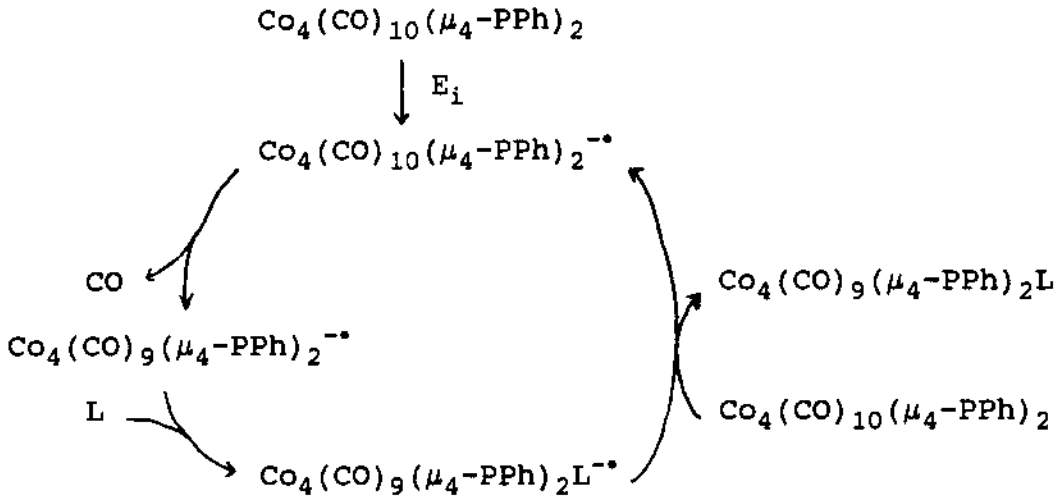

Scheme 3

B. Directed Synthesis of Arachno Fe_2/Pt Clusters

Synthetic routes and reactivity patterns of polynuclear metal clusters are not as well-understood in comparison to mononuclear organometallic complexes.[32] Interest in polynuclear metal clusters derives from their ability to function as working models for metal-containing proteins and nitrogenases,[33] redox transfer catalysts,[34] theoretical calculations related to band structure,[35] and multisite substrate activation as related to heterogeneous metal

catalysis.[36,37]

The chemistry of transition-metal chalcogenides is presently expanding at a rapid rate commensurate with the structural, spectroscopic, and chemical novelty of such compounds. Particularly of interest in this area of organometallic chemistry is the synthesis of models for important biological[38] and industrial[39] catalysts and the preparation of materials for energy storage and conversion.[40] Biological N_2 fixation is one of the fundamental synthetic processes of nature. Nitrogenase is the catalytic component of the biological nitrogen-fixation system which reduces atmospheric N_2 to ammonia. The dominating metal in all nitrogenases is iron in a coordination sphere of sulfur. Most nitrogenases also include molybdenum and some of them vanadium.[41] Recently the transformations of sulfur-containing ligands on cluster faces have been examined in detail with the aim to understand processes like the desulfurization of fossil fuels,[42] or the universal poisonous effects of sulfur on heterogeneous catalysts.[43]

One of the first sulfur-bridged clusters prepared was μ-dithio-bis(tricarbonyliron)[$Fe_2(CO)_6(\mu\text{-}S_2)$], **2**, which was first identified by Brendel in 1958.[44] Since this iron chalcogenide was prepared, it has been the subject of a number of investigations. Its solid-state structure was determined by Wei and Dahl[45] by X-ray diffraction analysis.

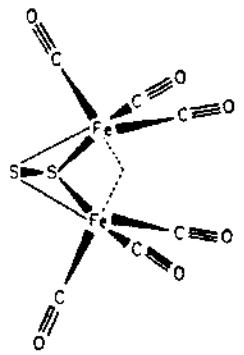

2

The complex adopts a butterfly shape (distorted Fe_2S_2 tetrahedron), with an S_2 ligand symmetrically bridging the two $Fe(CO)_3$ units. The two iron centers are connected by a bent metal-metal bond.[46] The S-S bond distance of 2.01 Å corresponds to the normal S-S single bond distance(2.04 Å, as found in S_2Cl_2 and S_8[47]). Several theoretical studies have dealt with the bonding and electronic structure of this species.[48,49]

Heiber and Zeidler[50] studied simple CO replacement by triphenylphosphine, a reaction which received more detailed study by later workers.[51] In 1980 Rauchfuss and coworkers observed that $Pt(PPh_3)_2$(ethylene) reacted with $Fe_2(CO)_6(\mu\text{-}S_2)$ to give the heterometallic arachno cluster $[Fe_2(CO)_6(\mu_3\text{-}S)_2Pt(PPh_3)_2]$, equation 2.[52] The repositioning of the bridging sulfido ligand is a notable feature of this reaction. The sulfur-sulfur bond undergoes a formal homolytic cleavage as the metal ligand species inserts into the sulfur-sulfur bond. At about this same time Seyferth

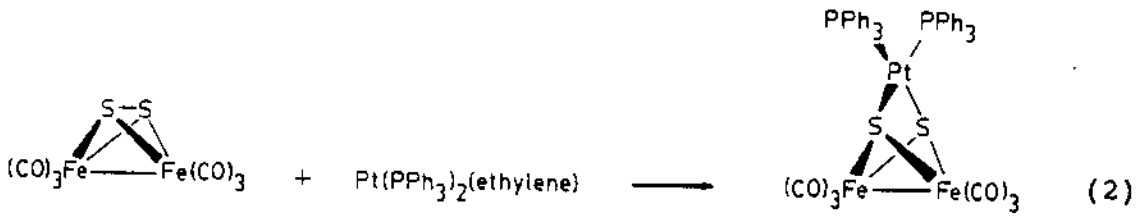

(2)

and coworkers had also begun to examine the chemistry of the corresponding dianion $[Fe_2(CO)_6(\mu\text{-}S)_2]^{2-}$. They proposed that treatment of a suitable metal or metal hydride with $Fe_2(CO)_6(\mu\text{-}S)_2$ might undergo nucleophilic cleavage, as shown in equation 3. In a subsequent step (eq 4), deprotonation

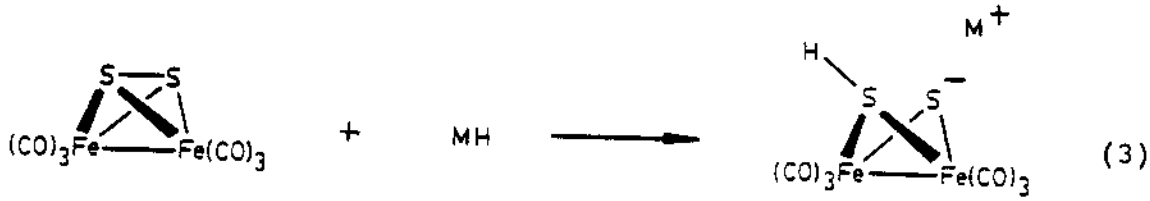

(3)

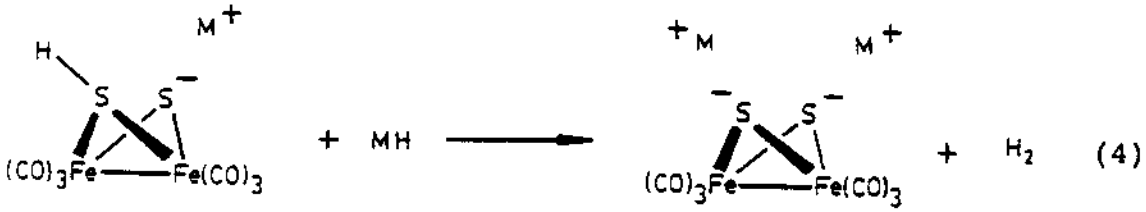

(4)

of the monoanionic intermediate by a second equivalent of metal hydride would then give the dianion. Addition of low-valent metal compounds to the dianion was extensively studied as a route to mixed-metal clusters, equation 5, ML_n = (diphos)$NiCl_2$, $(PPh_3)PtCl_2$, $CpCo(CO)I_2$.[53] These reactions involve halide displacement steps that bear resemblance to

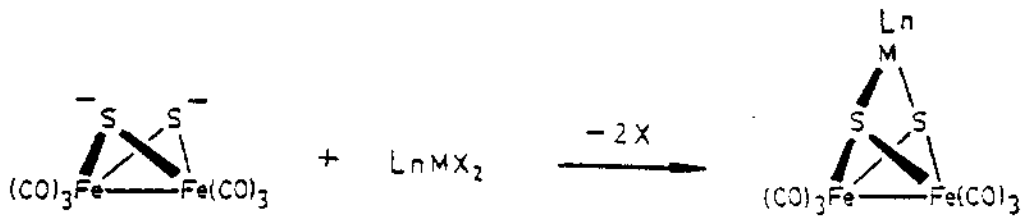

(5)

common S_N2 reactions. Recently, more synthetic studies involving $Fe_2(CO)_6(\mu\text{-}S)_2$ as a route to higher nuclearity clusters has been reported in the literature.[54,55] However, there has not been a detailed study concerning the reactivity of these kinds of clusters. Therefore, the analogous heterometallic chalcogenide clusters were explored for their reactivity under oxidation and reduction conditions. Also, it is hopeful that these clusters may prove useful as cluster catalysts in hydrogenation reactions and potential chemical vapor deposition (CVD) precursors.

C. Reactivity Studies in the Heterometallic Bridged Phosphinidine Capped Cluster $FeCo_2(CO)_9(\mu_3\text{-}PPh)$

Of the many diverse types of polynuclear compounds known, mixed-metal phosphinidene capped clusters represent a cluster subclass that has received much recent attention.[56] The low symmetry associated with these clusters facilitates mechanistic studies that deal with heterometallic metal-metal bond reactivity and site selectivity in ligand substitution processes.[57,58] For example, Huttner and coworkers were the first to demonstrate that P-ligands reversibly add to the iron center in the tetrahedral cluster

$MnFe_2(CO)_8Cp(\mu_3\text{-}PPh)$, via cleavage of the Mn-Fe bond, to give the corresponding arachno cluster $MnFe_2(CO)_8(PR_3)Cp(\mu_3\text{-}PPh)$.[59] Similar addition/elimination reactions have been reported by Vahrenkamp et al. for the clusters $FeCo_2(CO)_9(\mu_3\text{-}PMe)$ and $FeCoW(CO)_8Cp(\mu_3\text{-}PMe)$.[60,61] Site-specific substitutions need not involve heterometallic bond cleavage as shown by the work of Ohst and Kochi using the six-vertex closo cluster $Fe_3Rh(CO)_8Cp^*(\mu_4\text{-}PPh)_2$.[62] In that study, the unique iron opposite the Cp^*Rh center was shown to reversibly add and eliminate CO depending on the cluster's redox state.

Here the results are reported on the reduction pathways available to the phosphinidene-capped cluster $FeCo_2(CO)_9(\mu_3\text{-}PPh)$, **3**.[63] In 1983 Vahrenkamp and coworkers observed that

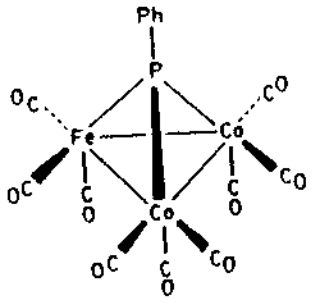

3

the easily accessible complexes $RPH_2\text{-}Fe(CO)_4$ (R = Me, t-Bu, Ph) contain two functional P-H units which can be reacted successively with $Co_2(CO)_8$ or $(\eta\text{-}C_3H_5)Co(CO)_3$ to yield the dinuclear complexes $(\mu\text{-}RPH)FeCo(CO)_7$. These mixed-metal

dimers react with additional cobalt carbonyls to give trinuclear cluster $FeCo_2(CO)_9(\mu_3\text{-}RP)$ (R = Me, t-Bu, Ph). The core of these clusters consist of a triangular array of cobalt and iron atoms ligated by the capping phosphinidene group. The overall geometry of this cluster is best considered as a nido cluster. The theoretical basis of such a polynuclear geometry is best viewed within the context of Polyhedral Skeletal Electron Pair (PSEP) Theory.[64-66]

As will be shown, the results provide the first detailed study on the reactivity of a tetrahedrane cluster toward anionic two-electron donor ligands. The impetus for this study stems from an earlier report describing the catalytic activity of **3** in 1-pentene and styrene hydroformylations[67] along with a recent paper dealing with the reactivity and stability of the structurally similar cluster $[Co_3(CO)_8(CHO)(\mu_3\text{-}CPh)^-]$, the product of hydride attack at a terminal cobalt-carbonyl group.[68] Besides reactivity comparisons made between **3** and the tricobalt clusters $Co_3(CO)_9(\mu_3\text{-}CR)$, the chemistry of **3** is also contrasted with the mixed-metal cluster $Fe_2Co_2(CO)_{11}(\mu_4\text{-}PPh)_2$, which has been shown to react with anionic nucleophiles exclusively at a terminal cobalt-carbonyl group.[69]

CHAPTER REFERENCES

1. Roth, J. F.; Craddock, J. H.; Hershman, A.; Paulik, F. E. Chem. Tech. **1971**, 1, 600.

2. Graff, J. L.; Wrighton, M. S. J. Am. Chem. Soc. **1980**, 102, 2123.

3. (a) Doi, Y.; Koshizuka, K.; Keii, T. Inorg. Chem. **1982**, 21, 2732. (b) Doi, Y.; Tamura, S.; Koshizuka, K. Inorg. Chim. Acta **1982**, 65, L63. (c) Doi, Y.; Tamura, S.; Koshizuka, K. J. Mol. Catal. **1983**, 19, 213.

4. (a) Lausarot, P. M.; Vaglio, G. A.; Valle, M. Inorg Chim. Acta **1977**, 25, L107. (b) Lausarot, P. M.; Vaglio, G. A.; Valle, M. Inorg. Chim. Acta **1979**, 36, 213.

5. (a) Bricker, J. C.; Nagel, C. C.; Shore, S. G. J. Am. Chem. Soc. **1982**, 104, 1444. (b) Bricker, J. C.; Nagel, C. C.; Bhattacharyya, A. A. J. Am. Chem. Soc. **1985**, 107, 377.

6. (a) Ryan, R. C.; Pittman, Jr. C. U.; O'Connor, J. P. J. Am. Chem. Soc. **1977**, 99, 1986. (b) Pittman, Jr. C. U.; Ryan, R. C. Chem. Technol. **1978**, 8, 170. (c) Pittman, Jr. C. U.; Wilemon, G. M.; Wilson, W. D.; Ryan, R. C. Angew. Chem., Int. Ed. Engl. **1980**, 19, 478.

7. Withers, H. P.; Seyferth, D. Inorg. Chem. **1983**, 22, 2931.

8. Taube, D. J.; Ford, P. C. Organometallics **1986**, 5, 99.

9. Langford, C. H.; Gray, H. B. in "Ligand Substitution Processes", New York: Benjamin, **1965**.

10. Darensbourg, D. J. in "The Chemistry of Metal Cluster Complexes," Shriver, D. F.; Kaesz, H. D.; Adams, R. D., Eds.; VCH Publishers; New York; **1990**; Ch 4.

11. Dahlinger, K.; Poë, A. J.; Sayal, P. K.; Sekhar, V. C. J. Chem. Soc., Dalton Trans. **1986**, 2145.

12. Browning, C. S.; Farrar, D. H.; Gukathasan, R. R.; Morris, S. A. Organometallics, **1985**, 4, 1750.

13. Basolo, F. Inorg. Chim. Acta **1981**, 50, 65.

14. Candlin, J. P.; Shortland, A. C. J. Organomet. Chem. **1969**, 16, 289.

15. Karel, K. J.; Norton, J. R. J. Am. Chem. Soc. **1974**, 96, 6812.

16. Shen, J. -K.; Shi, Y. -L.; Gao, Y. -C.; Shi, Q. -Z.; Basolo, F. J. Am. Chem. Soc. **1988**, 110, 2414.

17. Poë, A. J.; Twigg, M. V. Inorg. Chem. **1974**, 13, 2982.

18. Poë, A. J.; Sekhar, V. C. Inorg Chem. **1985**, 24, 4376.

19. Darensbourg, D. J.; Peterson, B. S.; Schmidt, Jr. R. E. Organometallics **1982**, 1, 306.

20. Richmond, M. G.; Kochi, J. K. Inorg. Chem. **1986**, 25, 1334.

21. Nomyia, K.; Suzuki, H. J. Organomet. Chem. **1979**, 168, 115.

22. John, G. R.; Johnson, B. F. G.; Lewis, J.; Mann, A. L. J. Organomet. Chem. **1979**, 171, C9.

23. Orpen, A. G. J. Chem. Soc., Chem. Commun. **1985**, 1310.

24. (a) Xiao, S. -X.; Trogler, W. C.; Ellis, D. E.; Berkovitch-Yellin, Z. J. Am. Chem. Soc. **1983**, 105, 7033. (b) Morris, R. J.; Girolami, G. S. Inorg. Chem. **1990**, 29, 4167.

25. Tolman, C. A. Chem. Rev. **1977**, 77, 313.

26. Pittman, Jr. C. U.; Richmond, M. G.; Wilemon, G. M.; Absi-Halabi, M. in "Catalysis of Organic Reactions", Kosak, J. R., Ed., Marcel Dekker: New York, **1984**, Ch. 5.

27. Don, M. J.; Richmond, M. G.; Watson, W. H.; Nagl, A. Acta Cryst. **1991**, C47, 93.

28. Richmond, M. G.; Kochi, J. K. Inorg. Chim. Acta **1987**, 126, 83.

29. Richmond, M. G.; Kochi, J. K. Inorg. Chem. **1986**, 25, 656.

30. Sonnenberger, D.; Atwood, J. D. Inorg. Chem. **1981**, 20, 3243.

31. Darensbourg, D. J.; Baldwin-Zuschke, B. J. J. Am. Chem. Soc. **1982**, 104, 3906.

32. (a) Vahrenkamp, H. Adv. Organomet. Chem. **1983**, 22, 169. (b) Vargas, M. D.; Nicholls, J. N. Adv. Inorg. Chem. Radiochem. **1986**, 30, 123. (c) Sappa, E.; Tiripicchio, A.; Carty, A. J.; Toogood, G. E. Prog. Inorg. Chem. **1987**, 35, 437. (d) Shriver, D. F.; Sailor, M. J. Acc. Chem. Res. **1988**, 21, 374.

33. (a) Lippard, S. J. Angew. Chem., Int. Ed. Engl. **1988**, 27, 344. (b) Orme-Johnson, W. H. Annu. Rev. Biophys. Biophys. Chem. **1985**, 14, 419. (c) Holm, R. H. Chem. Soc. Rev. **1981**, 10, 455. (d) Christou, G. Acc. Chem. Res. **1989**, 22, 328. (e) Coucouvanis, D. Acc. Chem. Res. **1981**, 14, 201.

34. (a) Kochi, J. K. J. Organomet. Chem. **1986**, 300, 139. (b) Astruc, D. Angew. Chem., Int. Ed. Engl. **1988**, 27, 643. (c) Astruc, D. Chem. Rev. **1988**, 88, 1189.

35. (a) Zonnevylle, M. C.; Silvestre, J.; Hoffmann, R. J. Am. Chem. Soc. **1986**, 108, 1509. (b) Mingos, D. M. P. Chem. Soc. Rev. **1986**, 15, 31. (c) Whangbo, M. H.; Hoffmann, R. J. Am. Chem. Soc. **1978**, 100, 6093. (d) Wheeler, R. A.; Piela, L.; Hoffmann, R. J. Am. Chem. Soc. **1988**, 110, 7302. (e) Wheeler, R. A.; Hoffmann, R. J. Am. Chem. Soc. **1988**, 110, 7315. (f) See also: Hoffmann, R. "Solids and Surfaces: A Chemist's View of Bonding in Extended Structures", VCH Publishers: New York, **1988**.

36. (a) Kaesz, H. D.; Knobler, C. B.; Andrews, M. A.; van Buskirk, G.; Szostak, R.; Strouse, C. E.; Lin, Y. C.; Mayr, A. Pure Appl. Chem. **1982**, 54, 131. (b) Knox, S. A. R. Pure Appl. Chem. **1984**, 56, 81. (c) Adams, R. D.; Babin, J. E.; Tasi, M.; Wolfe, T. A. J. Am. Chem. Soc. **1988**, 110, 7093. (d) Sappa, E.; Tiripicchio, A.; Braunstein, P. Coord. Chem. Rev. **1985**, 65, 219. (e) Albiez, T.; Powell, A. K.; Vahrenkamp, H. Chem. Ber. **1990**, 123, 667.

37. (a) Moskovits, M. Acc. Chem. Res. **1979**, 12, 229. (b) Muetterties, E. A.; Rhodin, T. N.; Band, E.; Brucker, C. F.; Pretzer, W. R. Chem. Rev. **1979**, 79, 91. (c) Muetterties, E. A. Science (Washington, D. C.) **1977**, 196, 839. (d) Gates, B. C.; Guczi, L.; Knozinger, H., Eds.; "Metal Clusters in Catalysis", Elsevier: New York, **1986**, and references therein. (e) Moskovits, M., Ed.; "Metal Clusters", Wiley: New York, **1986**, and

references therein. (f) Saillard, J. Y.; Hoffmann, R. J. Am. Chem. Soc. **1984**, 106, 2006. (g) Zheng, C.; Apeloig, Y.; Hoffmann, R. J. Am. Chem. Soc. **1988**, 110, 749.

38. Zimmerman, R.; Munch, E.; Brill, W.J.; Shah, V.K.;Henzl, M.T.; Rawlings, J.; Orme-Johnson, W.H. Biochim. Biophys. Acta **1978**, 537, 185.

39. Weisser, O.; Landa, S. "Sulfide Catalysis, Their Properties and Applications", Pergamon Press; New York, **1973**.

40. (a) Jacobson, A. J.; Whittingham, M. S.; Rich, S. M. J. Electrochem Soc. **1979**, 126, 891. (b) Jacobson, A. J.; Chianelli, R. R.; Rich, S. M.; Whittingham, M. S. Mater Res. Bull. **1979**, 14, 1437. (c) Kubiak, C. P.; Schneemeyer, L. F.; Wrighton, M. S. J. Am. Chem. Soc. 1980, 102, 6898.

41. (a) Hughes, M. N., Ed.; "The Inorganic Chemistry of Biological Process", Wiley: New York, **1984**. (b) Spiro, T. G. Ed, Molydenum Enzymes Wiley-Interscience : New York, **1986**. (c) Burgess, B. K. Chem. Rev. **1990**, 90, 1377. (d) Bergersen, F. J.; Postgate, J. R. "A Century of Nitrogen Fixation Research", The royal Society, London, **1987**.

42. (a) Schuman, S. C.; Shalit, H. Catal. Rev. **1970**, 4, 245. (b) Angelici, R. Acc. Chem. Res. **1988**, 21, 387. (c) Friend, C. M.; Roberts, J. T. Acc. Chem. Res. **1988**, 21, 394.

43. (a) Hegedus, L. L.; McCabe, R. W. "Catalyst poisoning", Marcel Decker, Ed.; New York, **1984**. (b) Bartholomew, C. H.; Agrawal, P. K.; Katzer, J. R. Adv. Catal. **1982**, 31, 135. (c) Qudar, J. J. Catal. Rev. Sci. Eng. **1980**, 22, 171.

44. Hieber, W.; Gruber, J. Z. Anorg. Allg. Chem. **1958**, 296, 91.

45. Wei, C. H.; Dahl, L. F. Inorg. Chem. **1965**, 4, 1.

46. Dahl, L. F.; Martell, C.; Wampler, D. L. J. Am. Chem. Soc. **1961**, 83, 1761.

47. (a) Ackermann, P. G.; Mayer, J. E. J. Chem. Phys. **1936**, 4, 377. (b) Abrahams, S. C. Acta Crystallogr. **1955**, 8, 661.

48. (a) Burdett, J. K. J. Chem. Soc. Dalton Trans. **1977**, 423. (b) Summerville, R. H.; Hoffmann, R. J. Am. Chem. Soc. **1976**, 98, 7240. (c) Mason, R.; Mingos, D. M. P. J. Organomet. Chem. **1973**, 50, 53.

49. (a) Teo, B. K.; Hall, M. B.; Fenske, R. G.; Dahl, L. F. J. Organomet. Chem. **1974**, 70, 413. (b) Teo, B. K.; Hall, M. B.; Fenske, R. G.; Dahl, L. F. Inorg. Chem. **1975**, 14, 3103.

50. Hieber, W.; Zeidler, A. Z. Anorg. Allg. Chem. **1964**, 329, 92.

51. Rossetti, R.; Gervasio, G.; Stanghellini, P. L. Inorg. Chim. Acta. **1979**, 35, 73.

52. Day, V. W.; Lesch, D. A.; Rauchfuss, T. B. J. Am. Chem. Soc. **1982**, 104, 1290.

53. Seyferth, D.; Henderson, R. S,; Song, L. C. Organometallics **1982**, 1, 125.

54. Seyferth, D.; Henderson, R. S.; Gallagher, M. K. Organometallics **1989**, 8, 119.

55. Wakatsuki, Y.; Yamazaki, H. J. Organomet. Chem. **1988**, 347, 151.

56. (a) Vahrenkamp, H. Phil. Trans. R. Soc. Lond. A **1982**, 308, 17. (b) Huttner, G.; Knoll, K. Angew. Chem., Int. Ed. Engl. **1987**, 26, 743.

57. (a) Geoffroy, G. L. Acc. Chem. Res. **1980**, 13, 469. (b) Gladfelter, W. L.; Geoffroy, G. L. Adv. Organomet. Chem. **1980**, 18, 207. (c) Roberts, D. A.; Geoffroy, G. L. in "Comprehensive Organometallic Chemistry," Wilkinson, G.; Stone, F. G. A.; Abels, E. W., Eds.; Pergamon Press: Oxford; U. K.; **1982**; Ch 40.

58. See also: (a) Stephan, D. W. Coord. Chem. Rev. **1989**, 95, 41. (b) Bullock, R. M.; Casey, C. P. Acc. Chem. Res. **1987**, 20, 167.

59. (a) Huttner, G,; Schneider, J.; Muller, H. D.; Mohr, G.; von Seyerl, J.; Wohlfahrt, L. Angew. Chem., Int. Ed. Engl. **1979**, 18, 76. (b) Schneider, J.; Minelli, M.; Huttner, G. J. Organomet. Chem. **1985**, 294, 75.

60. Planalp, R. P.; Vahrenkamp, H. Organometallics **1987**, 6, 492.

61. For related clusters exhibiting this phenomenon, see: (a) Richmond, M. G.; Kochi, J. K. Inorg. Chem. **1987**, 26, 541. (b) Vahrenkamp, H. J. Organomet. Chem. **1989**, 370, 65. (c) Gusbeth, P.; Vahrenkamp, H. Chem. Ber. **1985**, 118, 1758. (d) Albers, M. O.; Robinson, D. J.; Coville, N. J. Coord. Chem. Rev. **1986**, 69, 127, and references therein. (e) Lesch, D. A.; Rauchfuss, T. B. Inorg. Chem. **1983**, 22, 1854. (f) Bogan, L. E., Jr.; Lesch, D. A.; Rauchfuss, T. B. J. Organomet. Chem. **1983**, 250, 429.

62. (a) Ohst, H. H.; Kochi, J. K. Organometallics **1986**, 5, 1359. (b) Jaeger, T.; Aime, S.; Vahrenkamp, H. Organometallics **1986**, 5, 245.

63. (a) Richter, F.; Beurich, H.; Vahrenkamp, H. J. Organomet. Chem. **1979**, 166, C5. (b) Muller, M.; Vahrenkamp, H. Chem. Ber. **1983**, 116, 2311.

64. (a) Wade, K. Chem. Br. **1975**, 11, 177. (b) Wade, K. Adv. Inorg. Chem. Radiochem. **1976**, 18, 1. (c) Wade, K. in "Transition Metal Clusters", Johnson B. F. G. , Ed., Wiley, New York, **1980**; Ch 3. (d) Mingos, D. M. P. Acc. Chem. Res. **1984**, 17, 311. (e) Mingos, D. M. P. Nature (London), Phys. Sci. **1972**, 236, 99.

65. Also see: (a) Teo, B. K. Inorg. Chem. **1984**, 23, 1251. (b) Teo, B. K.; Longoni, G.; Chung, F. R. K. Inorg. Chem. **1984**, 23, 1257. (c) Teo, B. K. Inorg. Chem. **1985**, 24, 115. (d) Mingos, D. M. P. Inorg. Chem. **1985**, 24, 114.

66. For extended Huckel studies of $M_4(\mu_4\text{-}PR)_2$ clusters, see: Halet, J. F.; Hoffmann, R.; Saillard, J. Y. Inorg. Chem. **1985**, 24, 1695.

67. Richmond, M. G.; Absi-Halabi, M.; Pittman, Jr. C. U. J. Mol. Catal. **1984**, 22, 367.

68. Dumond, D. S.; Hwang, S.; Richmond, M. G. Inorg. Chim. Acta **1989**, 160, 135.

69. Richmond, M. G.; Kochi, J. K. J. Organomet. Chem. **1987**, 323, 219.

CHAPTER II

EXPERIMENTAL

A. Materials

1. Solvents

Toluene, THF, and 2-MeTHF were distilled from sodium/benzophenone ketyl and stored under argon in Schlenk vessels. CH_2Cl_2 and HMPA (Hexamethylphosphoramide) were distilled from calcium hydride and stored under argon in Schlenk vessels. The deuterated solvents benzene-d_6, THF-d_8, and toluene-d_8 were vacuum distilled from calcium hydride, while CD_2Cl_2 and $CDCl_3$ were distilled from P_2O_5 under argon and stored in Schlenk vessels.

2. Reagents

Dicobalt octacarbonyl and dichlorophenylphosphine were purchased from Pressure Chemical Co. and used as received. $Co_4(CO)_{10}(\mu_4\text{-PPh})_2$,[1] Bu_3SnH,[2] and Ph_2PH[3] were all prepared by known literature procedures. Trimethyl phosphite, triethyl phosphite, triisopropyl phosphite, and tributyl phosphine were purchased from Aldrich and distilled from sodium and stored under argon in Schlenk vessels. Triisopropyl phosphine and Bis(triphenylphosphoranylidene)ammonium chloride ([PPN][Cl]) were purchased from Aldrich and used as

received. Triphenyl phosphine and tricyclohexyl phosphine (Alfa) were recrystallized from absolute ethanol. The ^{13}C-enriched carbon monoxide (99% ^{13}C) was obtained from Isotec, Inc.

$Fe_2(CO)_6(\mu_2\text{-}S)_2$ was prepared according to the procedure of Hieber and Gruber.[4] Dichloro(1,5-cyclooctadiene)platinum was prepared by a known literature procedure.[5] Dichloro(1,10-phenanthroline)platinum and dichloro-1,2-bis(diphenylphosphine)ethane platinum were prepared by the method of Watt and Cuddeback,[6] while dichloro(2.2'-bipyridyl)platinum was prepared by essentially the same procedure as that used for the 1,10-phenanthroline complex. $FeCo_2(CO)_9(\mu_3\text{-}PPh)$[7], $Fe(1,10\text{-phen})_3(PF_6)_3$,[8] tris(4-bromophenyl)amine-hexachloroantimonate (magic green),[9] methyl triflate[10], and cobaltocene[11] (0.25 M in THF) were prepared by known literature procedures. Sodium naphthalide (0.5 M in THF) was prepared according to the method of Fieser and Fieser[12], while $[Cp_2Fe][BF_4]$ was synthesized using the procedure of Gray and coworkers.[13] $Cr(acac)_3$ was purchased from Alpha Chemicals and was used as a shiftless relaxation agent (~0.0001 M) in the ^{13}C NMR studies.[14]

$[Et_3BH][Li]$ (1.0 M in THF), K-Selectride (1.0 M in THF), MeLi (1.4 M in Et_2O), n-BuLi (2.5 M in hexanes), PhLi (2.0 M in C_6H_{12}/Et_2O; 70/30), MeMgBr (1.5 M in toluene/THF; 75/25), t-BuMgCl (2.0 M in THF), and trifluoroacetic acid were all purchased from Aldrich and used as received. MeLi

was titrated against diphenylacetic acid prior to use.[15] $[Et_4N][OH]$ (20% aqueous solution) was obtained from Lancaster Synthesis and dried under high vacuum to give solid $[Et_4N][OH]$. 1.3 M methanolic solutions of $[Et_4N][OH]$ were subsequently prepared under argon and transferred to Schlenk vessels for storage. All reactions were conducted under argon with Schlenk techniques.[16]

B. Instrumentation

All reactions were conducted under argon using Schlenk techniques[16] or in a nitrogen filled Vacuum Atmosphere ΔXL series inert-atmosphere Dri-box. Routine infrared spectra were recorded on a Nicolet 20SXB FT-IR spectrometer in 0.1 mm NaCl cells. Low-temperature IR spectra were recorded on the same spectrometer with a Specac Model P/N 21.000 variable-temperature cell equipped with inner and outer CaF_2 windows. Dry ice/acetone was used as coolant, and the reported cell temperature, taken to be accurate to $\pm$ 1 °C, was determined with a copper-constantan thermocouple, which was factory calibrated prior to purchase. ^1H, ^{13}C, and ^{31}P NMR spectra were recorded at 300, 75, and 121 MHz, respectively, on a Varian 300-VXR spectrometer. A Laude RC-6 constant-temperature bath was used to maintain the reactions at the desired temperatures, to within $\pm$ 0.1 °C. C and H analyses were performed by Atlantic Microlab, Atlanta, GA.

C. Preparation of Compounds

1. General Synthetic Procedure For Mono-substituted Tetracobalt Cluster $Co_4(CO)_9(L)(\mu_4\text{-}PPh)_2$ (where L = $P(OEt)_3$, Ph_2PH, $P(O\text{-}i\text{-}Pr)_3$, $P(n\text{-}Bu)_3$, PPh_3, $P(i\text{-}Pr)_3$, PCy_3)

The tetracobalt cluster compound $Co_4(CO)_{10}(\mu_4\text{-}PPh)_2$ and the desired ligand were dissolved in THF, after which a few drops of sodium benzophenone ketyl (0.25M THF solution) was added through a rubber septum. The solution was stirred for several hours at room temperature with monitoring by either IR spectroscopy or TLC analysis. Typically, TLC examination (petroleum ether/benzene, 8/2) revealed greater than 70% conversion to the mono-substituted cluster $Co_4(CO)_{10}(\mu_4\text{-}PPh)_2$, after which time the solvent was removed under vacuum. The desired product was purified by chromatography on silica gel using an 8:2 (v/v) mixture of petroleum ether and benzene. The resulting material was crystallized from a 1:1 mixture of toluene/heptane at -20 °C. The isolated yields of the desired products ranged from 50% to 70%. The microanalytical results and IR frequencies of all the mono-substituted clusters are given in Table 1 and Table 2, respectively.

2. Preparation of (dppf)PtCl2

(dppf)PtCl2 was synthesized in 1972,[19] but described here is a simpler synthetic approach, which affords

Table 1. Analytical Data for Mono-Substituted Tetracobalt Clusters

Cluster	% Found		% Calc.	
	C	H	C	H
$Co_4(CO)_9[P(OMe)_3](\mu_4\text{-}PPh)_2$[a] $C_{24}H_{19}Co_4O_{12}P_3$	-	-	-	-
$Co_4(CO)_9[P(OEt)_3](\mu_4\text{-}PPh)_2$ $C_{27}H_{25}Co_4O_{12}P_3$	37.33	2.91	37.27	2.90
$Co_4(CO)_9(Ph_2PH)(\mu_4\text{-}PPh)_2$ $C_{33}H_{21}Co_4O_9P_3$	44.63	2.40	44.53	2.38
$Co_4(CO)_9[P(O\text{-}i\text{-}Pr)_3](\mu_4\text{-}PPh)_2$ $C_{30}H_{31}Co_4O_{12}P_3$	39.16	3.45	39.50	3.43
$Co_4(CO)_9[P(n\text{-}Bu)_3](\mu_4\text{-}PPh)_2$ $C_{33}H_{37}Co_4O_9P_3$	43.81	4.15	43.73	4.11
$Co_4(CO)_9(PPh_3)(\mu_4\text{-}PPh)_2$[b] $C_{39}H_{25}Co_4O_9P_3$	-	-	-	-
$Co_4(CO)_9[P(i\text{-}Pr)_3](\mu_4\text{-}PPh)_2$ $C_{30}H_{31}Co_4O_9P_3$	41.79	3.64	41.69	3.62
$Co_4(CO)_9(PCy_3)(\mu_4\text{-}PPh)_2$ $C_{39}H_{43}Co_4O_9P_3 \cdot 1/4\ C_7H_8$	48.60	5.09	48.59	4.45

[a]See Ref. 17. [b]See Ref. 18.

Table 2. Infrared Spectra in the νCO Region of the Tetracobalt Cluster and Mono-Substituted Tetracobalt Clusters[a]

Cluster	IR band, cm^{-1}
$Co_4(CO)_{10}(\mu_4\text{-}PPh)_2$	2040(vs), 2029(s), 2016(s), 1879(m)
$Co_4(CO)_9[P(OMe)_3](\mu_4\text{-}PPh)_2$[b]	2058(m), 2023(vs), 2008(s), 1850(m)
$Co_4(CO)_9[P(OEt)_3](\mu_4\text{-}PPh)_2$	2058(m), 2021(vs), 2016(s), 2005(s), 1995(s), 1987(m), 1871(m), 1856(m)
$Co_4(CO)_9(Ph_2PH)(\mu_4\text{-}PPh)_2$[b]	2058(m), 2023(vs), 2015(s), 2006(s), 1995(m), 1873(m), 1862(m)
$Co_4(CO)_9[P(O\text{-}i\text{-}Pr)_3](\mu_4\text{-}PPh)_2$	2059(m), 2022(vs), 2015(m), 2005(m), 1994(m), 1987(m), 1871(m), 1856(m)
$Co_4(CO)_9[P(n\text{-}Bu)_3](\mu_4\text{-}PPh)_2$	2055(m), 2017(vs), 2004(m), 1985(m), 1979(m), 1871(m), 1846(m)
$Co_4(CO)_9(PPh_3)(\mu_4\text{-}PPh)_2$	2056(m), 2023(vs), 2013(s), 2000(vs), 1987(m), 1870(m), 1846(m)
$Co_4(CO)_9[P(i\text{-}Pr)_3](\mu_4\text{-}PPh)_2$	2057(m), 2020(vs), 2014(s), 2004(s), 1990(s), 1973.9(m), 1870(m), 1840(m)
$Co_4(CO)_9(PCy_3)(\mu_4\text{-}PPh)_2$	2054(m), 2018(vs), 2012(s), 2000(m), 1988(m), 1973.3(m), 1869(m), 1837(m)

[a]Spectrum measured in cyclohexane solvent to within ±2 cm^{-1} unless otherwise noted. [b]In CH_2Cl_2 solvent.

excellent yields of pure product. To a solution of 1.0 g (2.7 mmol) of (1,5-cod)$PtCl_2$ in 100 ml of CH_2Cl_2, 1.5 g (2.7 mmol) of dppf [1,1'-bis(diphenylphosphino)ferrocene] was added under argon atmosphere. After the solution was stirred overnight at room temperature, the solvent was removed under reduced pressure and then the solid was washed with petroleum ether and dried under vacuum to yield the desired product without complicated purification procedures. The yield of (dppf)$PtCl_2$ is ≥ 95%.

3. $Fe_2(CO)_6(\mu_2\text{-}LiS)_2$[4]

A 250-mL Schlenk flask equipped with septum cap and a stir bar was charged with 0.2 g (0.58 mmol) of $Fe_2(CO)_6(\mu_2\text{-}S)_2$ under argon atmosphere. THF (75 ml) was added and the reaction solution was cooled to -78 °C (dry ice/acetone). By syringe, 1.22 ml of 1 M [Et_3BH][Li] in THF was added dropwise over a 5 minutes time period. At the midpoint of the addition the reaction solution turned from red to a dark emerald green; further addition of [Et_3BH][Li] caused no further change in color of the reaction solution. IR (THF, -70 °C) : ν(CO) 2037(m), 2030(m), 2002(vs) 1992(vs), 1955(vs), and 1942(s) cm^{-1}.

4. $Fe_2(CO)_6(\mu_3\text{-}S)_2Pt(1,5\text{-cod})$

To the dianion of $Fe_2(CO)_6(\mu_2\text{-}LiS)_2$ in THF at -78 °C was added 0.22 g (0.58 mmol) (1,5-cod)$PtCl_2$ against a counterflow of argon. After the reaction mixture had been

stirred for 1 hour at -78 °C, the reaction solution acquired a red color. The reaction mixture was allowed to warm to room temperature while being stirred for an additional 2 hours. TLC examination (50% CH_2Cl_2/petroleum ether) revealed the presence of a single product. The solvent was removed under vacuum, leaving a red solid which was chromatographed on silica gel using CH_2Cl_2. The red solid was recrystallized from CH_2Cl_2 to give 0.31 g (0.48 mmol, 83% yield) of $Fe_2(CO)_6(\mu_3\text{-}S)_2Pt(1,5\text{-cod})$. IR ($CH_2Cl_2$): ν(CO) 2058(s), 2018(vs), and 1977(s) cm^{-1}. Anal. Calcd. for $C_{14}H_{12}Fe_2O_6PtS_2$: C, 25.98; H, 1.87. Found: C, 26.03; H, 1.91.

5. $Fe_2(CO)_6(\mu_3\text{-}S)_2Pt(bpy)$

To the dianion of $Fe_2(CO)_6(\mu_2\text{-}LiS)_2$ in THF at -78 °C was added 0.25 g (0.58 mmol) $(bpy)PtCl_2$ against a counterflow of argon. However, after 2 hours at -78 °C no reaction had taken place as assessed by IR analysis. The reaction mixture was warmed to room temperature while being stirred for an additional 2 hours. At this time IR analysis revealed that the reaction had gone to completion. The solvent was removed under vacuum to afford a red solid which was subsequently chromatographed on silica gel using CH_2Cl_2. The red solid was recrystallized from CH_2Cl_2 to give 0.33 g (0.47 mmol, 82% yield) of $Fe_2(CO)_6(\mu_3\text{-}S)_2Pt(bpy)$. IR ($CH_2Cl_2$): ν(CO) 2051(s), 2011(vs), and 1969(s) cm^{-1}. Anal.

Calcd. for $C_{16}H_8Fe_2N_2O_6PtS_2$: C, 27.65; H, 1.16. Found: C, 27.49; H, 1.22.

6. $Fe_2(CO)_6(\mu_3\text{-}S)_2Pt(1,10\text{-phen})$

This compound was prepared in a manner exactly analogous to $Fe_2(CO)_6(\mu_3\text{-}S)_2Pt(bpy)$ and was isolated in 84% yield. IR (CH_2Cl_2): ν(CO) 2051(s), 2011(vs), and 1969(s) cm^{-1}. Anal. Calcd. for $C_{18}H_8Fe_2N_2O_6PtS_2 \cdot 1/6\ C_7H_8$: C, 31.03; H, 1.24. Found: C, 31.34 ; H, 1.28.

7. $Fe_2(CO)_6(\mu_3\text{-}S)_2Pt(diphos)$

This compound was prepared in a manner exactly analogous to $Fe_2(CO)_6(\mu_3\text{-}S)_2Pt(bpy)$ and was isolated in 94% yield. IR (CH_2Cl_2): ν(CO) 2049(s), 2008(vs), 1968(s), and 1962(s) cm^{-1}. Anal. Calcd. for $C_{32}H_{24}Fe_2O_6P_2PtS_2 \cdot 1/4\ C_7H_8$: C, 42.21; H, 2.73. Found: C, 42.18; H, 2.80.

8. $Fe_2(CO)_6(\mu_3\text{-}S)_2Pt(dppf)$

This compound was prepared in a manner exactly analogous to $Fe_2(CO)_6(\mu_3\text{-}S)_2Pt(bpy)$ and was isolated in 88% yield. IR (CH_2Cl_2): ν(CO) 2048(s), 2007(vs), and 1969(s) cm^{-1}. Anal. Calcd. for $C_{40}H_{28}Fe_3O_6PtS_2 \cdot CH_2Cl_2$: C, 41.79; H, 2.57. Found: C, 41.76; H, 2.63.

9. Reactions of $Fe_2(CO)_6(\mu_3\text{-}S)_2Pt(L\frown L)$ with Reducing Agents ($L\frown L$ = 1,5-cod, bpy, 1,10-phen)

Since all the reduction reactions were conducted under similar conditions, only the reaction between $Fe_2(CO)_6(\mu_3$-

$S)_2Pt(1,5\text{-cod})$ and [Li][Et_3BH] will be described in detail. To 25 mg (0.039 mmol) of $Fe_2(CO)_6(\mu_3\text{-}S)_2Pt(1,5\text{-cod})$ in 25 ml of THF at -78 °C was added 1.0 mole equiv of Super-hydride. The reaction was instantaneous as determined by low-temperature IR spectroscopy to give paramagnetic $[Fe_2(CO)_6(\mu_3\text{-}S)_2Pt(1,5\text{-cod})]^{-\bullet}$. IR (THF, -70 °C) : ν(CO) 2034(s), 1991(vs), 1949(s), 1942(s), and 1929(m) cm^{-1}.

10. Reactions of $Fe_2(CO)_6(\mu_3\text{-}S)_2Pt(L\frown L)$ with Oxidizing Agents ($L\frown L$ = 1,5-cod, bpy, 1,10-phen, diphos, dppf)

Since all the oxidation reactions were conducted under similar conditions, only the reaction between $Fe_2(CO)_6(\mu_3\text{-}S)_2Pt(1,5\text{-cod})$ and magic green will be described in detail. To 25 mg (0.039 mmol) of $Fe_2(CO)_6(\mu_3\text{-}S)_2Pt(1,5\text{-cod})$ in 25 ml of CH_2Cl_2 at -78 °C was added 32 mg (0.039 mmol) of magic green. The reaction giving paramagnetic $[Fe_2(CO)_6(\mu_3\text{-}S)_2Pt(1,5\text{-cod})]^{+\bullet}$ was observed to be instantaneous as judged by low-temperature IR spectroscopy. IR (THF, -70 °C) : ν(CO) 2122(s), 2106(s), 2096(vs), 2077(s), 2056(s), and 2040(m) cm^{-1}.

11. Preparation of ^{13}CO Enriched $FeCo_2(CO)_9(\mu_3\text{-}PPh)$

To 0.50 g (0.94 mmol) of $FeCo_2(CO)_9(\mu_3\text{-}PPh)$ in ~75 ml of benzene in a 500 ml Schlenk storage vessel was added ~1.0 atm of ^{13}CO. The solution was stirred at room temperature for 12 hrs and then at 50 °C for 3.0 hrs. IR analysis

revealed negligible ^{13}CO incorporation in $FeCo_2(CO)_9(\mu_3$-PPh). The flask was recharged with fresh ^{13}CO and irradiated for 6.0 hrs using a medium pressure Hg lamp. After the solution was cooled and vented, IR analysis indicated ~15-25% ^{13}CO enrichment had occurred. ^{13}CO enriched $FeCo_2(CO)_9(\mu_3$-PPh) was purified by column chromatography under argon using florisil as the chromatographic adsorbent and benzene as the eluant. Integration of the ^{13}C NMR resonance of the different carbonyl groups revealed that statistical ^{13}CO enrichment had occurred. Yield: 0.42 g (~84 %). ^{13}C NMR (-80 °C; toluene-d_8) δ: 218.7 (1C, axial FeCO), 211.6 (2 C, equatorial FeCO), 201.0 (6C, $Co(CO)_3$). ^{31}P NMR {-80 °C; THF/benzene-d_6 (5:1, v/v)} δ: 429.3.

12. Reactions of $FeCo_2(CO)_9(\mu_3$-PPh) with Reducing Agents

Since all the reduction reactions were conducted under similar conditions, only the reaction between $FeCo_2(CO)_9(\mu_3$-PPh) and $[Et_3BH][Li]$ will be described in detail. To 20 mg (0.037 mmol) of $FeCo_2(CO)_9(\mu_3$-PPh) in 25 ml of THF at -78 °C was added 0.037 ml (0.037 mmol) of 1.0 M $[Et_3BH][Li]$ solution. The reaction was instantaneous as judged by the immediate discharge of the red color of the solution and low-temperature IR analysis which revealed only the presence of $[FeCo_2(CO)_9(\mu_2$-PPhH)$^-]$. ^{31}P NMR {-78 °C; 2-MeTHF/benzene-

d_6 (4:1, v/v)} δ: 143.2. ^{13}C NMR {-90 °C; 2-MeTHF/benzene-d_6 (4:1, (v/v)} δ: 222.9 (1C, J_{P-C} = 18.5 Hz, axial FeCO), 221.8 (3C, anionic $Co(CO)_3$), 215.8 (1C, equatorial FeCO), 214.0 (1C, equatorial FeCO), 208.6 (3C, neutral $Co(CO)_3$).

13. Preparation of the Sealed NMR Tube Reactions

Starting material and solvent (0.7 mL for a 5 mm NMR tube or 3.5 mL for a 10 mm NMR tube) were transferred into the NMR tube under argon. After the tube was shaken well, the NMR tube and its contents were cooled to -78 °C and the desired reagent was added. The tube was then evacuated to ca. 10^{-4} mmHg prior to flame sealing.

D. Kinetic Studies

All kinetic reactions involving the tetracobalt cluster $Co_4(CO)_9(L)(\mu_4\text{-}PPh)_2$ were carried out in Schlenk tubes under argon and conducted under pseudo-first-order conditions, with ligand concentrations which were greater than 10 times that of the reactant cluster. All high pressure kinetic reactions were carried out in the sealed Fischer-Porter tubes at constant pressure. The reactions were monitored for a minimum of two to three half-lives by following the IR absorbance of the highest energy ν(CO) band of the starting cluster. Plots of ln A_t vs. time gave the pseudo-first-order rate constants, k_{obsd}. Plots of k_{obsd} vs. the ligand concentration afforded the ligand-independent and ligand-dependent rate constants k_1 and k_2, respectively. The

activation parameters ($\Delta H^{\ddagger}$ and $\Delta S^{\ddagger}$) were determined by using the Eyring equation.[20] Error limits were calculated by using the available least-squares regression program.[21]

E. IR Band-Shape Analysis

Since the acid and ester carbonyl stretching bands of $[FeCo_2(CO)_8(CO_2H)(\mu_3\text{-}PPh)^-]$ and $[FeCo_2(CO)_8\{C(O))Me\}(\mu_3\text{-}PPh)^-]$ exhibit substantial overlap, the infrared band shapes of these CO bands were calculated using a numerical procedure in order to determine the ratio of their areas. Absorbances were digitized from 1670 cm^{-1} to 1560 cm^{-1} at 1 cm^{-1} intervals and entered into files of the university VAX 11/85 computer. Following baseline correction, the spectra were fit by a model consisting of Lorentzian bandshapes, each characterized by a peak frequency (ν), maximum intensity (I), and full width at half maximum (fwhm) (Δ). Since the instrument resolution (2 cm^{-1}) is far less than the observed bandwidths (~20 cm^{-1}), it was unnecessary to convolute the model spectrum with a resolution (slit) function. The parameters were varied to minimize the squared deviation between the experimental and calculated intensities using a non-linear regression procedure.[22] Given that the area of a Lorentzian peak is proportional to the product of the bandwidth and the maximum intensity, the area ratio of the different anionic clusters is calculated easily as $A_2/A_1 = (I_2 \cdot \Delta_2)/(I_1 \cdot \Delta_1)$. The same procedure

was also used in the area calculation of $[FeCo_2(CO)_8(COMe)(\mu_3\text{-}PPh)^-]$ and $[FeCo_2(CO)_8(COMe)(\mu_3\text{-}PPh)][Li]$.

F. X-Ray Crystallography

1. $Co_4(CO)_9(PCy_3)(\mu_4\text{-}PPh)_2$

Dark red single crystals of $Co_4(CO)_9(PCy_3)(\mu_4\text{-}PPh)_2$ were grown from a 1:1 toluene/heptane solution. A crystal of dimensions 0.15 x 0.28 x 0.35 mm was mounted on a Nicolet R3M/μ update of a $P2_1$ diffractometer. Cell constants were obtained from a least-squares refinement of 25 reflections in the range $38.64^\circ \leq 2\theta \leq 44.96^\circ$. Laue symmetry and statistics were consistent with space group $P2_1$. Intensity data in the range $3^\circ \leq 2\theta \leq 45^\circ$ were collected at 295 K in the ω-scan mode using a variable scan speed and graphite-monochromated Mo-K radiation (λ=0.71073). The angles were measured by a centering routine. Data collection required the use of a second reference reflection along with the 15 reflections from the automatic centering routine. Lorentz-polarization corrections and a ψ-scan based empirical absorption correction were applied (transmission factors 0.660 to 0.787). The structure was solved by direct methods and refined by a block-cascade least-squares technique. All hydrogen atoms were located in the difference map and refined with isotropic thermal parameters. The structure contained a molecule of toluene which was lost during data

collection, leading to a number of disordered solvent peaks in the difference Fourier maps. Seven of the largest peaks were refined, but no attempt was made to connect them into or restrain them as toluene molecules. Final R=0.044, wR=0.059 for 504 parameters and 2976 reflections (R=0.0517, wR=0.0609 for all data).

2. $Fe_2(CO)_6(\mu_3\text{-}S)_2Pt(1,5\text{-cod})$

Dark red single crystals of $Fe_2(CO)_6(\mu_3\text{-}S)_2Pt(1,5\text{-cod})$ were grown from CH_2Cl_2. A crystal of dimensions 0.23 x 0.35 x 0.38 mm was mounted on a Nicolet R3M/μ update of a P 1 diffractometer. Cell constants were obtained from a least-squares refinement of 25 reflections in the range $25.49^\circ \leq 2\theta \leq 34.88^\circ$. Laue symmetry and statistics were consistent with space group P 1. Intensity data in the range $3^\circ \leq 2\theta \leq 50^\circ$ were collected at 295 K in the ω-scan mode using a variable scan speed and graphite-monochromated Mo-K radiation (λ=0.71073). The angles were measured by a centering routine. Lorentz-polarization corrections and a ψ-scan based empirical absorption correction were applied (transmission factors 0.734 to 0.341). The structure was solved by direct methods and refined by a block-cascade least-squares technique. All hydrogen atoms were located in the difference map and refined with isotropic thermal parameters. Final R=0.0484, wR=0.0641 for 227 parameters and 3017 reflections (R=0.0495, wR=0.0646 for all data).

3. $Fe_2(CO)_6(\mu_3\text{-}S)_2Pt(1,10\text{-phen})$

Dark red single crystals of $Fe_2(CO)_6(\mu_3\text{-}S)_2Pt(1,10\text{-phen})$ were grown from CH_2Cl_2. A crystal of dimensions 0.05 x 0.15 x 0.38 mm was mounted on a Nicolet R3M/μ update of a P 1 diffractometer. Cell constants were obtained from a least-squares refinement of 25 reflections in the range $25.05^\circ \leq 2\theta \leq 29.08^\circ$. Laue symmetry and statistics were consistent with space group P 1. Intensity data in the range $3^\circ \leq 2\theta \leq 50^\circ$ were collected at 295 K in the ω-scan mode using a variable scan speed and graphite-monochromated Mo-K radiation (λ=0.71073). The angles were measured by a centering routine. Lorentz-polarization corrections and a ψ-scan based empirical absorption correction were applied (transmission factors 1.000 to 0.417). The structure was solved by direct methods and refined by a block-cascade least-squares technique. All hydrogen atoms were located in the difference map and refined with isotropic thermal parameters. Final R=0.0356, wR=0.0381 for 280 parameters and 3257 reflections (R=0.0416, wR=0.0388 for all data).

CHAPTER REFERENCES

1. Richmond, M. G.; Kochi, J. K. Inorg. Chem. **1986**, 25, 656.

2. Kuivila, H. G.; Beumel Jr, O. F. J. Am. Chem. Soc. **1961**, 83, 1246.

3. Bianco, V. D.; Doronzo, S. Inorg. Synth. **1976**, 13, 161.

4. Seyferth, D.; Henderson, R. S.; Song, L. C. Organometallics **1982**, 1, 125.

5. Drew, D.; Doyle, J. R. Inorg. Synth. **1973**, 13, 48.

6. Watt, G. W.; Cuddeback, J. E. J. Inorg. Nucl. Chem. **1971**, 33, 259.

7. (a) Richter, F.; Beurich, H.; Vahrenkamp, H. J. Organomet. Chem. **1979**, 166, C5. (b) Muller, M.; Vahrenkamp, H. Chem. Ber. **1983**, 116, 2311.

8. DeSimone, R. E.; Drago, R. S. J. Am. Chem. Soc. **1970**, 92, 2343.

9. Schmidt, W; Steckhan, E. Chem. Ber. **1980**, 113, 577.

10. Ahmed, M. G.; Alder, R. W.; James, G. H.; Sinnott, M. L.; Whiting, M. C. J. Chem. Soc., Chem. Commun. **1968**, 1523.

11. Eisch, J. J.; King, R. B. "Organometallic Syntheses", Academic Press: New York, **1965**, pp. 70-71.

12. Fieser, L. F.; Fieser, M. "Reagents for Organic Synthesis", Wiley: New York, **1967**, Vol 1.

13. Hendrickson, D. N.; Sohn, Y. S.; Gray, H. B. Inorg. Chem. **1971**, 10, 1559.

14. Gansow, O. A.; Burke, A. R.; LaMar, G. N. J. Chem. Soc., Chem. Commun. **1972**, 456.

15. Kofron, W. G.; Backlawski, L. M. J. Org. Chem. **1976**, 41, 1879.

16. Shriver, D. F. "The Manipulation of Air-Sensitive Compounds", McGraw-Hill: New York, **1969**.

17. Richmond, M. G.; Kochi, J. K. Inorg. Chem. **1986**, 25, 1334.

18. Ryan, R. C.; Pittman, Jr. C. U.; O'Connor, J. P.; Dahl, L. F. J. Organomat. Chem. **1980**, 193, 247.

19. Whitesides, G. M.; Goach, J. F.; Stedronsky, E. R. J. Am. Chem. Soc. **1972**, 94, 5258.

20. Drenth, W.; Kwart, H. "Kinetics Applied to Organic Reactions", Marcel Dekker: New York, **1980**.

21. Gordon, A. J.; Ford, R. A. "The Chemist's Companion. A Handbook of Practical Data, Techniques, and References", Wiley: New york, **1976**.

22. Program STEPT: Chandler, J. P., Oklahoma State University. Quantum Chemistry Exchange Program, No. 307.

CHAPTER III

RESULTS

A. Kinetics of Ligand Substitution of the Tetracobalt Clusters by Phosphine and Phosphite Ligands

In the reactions of $Co_4(CO)_{10}(\mu_4\text{-}PPh_2)$ [1] with $P(OMe)_3$, $P(OEt)_3$, PPh_2H, $P(O\text{-}i\text{-}Pr)_3$, $P(n\text{-}Bu)_3$, PPh_3, $P(i\text{-}Pr)_3$, and PCy_3, under pseudo-first order conditions, plots of ln A_t vs. time were linear for a mininum of 2-3 half-lives, as demonstrated in Figure 3. The pseudo-first-order rate constants, k_{obsd}, obtained from such plots at various temperatures and ligand concentrations investigated are summarized in Table 3 to Table 9. The infrared spectral changes for a typical reaction that leads to the production of the mono-substituted cluster $Co_4(CO)_9(L)(\mu_4\text{-}PPh)_2$ (L = Ph_2PH) are shown in Figure 4. Clearly visible are the isosbestic points at 2051, 2025, 2017, 2008, and 1862 cm^{-1}, which confirm the equilibrium nature of the substitution reaction. A plot of the various k_{obsd} values as a function of ligand concentration was linear with a nonzero intercept as shown in Figure 5 [$P(OEt)_3$] and Figure 6 (PPh_3), from which the ligand-independent and ligand-dependent rate constants k_1 and k_2, respectively, are readily obtained (Tables 10-16). The calculated ligand-independent and

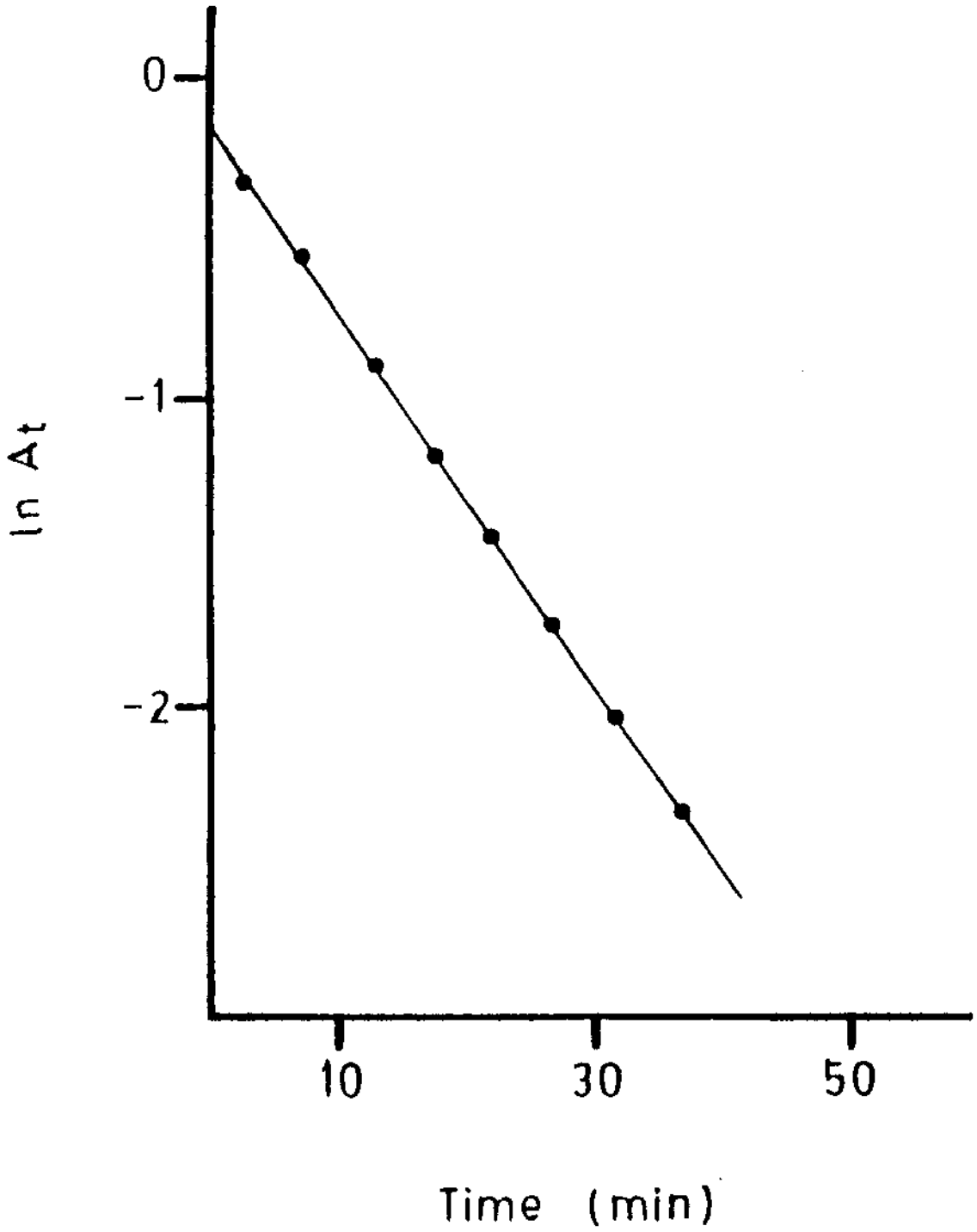

Figure 3. Plot of ln A_t vs. time from reaction of $Co_4(CO)_{10}(\mu_4\text{-}PPh)_2$ with Ph_2PH at 25.5 °C in toluene

Table 3. Experimental Rate Constants for the (Mono) Ligand Substitution of $Co_4(CO)_{10}(\mu_4\text{-}PPh)_2$ with Triethyl Phosphite.[a]

entry no.	temp,°C	$10^2[P(OEt)_3]$,M	10^5k_{obsd},s^{-1} [b]
1	15.0	21.0	12.8 ± 0.2
2	15.0	33.8	18 ± 1
3	15.0	50.2	24.9 ± 0.4
4	15.0	68.8	33 ± 1
5	26.2	15.2	31 ± 1
6	26.2	15.2	32 ± 1[c]
7	26.2	15.2	31 ± 1[d]
8	26.2	15.2	30 ± 1[e]
9	26.2	23.3	42 ± 1
10	26.2	32.8	57 ± 2
11	26.2	32.8	61 ± 2[f]
12	26.2	43.2	72 ± 2
13	30.0	12.8	40 ± 1
14	30.0	19.8	56 ± 2
15	30.0	32.8	87 ± 3
16	30.0	45.1	113 ± 4
17	42.6	8.2	94 ± 4
18	42.6	16.3	147 ± 6
19	42.6	28.0	227 ± 13
20	42.6	37.3	300 ± 10

Table 3. continued

[a]From 8.2×10-3 M $Co_4(CO)_{10}(\mu_4\text{-}PPh)_2$ in toluene by following the disappearance of the 2040 cm^{-1} IR band. All kinetic data quoted represent single experimental runs that have been appropriately rounded off. [b]Error limits at 95% confidence limit. [c]In the presence of 15psi of CO. [d]In the presence of 30psi of CO. [e]In the presence of 100psi of CO. [f]In the presence of 0.04M of tri-n-butyltin hydride.

Table 4. Experimental Rate Constants for the (Mono) Ligand Sbstitution of $Co_4(CO)_{10}(\mu_4\text{-}PPh)_2$ with Triisopropyl Phosphite.[a]

entry no.	temp,°C	$10^2[P(O\text{-}i\text{-}pr)_3]$,M	10^5k_{obsd},s^{-1} [b]
1	22.4	16.3	12.3 ± 0.4
2	22.4	32.7	20.2 ± 0.2
3	22.4	49.0	28 ± 1
4	35.2	16.3	43 ± 1
5	35.2	25.0	58 ± 1
6	35.2	36.5	76 ± 3
7	45.4	12.5	85 ± 1
8	45.4	20.2	116 ± 2
9	45.4	32.7	169 ± 4

[a]From 8.2×10^{-3} M $Co_4(CO)_{10}(\mu_4\text{-}PPh)_2$ in toluene by following the disappearance of the 2040 cm^{-1} IR band. All kinetic data quoted represent single experimental runs that have been appropriately rounded off. [b]Error limits at 95% confidence limit.

Table 5. Experimental Rate Constants for the (Mono) Ligand Substitution of $Co_4(CO)_{10}(\mu_4\text{-}PPh)_2$ with Diphenyl Phosphine.[a]

entry no.	temp,°C	$10^2[Ph_2PH]$,M	10^5k_{obsd},s^{-1} [b]
1	19.6	8.6	25 ± 1
2	19.6	16.1	34 ± 1
3	19.6	24.7	45 ± 2
4	25.5	8.6	42 ± 1
5	25.5	16.1	62 ± 2
6	25.5	16.1	68 ± 1[c]
7	25.5	16.1	68 ± 1[d]
8	25.5	32.2	102 ± 3
9	32.3	8.6	77 ± 2
10	32.3	16.1	113 ± 2
11	32.3	28.0	171 ± 5
12	32.3	32.2	195 ± 8
13	40.8	16.1	234 ± 8
14	40.8	22.6	306 ± 4
15	40.8	29.0	369 ± 12

[a]From 8.2×10^{-3} M $Co_4(CO)_{10}(\mu_4\text{-}PPh)_2$ in toluene by following the disappearance of the 2040 cm^{-1} IR band. All kinetic data quoted represent single experimental runs that have been appropriately rounded off. [b]Error limits at 95% confidence limit. [c]In the presence of 0.04 M tri-n-butyltin hydride. [d]In the presence of 1 atm of CO.

Table 6. Experimental Rate Constants for the (Mono) Ligand Substitution of $Co_4(CO)_{10}(\mu_4\text{-}PPh)_2$ with Tri-n-butyl Phosphine.[a]

entry no.	temp,°C	$10^2[P(n\text{-}Bu)_3]$,M	10^5k_{obsd},s^{-1} [b]
1	15.0	10.4	15.6 ± 0.2
2	15.0	20.5	24 ± 1
3	15.0	36.9	41 ± 1
4	26.0	12.4	48 ± 1
5	26.0	20.5	72 ± 1
6	26.0	28.5	97 ± 2
7	35.0	6.0	70 ± 1
8	35.0	14.5	118 ± 3
9	35.0	20.5	164 ± 4
10	35.0	26.5	198 ± 7
11	42.7	4.0	113 ± 2
12	42.7	10.4	185 ± 3
13	42.7	18.5	278 ± 13

[a]From 8.2×10^{-3} M $Co_4(CO)_{10}(\mu_4\text{-}PPh)_2$ in toluene by following the disappearance of the 2040 cm^{-1} IR band. All kinetic data quoted represent single experimental runs that have been appropriately rounded off. [b]Error limits at 95% confidence limit.

Table 7. Experimental Rate Constants for the (Mono) Ligand Substitution of $Co_4(CO)_{10}(\mu_4\text{-}PPh)_2$ with Triphenyl Phosphine.[a]

entry no.	temp,°C	$10^2[PPh_3]$,M	10^5k_{obsd},s^{-1} [b]
1	42.2	8.2	1.2 ± 0.1
2	42.2	20.5	3.0 ± 0.1
3	42.2	32.8	4.7 ± 0.1
4	42.2	45.1	6.3 ± 0.2
5	42.2	57.4	8.1 ± 0.2
6	50.9	8.0	2.7 ± 0.1
7	50.9	20.5	6.6 ± 0.2
8	50.9	32.8	10.3 ± 0.4
9	50.9	45.1	13.9 ± 0.1
10	59.8	16.4	11.9 ± 0.3
11	59.8	16.4	9 ± 1[c]
12	59.8	28.7	20 ± 1
13	59.8	28.7	14 ± 1[c]
14	59.8	36.9	24.7 ± 0.3
15	59.8	36.9	20 ± 1[c]
16	59.8	45.1	30.0 ± 0.4
17	59.8	45.1	29 ± 1[d]
18	59.8	45.1	30 ± 2[e]
19	59.8	45.1	22 ± 1[c]
20	65.6	8.2	12.2 ± 0.1
22	65.6	16.4	21.7 ± 0.3

Table 7. continued

23	65.6	28.7	34.2 ± 0.4
24	65.6	41.0	47 ± 1
25	70.5	20.5	40 ± 1
26	70.5	28.7	52 ± 1
27	70.5	36.9	65 ± 1
28	70.5	45.1	78 ± 2
29	75.5	6.6	32.5 ± 0.4
30	75.5	12.3	47 ± 1
31	75.5	18.0	61 ± 1
32	75.5	24.6	75 ± 1

[a]From 8.2×10^{-3} M $Co_4(CO)_{10}(\mu_4\text{-PPh})_2$ in toluene by following the disappearance of the 2040 cm^{-1} IR band. All kinetic data quoted represent single experimental runs that have been appropriately rounded off. [b]Error limits at 95% confidence limit. [c]In the presence of 100psi of CO. [d]In the presence of 1 atm of CO. [e]In the presence of 0.04 M tri-n-butyltin hydride.

Table 8. Experimental Rate Constants for the (Mono) Ligand Substitution of $Co_4(CO)_{10}(\mu_4\text{-}PPh)_2$ with Triisopropyl Phosphine.[a]

entry no.	temp,°C	$10^2[P(i\text{-}Pr)_3]$,M	10^5k_{obsd},s^{-1} [b]
1	53.8	25.0	6 ± 1
2	53.8	32.5	8 ± 1
3	53.8	41.3	9 ± 1
4	53.8	50.0	11 ± 1
5	60.1	12.5	7 ± 1
6	60.1	25.0	12 ± 1
7	60.1	32.5	15 ± 1
8	60.1	43.8	19 ± 2
9	65.7	17.5	15 ± 1
10	65.7	23.8	19 ± 2
11	65.7	32.5	24 ± 2
12	65.7	41.3	30 ± 1
13	75.2	8.3	26 ± 1
14	75.2	16.4	34 ± 3
15	75.2	25.0	44 ± 5
16	75.2	32.5	53 ± 4

[a]From 8.2×10^{-3} M $Co_4(CO)_{10}(\mu_4\text{-}PPh)_2$ in toluene by following the disappearance of the 2040 cm^{-1} IR band. All kinetic data quoted represent single experimental runs that have been appropriately rounded off. [b]Error limits at 95% confidence limit.

Table 9. Experimental Rate Constants for the (Mono) Ligand Substitution of $Co_4(CO)_{10}(\mu_4\text{-}PPh)_2$ with Tricyclohexyl Phosphine.[a]

entry no.	temp,°C	$10^2[PCy_3]$,M	10^5k_{obsd},s^{-1} [b]
1	55.0	11.7	1.4 ± 0.1
2	55.0	15.0	1.7 ± 0.1
3	55.0	18.3	1.9 ± 0.1
4	55.0	21.4	2.0 ± 0.1
5	55.0	25.1	2.2 ± 0.1
6	65.2	11.7	5.3 ± 0.1
7	65.2	15.0	5.8 ± 0.1
8	65.2	19.4	6.3 ± 0.1
9	65.2	21.4	6.6 ± 0.1
10	72.7	16.4	16.8 ± 0.4
11	72.7	32.8	21 ± 1
12	72.7	41.0	22 ± 1

[a]From 8.2×10^{-3} M $Co_4(CO)_{10}(\mu_4\text{-}PPh)_2$ in toluene by following the disappearance of the 2040 cm^{-1} IR band. All kinetic data quoted represent single experimental runs that have been appropriately rounded off. [b]Error limits at 95% confidence limit.

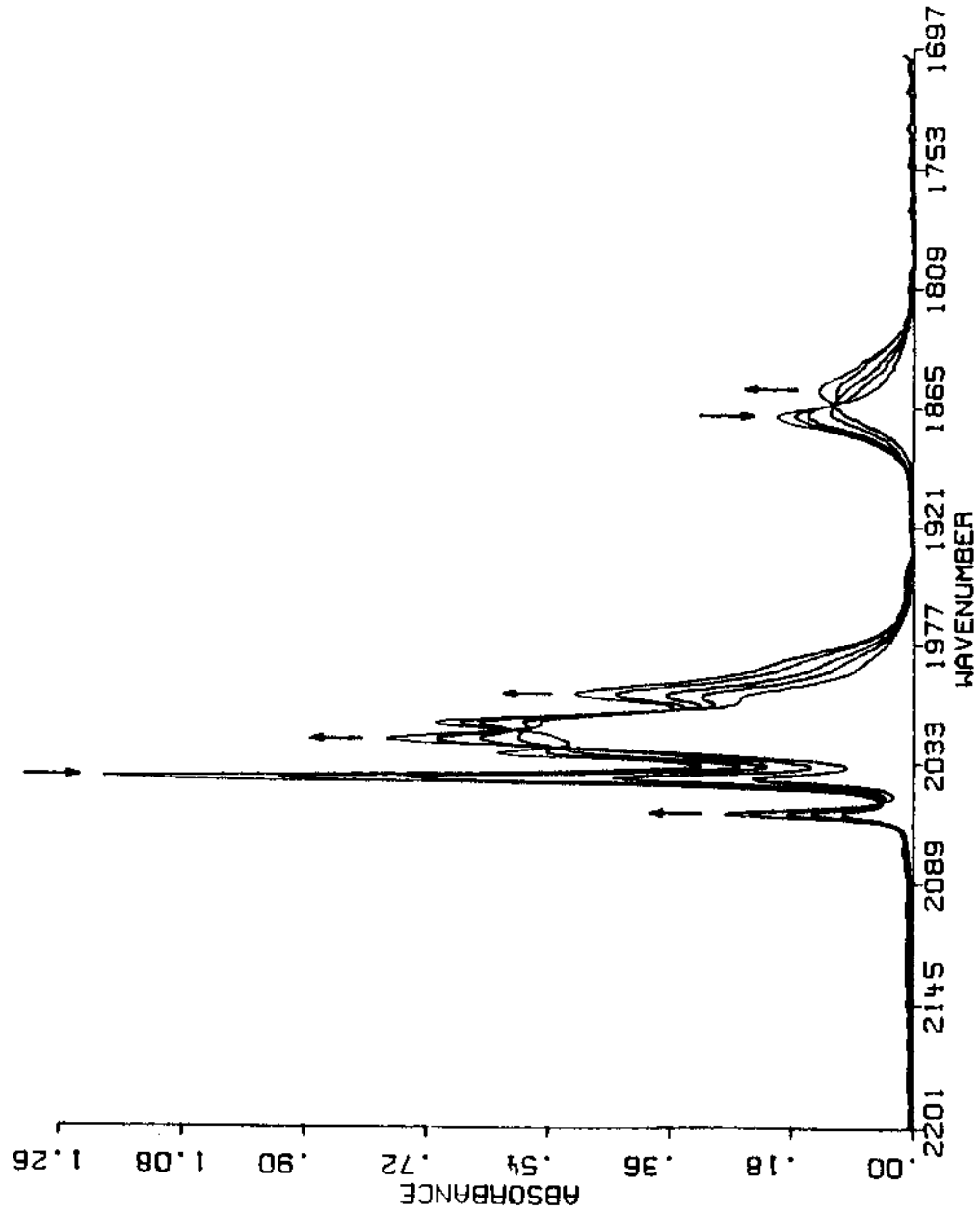

Figure 4. Typical infrared spectral changes accompanying the ligand substitution of $Co_4(CO)_{10}(\mu_4\text{-}PPh)_2$ with Ph_2PH to afford $Co_4(CO)_9(Ph_2PH)(\mu_4\text{-}PPh)_2$

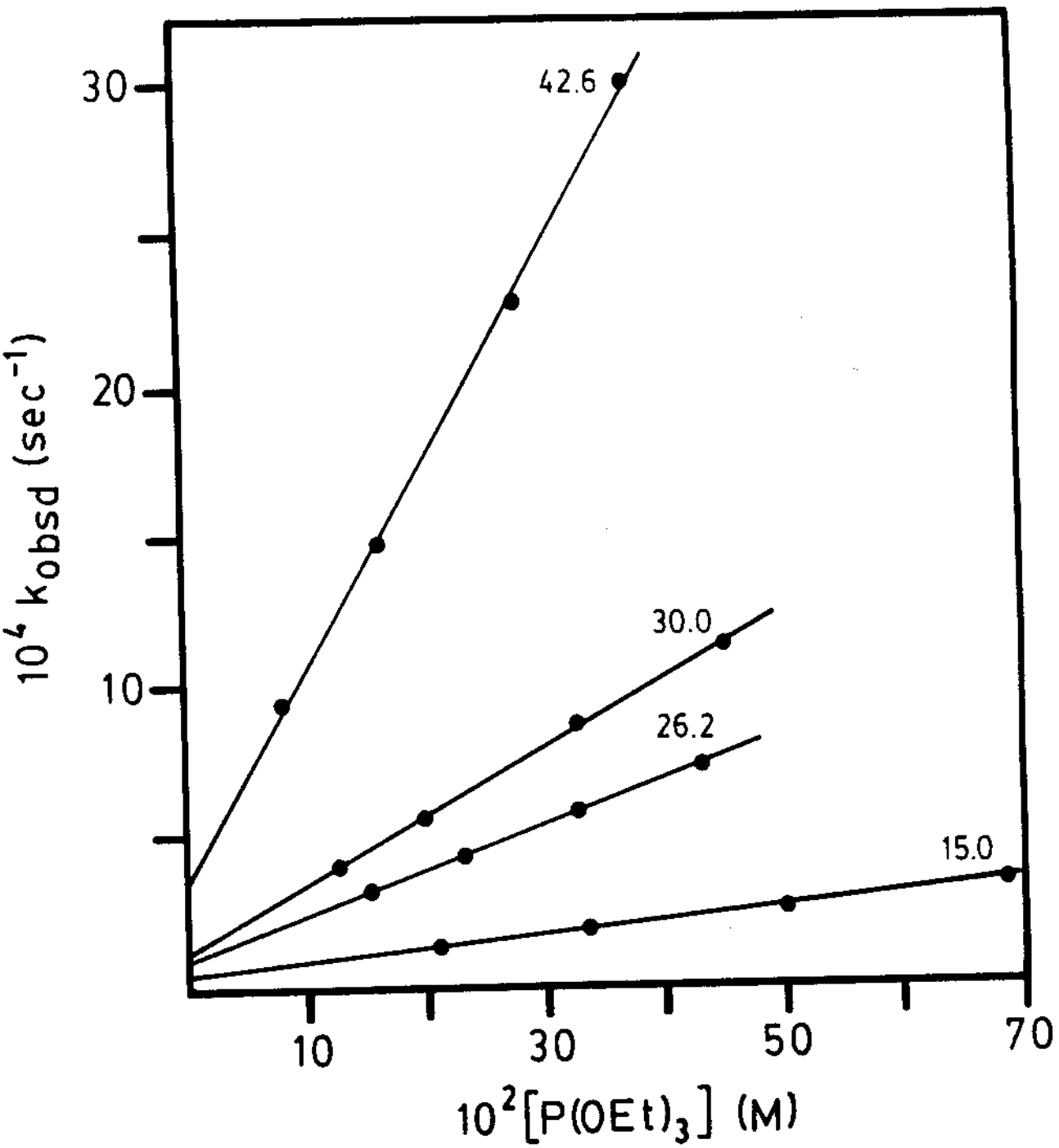

Figure 5. Plot of k_{obsd} vs. $P(OEt)_3$ concentration for the reaction of $Co_4(CO)_{10}(\mu_4\text{-}PPh)_2$ with $P(OEt)_3$ at various temperatures, as indicated

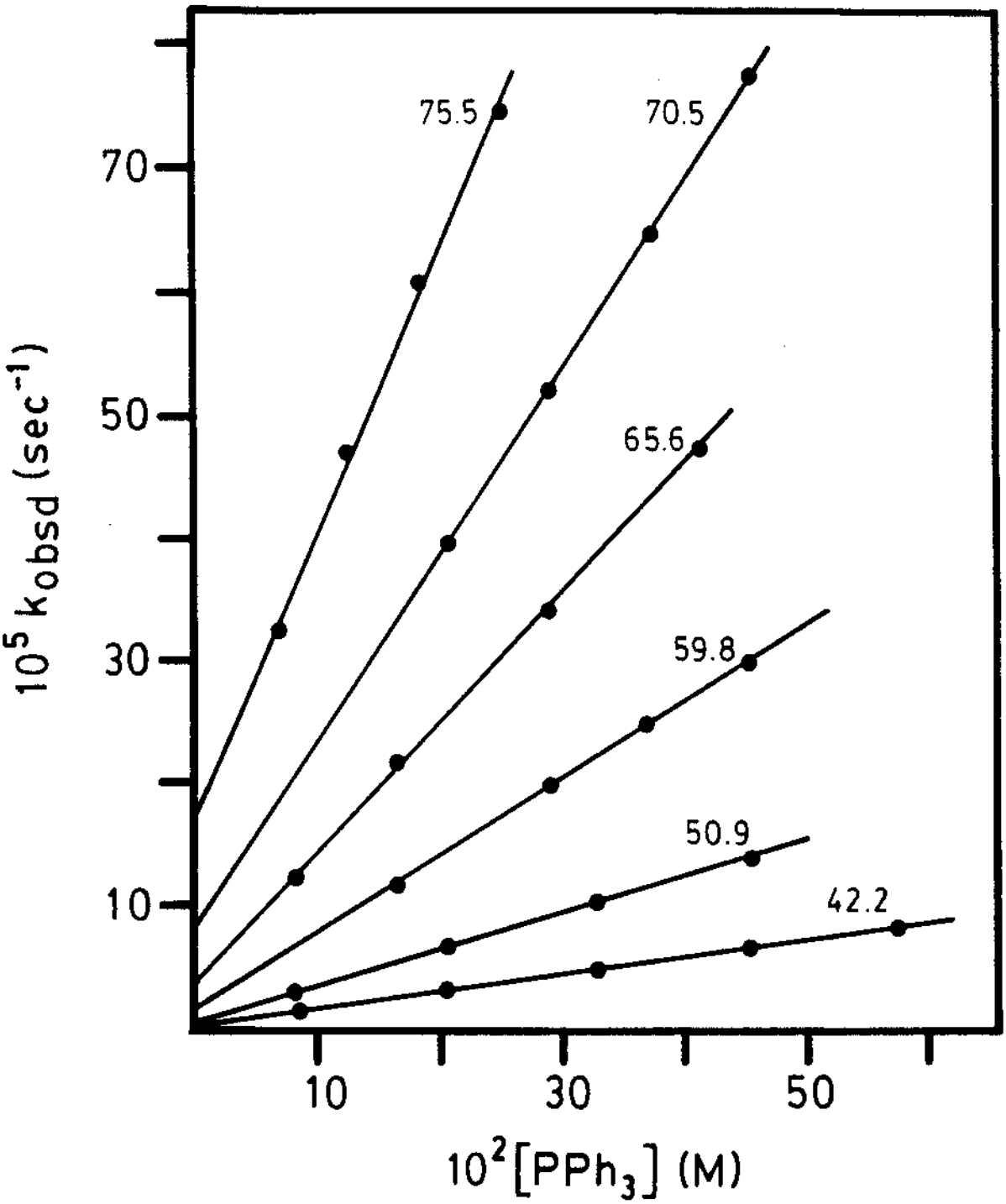

Figure 6. Plot of k_{obsd} vs. PPh_3 concentration for the reaction of $Co_4(CO)_{10}(\mu_4\text{-}PPh)_2$ with PPh_3 at various temperatures, as indicated

Table 10. Ligand-Independent and Ligand-Dependent Rate Constant for the Ligand Substitution of $Co_4(CO)_{10}(\mu_4\text{-}PPh)_2$ with Triethyl Phosphite.[a]

temp,°C	$10^5k_1,s^{-1}$	$10^4k_2,M^{-1}s^{-1}$
15.0	4 ± 1	4.3 ± 0.2
26.2	8 ± 3	15 ± 1
30.0	11 ± 5	23 ± 1
42.6	34 ± 15	71 ± 6

[a]The quoted rate constants have been appropriately rounded off. Error limits at the 95% confidence level.

Table 11. Ligand-Independent and Ligand-Dependent Rate Constant for the Ligand Substitution of $Co_4(CO)_{10}(PPh)_2$ with Triisopropyl Phosphite.[a]

temp,°C	$10^5k_1,s^{-1}$	$10^4k_2,M^{-1}s^{-1}$
22.4	5 ± 1	4.7 ± 0.3
35.2	16 ± 3	17 ± 1
45.4	32 ± 4	42 ± 2

[a]The quoted rate constants have been appropriately rounded off. Error limits at the 95% confidence level.

Table 12. Ligand-Independent and Ligand-Dependent Rate Constant for the Ligand Substitution of $Co_4(CO)_{10}(PPh)_2$ with Diphenyl Phosphine.[a]

temp,°C	$10^5k_1, s^{-1}$	$10^4k_2, M^{-1}s^{-1}$
19.6	15.1 ± 0.3	12 ± 2
25.5	21 ± 2	25 ± 10
32.3	34 ± 5	49 ± 2
40.8	65 ± 26	105 ± 11

[a]The quoted rate constants have been appropriately rounded off. Error limits at the 95% confidence level.

Table 13. Ligand-Independent and Ligand-Dependent Rate Constant for the Ligand Substitution of $Co_4(CO)_{10}(PPh)_2$ with Tri-n-butyl Phosphine.[a]

temp,°C	$10^5k_1,s^{-1}$	$10^4k_2,M^{-1}s^{-1}$
15.0	5 ± 3	10 ± 1
26.0	11 ± 4	30 ± 2
35.0	31 ± 12	63 ± 7
42.7	66 ± 4	115 ± 3

[a]The quoted rate constants have been appropriately rounded off. Error limits at the 95% confidence level.

Table 14. Ligand-Independent and Ligand-Dependent Rate Constant for the Ligand Substitution of $Co_4(CO)_{10}(PPh)_2$ with Triphenyl Phosphine.[a]

temp,°C	$10^5k_1,s^{-1}$	$10^4k_2,M^{-1}s^{-1}$
42.2	0.08 ± 0.08	1.4 ± 0.2
50.9	0.3 ± 0.3	3 ± 1
59.8	2 ± 1	6 ± 3
65.6	4 ± 1	11 ± 1
70.5	8 ± 2	15.4 ± 0.4
75.5	18 ± 4	23 ± 2

[a]The quoted rate constants have been appropriately rounded off. Error limits at the 95% confidence level.

Table 15. Ligand-Independent and Ligand-Dependent Rate Constant for the Ligand Substitution of $Co_4(CO)_{10}(PPh)_2$ with Triisopropyl Phosphine.[a]

temp,°C	$10^5k_1,s^{-1}$	$10^4k_2,M^{-1}s^{-1}$
53.8	1 ± 1	2.1 ± 0.2
60.1	2 ± 1	4.0 ± 0.3
65.7	4 ± 1	6.2 ± 0.3
75.2	16 ± 2	11 ± 1

[a]The quoted rate constants have been appropriately rounded off. Error limits at the 95% confidence level.

Table 16. Ligand-Independent and Ligand-Dependent Rate Constant for the Ligand Substitution of $Co_4(CO)_{10}(PPh)_2$ with Tricyclohexyl Phosphine.[a]

temp,°C	$10^5k_1,s^{-1}$	$10^4k_2,M^{-1}s^{-1}$
55.0	0.8 ± 0.2	0.6 ± 0.1
65.2	3.9 ± 0.3	1.3 ± 0.2
72.7	13.1 ± 0.4	2.2 ± 0.1

[a]The quoted rate constants have been appropriately rounded off. Error limits at the 95% confidence level.

ligand-dependent rate constants from the experimental rate data have been extrapolated to 40 °C for comparative purposes and are listed in Table 17. The activation parameters for the kinetic reactions with these ligands are also listed in Table 17.

The effect of tri-n-butyltin hydride on the substitution rate k_{obsd} was next examined because **1** is known to undergo facile electron-transfer-chain (ETC) catalyzed ligand substitution.[1,2] This additive was chosen due to its ability to function as an efficient inhibitor of free-radical-chain processes involving metal carbonyls.[3] Furthermore, tri-n-butyltin hydride effectively terminates the ETC catalyzed substitution pathway in **1**.[1] Since there is no obvious decrease in the observed rate constant in the presence of added tri-n-butyltin hydride (entry 11, Table 3; entry 6, Table 5; entry 18, Table 7), it may be safely concluded that the substitution reaction proceeds via a thermal process devoid of radical-chain character. The possible inhibitory effect of CO on the reaction rate was also investigated. Entry 7 (Table 5) and entry 17 (Table 7) show that the pseudo-first-order rate constant remains essentially unaffected in the presence 1 atm of CO. Entry 8 (table 3) also reveals that the pseudo-first-order rate constant is essentially unaffected in the presence 100 psi of CO. However, entries 11, 13, 15, 19 (Table 7) reveal that the pseudo-first-order rate constant is retarded in the

Table 17. Ligand-Independent and Ligand-Dependent Rate Constants and Activation Parameters for $Co_4(CO)_{10}(\mu_4\text{-}PPh)_2$ + Ligand

Ligand	ligand-independent[a]			ligand-dependent		
	k_1[b]	$\Delta H^{\ddagger}$	$\Delta S^{\ddagger}$	k_2[c]	$\Delta H^{\ddagger}$	$\Delta S^{\ddagger}$
$P(OMe)_3$	6.8	15.0±3.0	-25.0±10.0	9.2	19.1±4.6	-8.7±1.5
$P(OEt)_3$	5.8	14.7±1.8	-28.1±6.1	15.5	18.7±0.8	-9.2±2.5
$P(O\text{-}i\text{-}Pr)_3$	4.7	15.4±2.1	-26.0±6.8	6.2	17.8±0.1	-13.5±0.1
Ph_2PH	11.2	12.6±1.1	-33.1±3.7	26.5	18.4±0.9	-8.9±2.9
$P(n\text{-}Bu)_3$	11.5	17.2±2.6	-18.7±8.4	22.2	16.5±0.5	-15.2±1.8
PPh_3	0.03	35.5±0.6	26.1±1.8	2.7	18.5±0.4	-17.8±1.3
$P(i\text{-}Pr)_3$	0.03	34.3±0.8	22.4±2.5	1.6	17.5±2.3	-21.9±6.8
PCy_3	0.03	36.4±0.7	28.8±2.0	0.4	16.7±0.5	-27.3±1.4

[a]Calculated from the experimental rate data extrapolated to 50°C. The quoted activation parameters have been appropriately rounded off and are reported at the 95% confidence limit. $\Delta H^{\ddagger}$ values are in kcal mol^{-1} and $\Delta S^{\ddagger}$ in eu. [b]10^4 s^{-1}. [c]10^3 $M^{-1}s^{-1}$

presence of 100 psi of CO.

B. X-Ray Crystallographic Structure of $Co_4(CO)_9(PCy_3)(\mu_4$-PPh)$_2$

Single crystals of $Co_4(CO)_9(PCy_3)(\mu_4$-PPh)$_2$ were successfully grown, and subjected to X-ray diffraction analysis in order to probe for unusual cluster/ligand interactions. The X-ray crystallographic data for $Co_4(CO)_9(PCy_3)(\mu_4$-PPh)$_2$ are summarized in Table 18. The final fractional coordinates are listed in Table 19, while the molecular configuration and the numbering scheme of $Co_4(CO)_9(PCy_3)(\mu_4$-PPh)$_2$ is presented in the ORTEP diagram in Figure 7. The structure of $Co_4(CO)_9(PCy_3)(\mu_4$-PPh)$_2$ consists of four Co atoms in a planar, rectangular array and is capped by a pair of μ_4-phenylphosphinidene groups to give a closo octahedral Co_4P_2 core commonly observed in this genre of cluster. Selected bond distances and bond angles for $Co_4(CO)_9(PCy_3)(\mu_4$-PPh)$_2$ are presented in Table 20 and Table 21, respectively.

C. Synthesis of $Fe_2(CO)_6(\mu_3$-S)$_2$Pt(L^L) (where L^L = 1,5- cod, bpy, 1,10-phen, diphos, dppf)

The addition of 2 mol equiv of [BEt3H][Li] ("Super-Hydride") to a THF solution of Fe2(CO)6(μ-S)2 [**2**] at -78 °C produced dianion [Fe2(CO)6(μ-S)2]2- in essentially quantitative yield. The reaction of $[Fe_2(CO)_6(\mu$-S)$_2]^{2-}$ with various (L^L)$PtCl_2$ complexes (where L^L = 1,5-

Table 18. X-ray Crystallographic Collection and Processing Data for $Co_4(CO)_9(PCy_3)(\mu_4\text{-}PPh)_2$

Space group	P 2_1
Cell constants	
a, Å	10.634 (2)
b, Å	20.674 (4)
c, Å	12.189 (2)
α, Å	90
β, Å	112.44 (1)
γ, Å	90
V, Å^3	2477.0 (6)
Molecular formula	$C_{39}H_{43}O_9P_3Co_4 \cdot C_7H_8$
fw	1076.57
Formula units per cell (Z)	2
ρ, g cm^{-1}	1.443
Abs. coeff. (μ), cm^{-1}	14.59
Radiation (λ), Å	0.71073
Collection range, deg	$3^\circ \leq 2\theta \leq 45^\circ$
Independent data, I > 3σ(I)	2976
Total variables	504
R	0.044
R_w	0.059
Weights	$w = [\sigma^2(F_o)+0.00207F_o^2]^{-1}$

Table 19. Atomic Coordinates ($x10^4$) and Isotropic Thermal Parameters ($Å^2x10^3$) for $Co_4(CO)_9(PCy_3)(\mu_4\text{-}PPh)_2$

atom	x	y	z	u
Co(1)	3767(1)	6140	7643(1)	27(1)*
Co(2)	5157(1)	6259(1)	6358(1)	31(1)
Co(3)	2908(1)	6260(1)	4371(1)	33(1)
Co(4)	1416(1)	6174(1)	5555(1)	33(1)
C(1)	3281(9)	5442(5)	8213(7)	38(4)
O(1)	2890(7)	4984(3)	8499(6)	57(3)
C(2)	5685(9)	6067(4)	8090(8)	38(4)
O(2)	6688(6)	5922(4)	8841(5)	52(3)
C(3)	6165(11)	5642(5)	6067(9)	46(4)
O(3)	6841(9)	5277(4)	5883(8)	82(4)
C(4)	6266(10)	6926(5)	6466(8)	40(4)
O(4)	7051(8)	7323(4)	6523(7)	66(4)
C(5)	3203(11)	5626(6)	3486(9)	49(4)
O(5)	3404(10)	5250(4)	2917(8)	84(5)
C(6)	3040(11)	6968(5)	3549(9)	46(4)
O(6)	3181(10)	7384(4)	3007(7)	76(4)
C(7)	972(9)	6210(6)	3834(8)	49(4)
O(7)	14(7)	6176(5)	2975(6)	75(3)
C(8)	524(11)	5467(5)	5682(10)	54(5)
O(8)	-67(10)	5045(5)	5770(10)	101(5)
C(9)	148(11)	6758(5)	5514(8)	50(4)
O(9)	-715(8)	7083(5)	5445(8)	85(4)

Table 19. continued

P(1)	3342(2)	5614(1)	5940(2)	31(1)
C(10)	3443(10)	4732(4)	5884(8)	36(4)
C(11)	4431(11)	4405(5)	6735(10)	51(5)
C(12)	4491(15)	3727(6)	6706(11)	65(6)
C(13)	3542(16)	3410(5)	5842(14)	74(8)
C(14)	2558(15)	3730(6)	4978(12)	73(6)
C(15)	2468(13)	4394(5)	4994(10)	62(5)
P(2)	3258(2)	6839(1)	6090(2)	29(1)
C(20)	3108(9)	7718(5)	5959(7)	35(4)
C(21)	3962(9)	8082(4)	5561(8)	38(4)
C(22)	3841(11)	8752(5)	5485(9)	49(5)
C(23)	2849(12)	9059(5)	5771(9)	55(5)
C(24)	2005(11)	8709(4)	6153(9)	54(5)
C(25)	2131(10)	8039(4)	6251(8)	42(4)
P(3)	4029(2)	6769(1)	9268(2)	28(1)
C(30)	5355(8)	6451(4)	10690(7)	30(3)
C(31)	5296(10)	6726(5)	11814(8)	51(4)
C(32)	6563(12)	6550(5)	12877(9)	58(5)
C(33)	6749(11)	5829(5)	13014(9)	54(40
C(34)	6710(10)	5526(5)	11864(8)	49(4)
C(35)	5435(10)	5706(4)	10812(8)	42(4)
C(40)	4617(8)	7620(4)	9161(8)	33(3)
C(41)	4543(10)	8129(4)	10026(10)	49(4)
C(42)	4811(12)	8800(5)	9645(10)	62(5)
C(43)	6154(12)	8817(5)	9522(10)	63(5)

Table 19. continued

C(44)	6332(12)	8291(5)	8740(10)	62(5)
C(45)	6014(10)	7635(5)	9094(9)	50(4)
C(50)	2485(8)	6879(4)	9615(7)	32(3)
C(51)	1380(9)	7270(5)	8630(8)	45(4)
C(52)	176(11)	7417(5)	8997(11)	60(5)
C(53)	-415(10)	6800(7)	9256(12)	79(6)
C(54)	647(11)	6393(6)	10175(11)	73(6)
C(55)	1884(9)	6271(5)	9825(9)	53(4)
C(60)'	10306	9388	-1569	150
C(61)'	9284	7965	2773	150
C(62)'	10073	8288	1914	150
C(63)'	10787	9020	1902	150
C(64)'	10113	8571	2666	150
C(65)'	10762	9374	585	150
C(66)'	10951	9510	-429	150

* Equivalent isotropic U defined as one third of the trace of the orthogonalised U_{ij} tensor

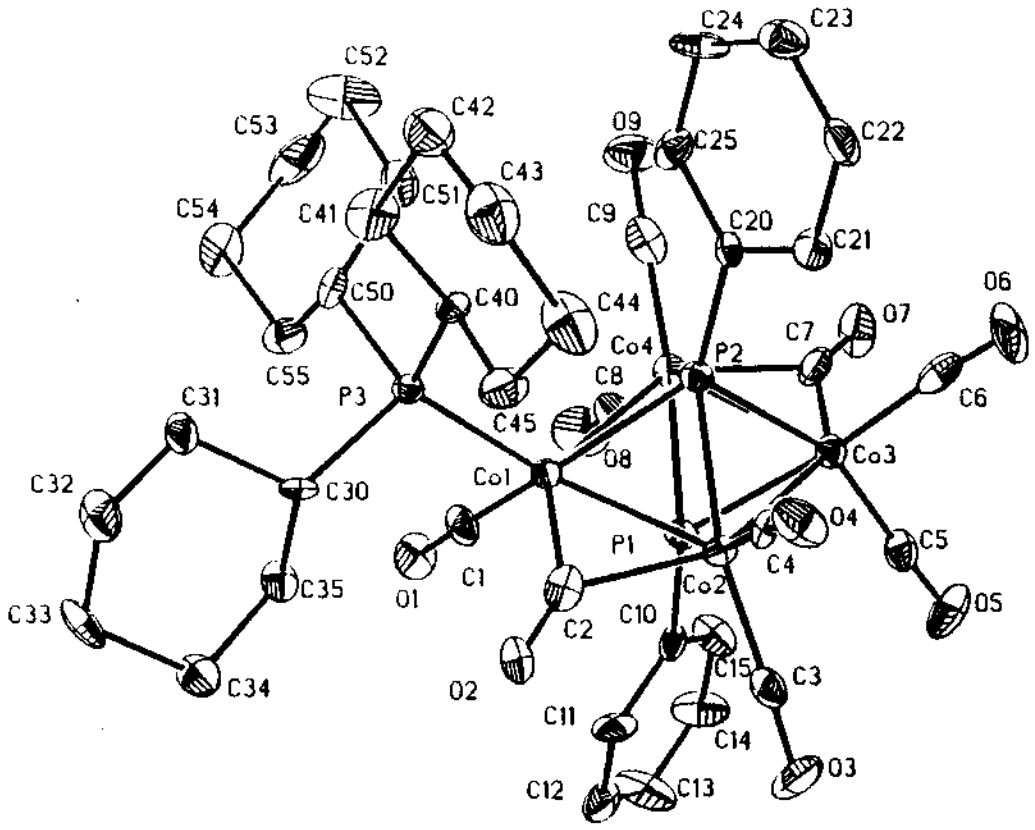

Figure 7. ORTEP diagram of $Co_4(CO)_9(PCy_3)(\mu_4\text{-}PPh)_2$ with the thermal ellipsoids drawn at the 30% probability level. H atoms are omitted for clarity. Structure determined by W. H. Watson and A. Nagl, Texas Christian University

Table 20. Bond Distances (Å) for $Co_4(CO)_9(PCy_3)(\mu_4\text{-}PPh)_2$

Co(1)-Co(2)	2.544(2)	Co(1)-Co(4)	2.806(1)
Co(1)-C(1)	1.763(10)	Co(1)-C(2)	1.906(9)
Co(1)-P(1)	2.232(2)	Co(1)-P(2)	2.277(2)
Co(1)-P(3)	2.296(2)	Co(2)-Co(3)	2.677(1)
Co(2)-C(2)	2.006(9)	Co(2)-C(3)	1.788(12)
Co(2)-C(4)	1.785(10)	Co(2)-P(1)	2.239(3)
Co(2)-P(2)	2.263(3)	Co(3)-Co(4)	2.526(2)
Co(3)-C(5)	1.798(12)	Co(3)-C(6)	1.809(11)
Co(3)-C(7)	1.910(9)	Co(3)-P(1)	2.231(3)
Co(3)-P(2)	2.318(2)	Co(4)-C(7)	1.968(9)
Co(4)-C(8)	1.782(12)	Co(4)-C(9)	1.796(12)
Co(4)-P(1)	2.241(3)	Co(4)-P(2)	2.275(2)
C(1)-O(1)	1.140(13)	C(2)-O(2)	1.149(9)
C(3)-O(3)	1.122(16)	C(4)-O(4)	1.155(13)
C(5)-O(5)	1.116(16)	C(6)-O(6)	1.129(15)
C(7)-O(7)	1.151(9)	C(8)-O(8)	1.104(16)
C(9)-O(9)	1.115(15)	P(1)-C(10)	1.829(9)
P(1)-P(2)	2.544(3)	C(10)-C(11)	1.344(13)
C(10)-C(15)	1.373(13)	C(11)-C(12)	1.403(15)
C(12)-C(13)	1.321(17)	C(13)-C(14)	1.342(18)
C(14)-C(15)	1.376(17)	P(2)-C(20)	1.826(10)
C(20)-C(21)	1.401(15)	C(20)-C(25)	1.388(15)
C(21)-C(22)	1.391(13)	C(22)-C(23)	1.385(18)
C(23)-C(24)	1.365(18)	C(24)-C(25)	1.393(13)

Table 20. continued

P(3)-C(30)	1.887(7)	P(3)-C(40)	1.889(9)
P(3)-C(50)	1.858(10)	C(30)-C(31)	1.506(14)
C(30)-C(35)	1.547(12)	C(31)-C(32)	1.515(13)
C(32)-C(33)	1.505(15)	C(33)-C(34)	1.522(16)
C(34)-C(35)	1.514(12)	C(40)-C(41)	1.513(14)
C(40)-C(45)	1.519(16)	C(41)-C(42)	1.524(15)
C(42)-C(43)	1.492(19)	C(43)-C(44)	1.503(17)
C(44)-C(45)	1.500(15)	C(50)-C(51)	1.548(11)
C(50)-C(55)	1.476(15)	C(51)-C(52)	1.539(18)
C(52)-C(53)	1.507(19)	C(53)-C(54)	1.508(16)
C(54)-C(55)	1.551(18)		

Table 21. Bond Angles (deg) for $Co_4(CO)_9(PCy_3)(\mu_4\text{-}PPh)_2$

Co(2)-Co(1)-Co(4)	88.0(1)	Co(2)-Co(1)-C(1)	130.5(4)
Co(4)-Co(1)-C(1)	94.9(2)	Co(2)-Co(1)-C(2)	51.2(3)
Co(4)-Co(1)-C(2)	138.3(3)	C(1)-Co(1)-C(2)	105.4(4)
Co(2)-Co(1)-P(1)	55.5(1)	Co(4)-Co(1)-P(1)	51.3(1)
C(1)-Co(1)-P(1)	89.0(3)	C(2)-Co(1)-P(1)	92.4(3)
Co(2)-Co(1)-P(2)	55.7(1)	Co(4)-Co(1)-P(2)	51.9(1)
C(1)-Co(1)-P(2)	146.7(3)	C(2)-Co(1)-P(2)	100.2(3)
P(1)-Co(1)-P(2)	68.7(1)	Co(2)-Co(1)-P(3)	124.7(1)
Co(4)-Co(1)-P(3)	122.7(1)	C(1)-Co(1)-P(3)	94.7(3)
C(2)-Co(1)-P(3)	92.0(3)	P(1)-Co(1)-P(3)	173.4(1)
P(2)-Co(1)-P(3)	105.6(1)	Co(1)-Co(2)-Co(3)	91.6(1)
Co(1)-Co(2)-C(2)	47.8(3)	Co(3)-Co(2)-C(2)	138.3(3)
Co(1)-Co(2)-C(3)	125.9(4)	Co(3)-Co(2)-C(3)	102.5(3)
C(2)-Co(2)-C(3)	96.8(4)	Co(1)-Co(2)-C(4)	123.5(4)
Co(3)-Co(2)-C(4)	113.8(3)	C(2)-Co(2)-C(40	99.4(4)
C(3)-Co(2)-C(4)	97.9(5)	Co(1)-Co(2)-P(1)	55.2(1)
Co(3)-Co(2)-P(1)	53.1(1)	C(2)-Co(2)-P(1)	89.6(3)
C(3)-Co(2)-P(1)	93.4(4)	C(4)-Co(2)-P(1)	164.6(3)
Co(1)-Co(2)-P(2)	56.2(1)	Co(3)-Co(2)-P(2)	55.2(1)
C(2)-Co(2)-P(2)	97.6(3)	C(3)-Co(2)-P(2)	156.9(3)
C(4)-Co(2)-P(2)	97.5(3)	P(1)-Co(2)-P(2)	68.8(1)
Co(2)-Co(3)-Co(4)	91.3(1)	Co(2)-Co(3)-C(5)	104.0(3)
Co(4)-Co(3)-C(5)	125.7(4)	Co(2)-Co(3)-C(6)	105.6(3)
Co(4)-Co(3)-C(6)	124.8(4)	C(5)-Co(3)-C(6)	100.9(5)

Table 21. continued

Co(2)-Co(3)-C(7)	141.6(3)	Co(4)-Co(3)-C(7)	50.4(3)
C(5)-Co(3)-C(7)	99.7(5)	C(6)-Co(3)-C(7)	98.9(5)
Co(2)-Co(3)-P(1)	53.4(1)	Co(4)-Co(3)-P(1)	55.8(1)
C(5)-Co(3)-P(1)	93.0(4)	C(6)-Co(3)-P(1)	157.5(3)
C(7)-Co(3)-P(1)	96.0(3)	Co(2)-Co(3)-P(2)	53.3(1)
Co(4)-Co(3)-P(2)	55.8(1)	C(5)-Co(3)-P(2)	156.1(3)
C(6)-Co(3)-P(2)	93.6(4)	C(7)-Co(3)-P(2)	96.7(3)
P(1)-Co(3)-P(2)	68.0(1)	Co(1)-Co(4)-Co(3)	89.1(1)
Co(1)-Co(4)-C(7)	137.4(3)	Co(3)-Co(4)-C(7)	48.4(3)
Co(1)-Co(4)-C(8)	102.7(3)	Co(3)-Co(4)-C(8)	125.3(4)
C(7)-Co(4)-C(8)	101.8(5)	Co(1)-Co(4)-C(9)	116.2(3)
Co(3)-Co(4)-C(9)	124.5(4)	C(7)-Co(4)-C(9)	94.2(5)
C(8)-Co(4)-C(9)	97.8(5)	Co(1)-Co(4)-P(1)	51.0(1)
Co(3)-Co(4)-P(1)	55.4(1)	C(7)-Co(4)-P(1)	94.0(3)
C(8)-Co(4)-P(1)	91.8(4)	C(9)-Co(4)-P(1)	165.8(3)
Co(1)-Co(4)-P(2)	52.0(1)	Co(3)-Co(4)-P(2)	57.5(1)
C(7)-Co(4)-P(2)	96.5(3)	C(8)-Co(4)-P(2)	154.1(3)
C(9)-Co(4)-P(2)	99.0(4)	P(1)-Co(4)-P(2)	68.6(1)
Co(1)-C(1)-O(1)	174.8(7)	Co(1)-C(2)-Co(2)	81.1(3)
Co(1)-C(2)-O(2)	144.6(9)	Co(2)-C(2)-O(2)	133.8(9)
Co(2)-C(3)-O(3)	176.6(11)	Co(2)-C(4)-O(4)	174.8(10)
Co(3)-C(5)-O(5)	177.4(12)	Co(3)-C(6)-O(6)	175.0(11)
Co(3)-C(7)-Co(4)	81.3(3)	Co(3)-C(7)-O(7)	141.2(9)
Co(4)-C(7)-O(7)	137.4(9)	Co(4)-C(8)-O(8)	177.0(13)
Co(4)-C(9)-O(9)	174.4(10)	Co(1)-P(1)-Co(2)	69.3(1)

Table 21. continued

Co(1)-P(1)-Co(3)	114.1(1)	Co(2)-P(1)-Co(3)	73.6(1)
Co(1)-P(1)-Co(4)	77.7(1)	Co(1)-P(1)-Co(4)	112.3(1)
Co(3)-P(1)-Co(4)	68.8(1)	Co(1)-P(1)-C(10)	121.7(3)
Co(2)-P(1)-C(10)	123.0(4)	Co(3)-P(1)-C(10)	124.1(3)
Co(4)-P(1)-C(10)	124.7(4)	Co(1)-P(1)-P(2)	56.5(1)
Co(2)-P(1)-P(2)	56.0(1)	Co(3)-P(1)-P(2)	57.6(1)
Co(4)-P(1)-P(2)	56.4(1)	C(10)-P(1)-P(2)	178.0(3)
P(1)-C(10)-C(11)	120.9(7)	P(1)-C(10)-C(15)	120.0(7)
C(11)-C(10)-C(15)	119.1(9)	C(10)-C(11)-C(12)	120.9(11)
C(11)-C(12)-C(13)	119.2(10)	C(12)-C(13)-C(14)	120.6(11)
C(13)-C(14)-C(15)	121.2(11)	C(10)-C(15)-C(14)	118.9(10)
Co(1)-P(2)-Co(2)	68.1(1)	Co(1)-P(2)-Co(3)	109.2(1)
Co(2)-P(2)-Co(3)	71.5(1)	Co(1)-P(2)-Co(4)	76.1(1)
Co(2)-P(2)-Co(4)	110.2(1)	Co(3)-P92)-Co(4)	66.7(1)
Co(1)-P(2)-P(1)	54.8(1)	Co(2)-P(2)-P(1)	55.2(1)
Co(3)-P(2)-P(1)	54.4(1)	Co(4)-P(2)-P(1)	55.1(1)
Co(1)-P(2)-C(20)	133.6(3)	Co(2)-P(2)-C(20)	125.7(3)
Co(3)-P(2)-C(20)	117.2(3)	Co(4)-P(2)-C(20)	122.7(3)
P(1)-P(2)-C(20)	171.5(3)	P(2)-C(20)-C(21)	121.3(8)
P(2)-C(20)-C(25)	120.1(8)	C(21)-C(20)-C(25)	118.7(9)
C(20)-C(21)-C(22)	120.2(10)	C(21)-C(22)-C(23)	119.9(11)
C(22)-C(23)-C(24)	120.4(10)	C(23)-C(24)-C(25)	120.1(11)
C(20)-C(25)-C(24)	120.7(10)	Co(1)-P(3)-C(30)	113.4(3)
Co(1)-P(3)-C(40)	113.7(3)	C(30)-P(3)-C(40)	103.7(3)
Co(1)-P(3)-C(50)	116.0(3)	C(30)-P(3)-C(50)	104.4(4)

Table 21. continued

C(40)-P(3)-C(50)	104.3(4)	P(3)-C(30)-C(31)	115.3(6)
P(3)-C(30)-C(35)	115.5(5)	C(31)-C(30)-C(35)	108.0(8)
C(30)-C(31)-C(32)	110.8(9)	C(31)-C(32)-C(33)	111.7(8)
C(32)-C(33)-C(34)	110.5(9)	C(33)-C(34)-C(35)	112.3(9)
C(30)-C(35)-C(34)	109.0(7)	P(3)-C(40)-C(41)	119.6(8)
P(3)-C(40)-C(45)	112.3(6)	C(41)-C(40)-C(45)	109.6(7)
C(40)-C(41)-C(42)	110.8(10)	C(41)-C(42)-C(43)	110.4(9)
C(42)-C(43)-C(44)	113.8(9)	C(43)-C(44)-C(45)	112.0(11)
C(40)-C(45)-C(44)	111.5(9)	P(3)-C(50)-C(51)	111.3(7)
P(3)-C(50)-C(55)	114.4(7)	C(51)-C(50)-C(55)	109.1(7)
C(50)-C(51)-C(52)	110.3(9)	C(51)-C(52)-C(53)	110.7(10)
C(52)-C(53)-C(54)	112.0(9)	C(53)-C(54)-C(55)	111.1(11)
C(50)-C(55)-C(54)	112.3(9)		

cyclooctadiene, 2,2'-dipyridine, 1,10-phenanthroline, and diphos) affords the corresponding mixed-metal arachno clusters $Fe_2(CO)_6(\mu_3\text{-}S)_2Pt(L\frown L)$ [**5**] in high yield. All of the new clusters have been characterized by IR and NMR spectroscopy. These data are summarized in Tables 22 and 23.

D. Reactions of $Fe_2(CO)_6(\mu_3\text{-}S)_2Pt(L\frown L)$ with Reducing Agents (where L⌢L = 1,5-cod, bpy, 1,10-phen)

The reaction of the arachno Fe_2/Pt chalcogenide clusters **5** (where L⌢L = 1,5-cod, bpy, and 1,10-phen) with reducing agents such as Super-Hydride, methyl lithium, cobaltocene, and sodium naphthalide has been examined in THF at -78 °C. All reducing agents react with $Fe_2(CO)_6(\mu_3\text{-}S)_2Pt(1,5\text{-cod})$ to yield the corresponding radical anion $[Fe_2(CO)_6(\mu_3\text{-}S)_2Pt(1,5\text{-cod})^{-\bullet}]$ [$\mathbf{6a}^{-\bullet}$] without the spectroscopic observation of any intermediates. The remaining clusters react similarily with all of the reducing agents with the exception of cobaltocene. The IR spectral data of these cluster radical anions are summarized in Table 24.

These paramagnetic clusters are thermally unstable. Upon warming from -78 °C to room temperature, approximately 20% of the radical anion reverts back to starting material while 80% decomposes to non-carbonyl containing material. If the temperature is maintained at -78 °C, the radical

Table 22. Infrared Spectral Data in the Carbonyl Region for Mixed-Metal Arachno Clusters $Fe_2(CO)_6(\mu_3\text{-}S)_2Pt(L\frown L)$[a]

$Fe_2(CO)_6(\mu_3\text{-}S)_2Pt(1,5\text{-cod})$	2058(s), 2018(vs), 1977(s)
$Fe_2(CO)_6(\mu_3\text{-}S)_2Pt(bpy)$	2051(s), 2011(vs), 1969(s)
$Fe_2(CO)_6(\mu_3\text{-}S)_2Pt(1,10\text{-phen})$	2051(s), 2011(vs), 1969(s)
$Fe_2(CO)_6(\mu_3\text{-}S)_2Pt(diphos)$	2049(s), 2008(vs), 1968(s), 1962(s)
$Fe_2(CO)_6(\mu_3\text{-}S)_2Pt(dppf)$	2048(s), 2007(vs), 1969(s)

[a]All spectra recorded in CH_2Cl_2 at room temperature.

Table 23. ^{1}H-NMR, ^{13}C-NMR, and ^{31}P-NMR Chemical Shifts for Mixed-Metal Arachno Clusters $Fe_2(CO)_6(\mu_3\text{-}S)_2Pt(L\frown L)$[a]

Cluster	^{31}P-NMR, ppm	^{1}H-NMR, ppm	^{13}C-NMR, ppm
$Fe_2(CO)_6(\mu_3\text{-}S)_2Pt(1,5\text{-cod})$		2.39 2.57 5.05 ($J_{Pt,H}$=90Hz)	30.4 99.9 211.2
$Fe_2(CO)_6(\mu_3\text{-}S)_2Pt(bpy)$[b]		7.85(t) 8.37(t) 8.55(d) 8.95(d) ($J_{Pt,H}$=36Hz)	
$Fe_2(CO)_6(\mu_3\text{-}S)_2Pt(1,10\text{-phen})$[b]		8.20(dd) 8.30(s) 8.98(d) 9.21(d) ($J_{Pt,H}$=36Hz)	
$Fe_2(CO)_6(\mu_3\text{-}S)_2Pt(diphos)$	39.9 ($J_{Pt,P}$=2721 Hz)		
$Fe_2(CO)_6(\mu_3\text{-}S)_2Pt(dppf)$	19.1 ($J_{Pt,P}$=2849 Hz)		

[a]Solvent $CDCl_3$ [b]Solvent Acetone-d_6

Table 24. Infrared Spectral Data in the Carbonyl Region for Mixed-Metal Clusters $Fe_2(CO)_6(\mu_3\text{-}S)_2Pt(L\frown L)$ and Related Radical Anion Clusters[a]

$Fe_2(CO)_6(\mu_3\text{-}S)_2Pt(1,5\text{-cod})$	2057(s), 2016(vs), 1976(s), 1957(m)
$Fe_2(CO)_6(\mu_3\text{-}S)_2Pt(1,5\text{-cod})^{-\bullet}$	2034(s), 1991(vs), 1949(s), 1942(s), 1929(m)
$Fe_2(CO)_6(\mu_3\text{-}S)_2Pt(bpy)$	2049(s), 2008(vs), 1968(s), 1962(s), 1947(m)
$Fe_2(CO)_6(\mu_3\text{-}S)_2Pt(bpy)^{-\bullet}$	2037(s), 1995(vs), 1949(s), 1934(m)
$Fe_2(CO)_6(\mu_3\text{-}S)_2Pt(1,10\text{-phen})$	2049(s), 2008(vs), 1968(s), 1962(s), 1947(m)
$Fe_2(CO)_6(\mu_3\text{-}S)_2Pt(1,10\text{-phen})^{-\bullet}$	2037(s), 1996(vs), 1948(s), 1934(m)

[a]All spectra recorded in THF at -70 °C.

anion appears to be indefinitely stable. Treatment of the radical anion with the one-electron oxidant $[Cp_2Fe][BF_4]$ (ferricenium tetrafluoroborate) results in the regeneration of starting material and provides additional proof for the presence of a cluster radical anion.

E. Reactions of $Fe_2(CO)_6(\mu_3\text{-}S)_2Pt(L\frown L)$ with Oxidizing Agents (where L⁀L = 1,5-cod, bpy, 1,10-phen, diphos, dppf)

The reaction of the arachno Fe_2/Pt chalcogenide clusters **5** (where L⁀L = 1,5-cod, bpy, 1,10-phen, diphos, and dppf) with oxidants such as magic green and $Fe(1,10\text{-phen})_3^{3+}$ has been examined in CH_2Cl_2 or acetone at -78 °C. All of the oxidants yield the corresponding radical cation $[Fe_2(CO)_6(\mu_3\text{-}S)_2Pt(L\frown L)^{+\bullet}]$ [$7^{+\bullet}$] without the spectroscopic intervention of any intermediates. The IR spectral data of these cluster radical cations are summarized in Table 25.

These paramagnetic clusters are thermally unstable. Upon warming to room temperature, approximately 10% of the radical anion goes back to starting material while 90% decomposes to non-carbonyl containing material. Treatment of the radical cation with Cp_2Co (Cobaltocene) leads to the regeneration of starting material and provides additional proof for the prescence of an oxidized cluster.

Table 25. Infrared Spectral Data in the Carbonyl Region for Mixed-Metal Clusters Radical Cation Clusters $Fe_2(CO)_6(\mu_3\text{-}S)_2Pt(L\frown L)^{+\bullet}$ [a]

$Fe_2(CO)_6(\mu_3\text{-}S)_2Pt(1,5\text{-cod})^{+\bullet}$	2122(s), 2106(s), 2096(vs), 2077(s), 2056(s), 2040(s)
$Fe_2(CO)_6(\mu_3\text{-}S)_2Pt(bpy)^{+\bullet}$	2114(s), 2096(vs), 2062(s), 2038(s)
$Fe_2(CO)_6(\mu_3\text{-}S)_2Pt(1,10\text{-phen})^{+\bullet}$	2114(s), 2096(vs), 2062(s), 2038(s)
$Fe_2(CO)_6(\mu_3\text{-}S)_2Pt(diphos)^{+\bullet}$	2113(s), 2096(vs), 2064(s), 2029(s)
$Fe_2(CO)_6(\mu_3\text{-}S)_2Pt(dppf)^{+\bullet}$	2113(s), 2096(vs), 2058(s), 2033(s)

[a]All spectra recorded in CH_2Cl_2 at -70 °C.

F. X-Ray Crystallographic Structure of $Fe_2(CO)_6(\mu_3$-S$)_2$Pt(1,5-cod)

Single crystals of $Fe_2(CO)_6(\mu_3$-S$)_2$Pt(1,5-cod) were successfully grown, and the X-ray crystallographic data for $Fe_2(CO)_6(\mu_3$-S$)_2$Pt(1,5-cod) are summarized in Table 26. The final fractional coordinates are listed in Table 27. The molecular configuration and the numbering scheme of $Fe_2(CO)_6(\mu_3$-S$)_2$Pt(1,5-cod) are presented in the ORTEP diagram shown in Figure 8. Selected bond distances and bond angles for $Fe_2(CO)_6(\mu_3$-S$)_2$Pt(1,5-cod) are presented in Table 28 and Table 29, respectively.

G. X-Ray Crystallographic Structure of $Fe_2(CO)_6(\mu_3$-S$)_2$Pt(1,10-phen)

Single crystals of $Fe_2(CO)_6S_2$Pt(1,10-phen) were successfully grown, and the X-ray crystallographic data for $Fe_2(CO)_6S_2$Pt(1,10-phen) are summarized in Table 30. The final fractional coordinates are listed in Table 31. The molecular configuration and the numbering scheme of $Fe_2(CO)_6S_2$Pt(1,10-phen) are presented in the ORTEP diagram shown in Figure 9. Selected bond distances and bond angles for $Fe_2(CO)_6S_2$Pt(1,5-cod) are presented in Table 32 and Table 33, respectively.

H. Reactions of $FeCo_2(CO)_9(\mu_3$-PPh) with Reducing Agents

The reaction of the mixed-metal tetrahedrane cluster $FeCo_2(CO)_9(\mu_3$-PPh), 3, with various reducing agents has been

Table 26. X-ray Crystallographic Collection and Processing Data for $Fe_2(CO)_6(\mu_3\text{-}S)_2Pt(1,5\text{-cod})$

Space group	P 1
Cell constants	
a, Å	7.685 (1)
b, Å	11.363 (2)
c, Å	11.403 (2)
α, Å	113.92 (1)
β, Å	100.57 (1)
γ, Å	90.78 (1)
V, $Å^3$	890.5 (2)
Molecular formula	$C_{14}H_{12}O_6S_2Fe_2Pt$
fw	647.15
Formula units per cell (Z)	2
ρ, g cm^{-1}	2.41
Abs. coeff. (μ), cm^{-1}	101.0
Radiation (λ), Å	0.71073
Collection range, deg	$3^\circ \leq 2\theta \leq 50^\circ$
Independent data, $I > 3\sigma(I)$	3017
Total variables	227
R	0.0484
R_w	0.0641
Weights	$w = [\sigma^2(F_o)+0.00295F_o^2]^{-1}$

Table 27. Atomic Coordinates ($x10^4$) and Isotropic Thermal Parameters ($Å^2x10^3$) for $Fe_2(CO)_6(\mu_3\text{-}S)_2Pt(1,5\text{-cod})$

atom	x	y	z	u
Pt	7381(1)	-773(1)	7175(1)	21(1)*
Fe(1)	9247(2)	2132(1)	7826(1)	28(1)*
Fe(2)	6685(2)	2165(1)	8908(1)	29(1)*
S(1)	8982(3)	924(2)	8972(2)	30(1)*
S(2)	6582(3)	961(2)	6735(2)	29(1)*
C(1)	6333(13)	-2338(8)	5202(9)	37(3)*
C(2)	5022(11)	-2079(8)	5911(9)	35(3)*
C(3)	4442(12)	-2793(10)	6666(10)	48(4)*
C(4)	6009(13)	-3235(10)	7401(11)	50(4)*
C(5)	7656(11)	-2276(8)	7958(8)	32(3)*
C(6)	9012(11)	-2287(8)	7355(9)	34(2)*
C(7)	9151(14)	-3202(11)	5978(9)	50(4)*
C(8)	7425(16)	-3470(10)	4993(9)	59(4)*
C(9)	10811(12)	3277(9)	9214(10)	41(4)*
O(9)	11775(11)	4004(7)	10086(8)	67(3)*
C(10)	8767(13)	3257(8)	7095(9)	39(3)*
O(10)	8352(13)	3933(8)	6610(8)	70(4)*
C(11)	10727(12)	1203(10)	6858(9)	43(4)*
O(11)	11698(11)	577(10)	6260(8)	78(4)*
C(12)	7583(12)	3293(9)	10566(10)	42(4)*
O(12)	8157(11)	4001(7)	11621(7)	62(3)*
C(13)	5473(12)	3323(9)	8509(9)	40(4)*

Table 27. Continued

O(13)	4724(11)	4054(7)	8239(8)	62(4)*
C(14)	4886(13)	1289(10)	9129(9)	42(4)*
O(14)	3775(11)	708(9)	9250(9)	69(4)*

* Equivalent isotropic U defined as one third of the trace of the orthogonalised U_{ij} tensor

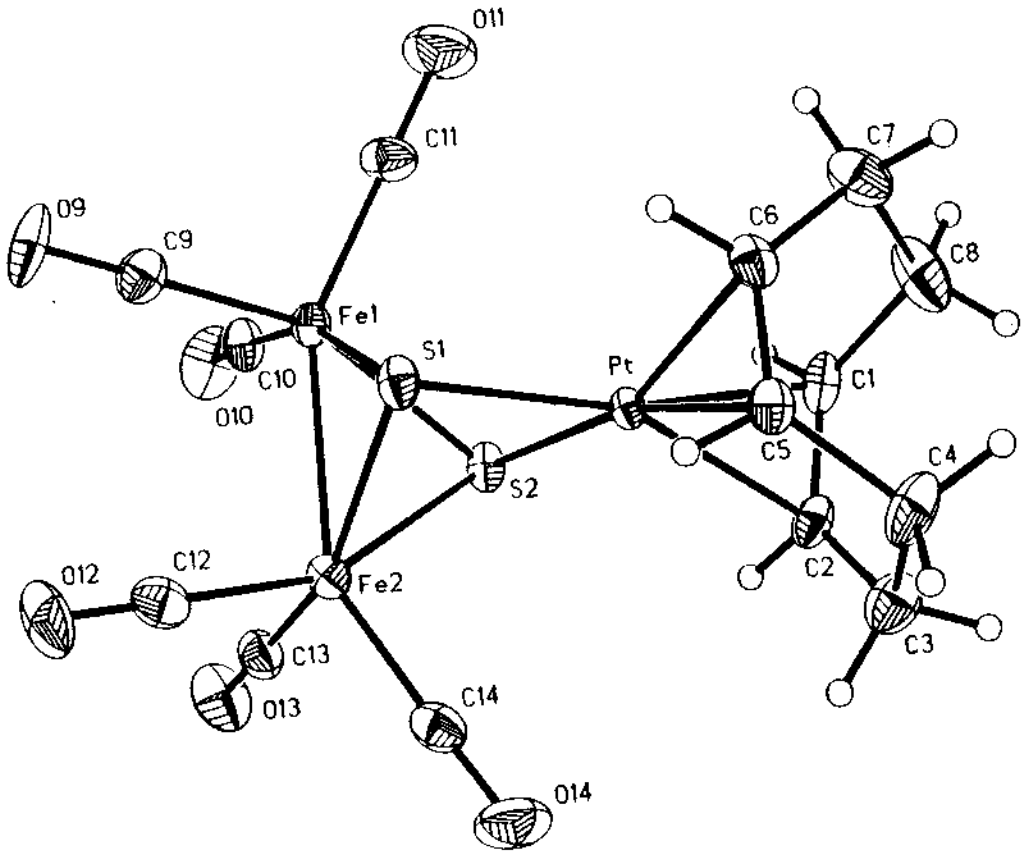

Figure 8. ORTEP diagram of $Fe_2(CO)_6(\mu_3\text{-}S)_2Pt(1,5\text{-cod})$ with the thermal ellipsoids drawn at the 30% probability level. H atoms are omitted for clarity. Structure determined by W. H. Watson and A. Nagl, Texas Christian University

Table 28. Bond Distances (Å) for $Fe_2(CO)_6(\mu_3\text{-}S)_2Pt(1,5\text{-cod})$

Pt-S(1)	2.288(2)	Pt-S(2)	2.287(2)
Pt-C(1)	2.219(7)	Pt-C(2)	2.191(7)
Pt-C(5)	2.223(11)	Pt-C(6)	2.196(10)
Fe(1)-Fe(2)	2.501(2)	Fe(1)-S(1)	2.276(3)
Fe(1)-S(2)	2.272(2)	Fe(1)-C(9)	1.797(8)
Fe(1)-C(10)	1.797(11)	Fe(1)-C(11)	1.782(10)
Fe(2)-S(1)	2.284(3)	Fe(2)-S(2)	2.279(2)
Fe(2)-C(12)	1.796(8)	Fe(2)-C(13)	1.781(11)
Fe(2)-C(14)	1.805(11)	C(1)-C(2)	1.368(14)
C(1)-C(8)	1.506(15)	C(2)-C(3)	1.515(18)
C(3)-C(4)	1.547(16)	C(4)-C(5)	1.516(12)
C(5)-C(6)	1.348(14)	C(6)-C(7)	1.516(13)
C(7)-C(8)	1.510(14)	C(9)-O(9)	1.126(10)
C(10)-O(10)	1.133(16)	C(11)-O(11)	1.155(13)
C(12)-O(12)	1.140(10)	C(13)-O(13)	1.126(14)
C(14)-O(14)	1.134(15)		

Table 29. Bond Angles (deg) for $Fe_2(CO)_6(\mu_3\text{-}S)_2Pt(1,5\text{-cod})$

S(1)-Pt-S(2)	77.9(1)	S(1)-Pt-C(1)	166.2(3)
S(2)-Pt-C(1)	98.7(3)	S(1)-Pt-C(2)	156.7(2)
S(2)-Pt-C(2)	96.1(3)	C(1)-Pt-C(2)	36.1(4)
S(1)-Pt-C(5)	98.4(2)	S(2)-Pt-C(5)	164.8(2)
C(1)-Pt-C(5)	88.2(3)	C(2)-Pt-C(5)	81.5(3)
S(1)-Pt-C(6)	96.9(2)	S(2)-Pt-C(6)	158.8(3)
C(1)-Pt-C(6)	81.4(3)	C(2)-Pt-C(6)	96.1(3)
C(5)-Pt-C(6)	35.5(4)	Fe(2)-Fe(1)-S(1)	56.9(1)
Fe(2)-Fe(1)-S(2)	56.8(1)	S(1)-Fe(1)-S(2)	78.5(1)
Fe(2)-Fe(1)-C(9)	99.0(4)	S(1)-Fe(1)-C(9)	89.6(4)
S(2)-Fe(1)-C(9)	155.8(4)	Fe(2)-Fe(1)-C(10)	103.7(3)
S(1)-Fe(1)-C(10)	160.6(3)	S(2)-Fe(1)-C(10)	91.2(3)
C(9)-Fe(1)-C(10)	93.6(5)	Fe(2)-Fe(1)-C(11)	148.0(4)
S(1)-Fe(1)-C(11)	98.2(4)	S(2)-Fe(1)-C(11)	102.0(3)
C(9)-Fe(1)-C(11)	100.5(4)	C(10)-Fe(1)-C(11)	100.1(5)
Fe(1)-Fe(2)-S(1)	56.6(1)	Fe(1)-Fe(2)-S(2)	56.5(1)
S(1)-Fe(2)-S(2)	78.2(1)	Fe(1)-Fe(2)-C(12)	101.7(3)
S(1)-Fe(2)-C(12)	90.6(3)	S(2)-Fe(2)-C(12)	158.2(4)
Fe(1)-Fe(2)-C(13)	99.7(4)	S(1)-Fe(2)-C(13)	156.3(4)
S(2)-Fe(2)-C(13)	89.7(3)	C(12)-Fe(2)-C(13)	93.6(4)
Fe(1)-Fe(2)-C(14)	148.9(3)	S(1)-Fe(2)-C(14)	102.8(4)
S(2)-Fe(2)-C(14)	99.3(3)	C(12)-Fe(2)-C(14)	101.4(5)
C(13)-Fe(2)-C(14)	99.2(5)	Pt-S(1)-Fe(1)	93.2(1)
Pt-S(1)-Fe(2)	89.8(1)	Fe(1)-S(1)-Fe(2)	66.5(1)

Table 29. Continued

Pt-S(2)-Fe(1)	93.3(1)	Pt-S(2)-Fe(2)	90.0(1)
Fe(1)-S(2)-Fe(2)	66.7(1)	Pt-C(1)-C(2)	70.8(4)
Pt-C(1)-C(8)	109.6(6)	C(2)-C(1)-C(8)	124.2(11)
Pt-C(2)-C(1)	73.1(5)	Pt-C(2)-C(3)	106.7(6)
C(1)-C(2)-C(3)	128.4(9)	C(2)-C(3)-C(4)	113.4(9)
C(3)-C(4)-C(5)	113.2(10)	Pt-C(5)-C(4)	110.6(7)
Pt-C(5)-C(6)	71.2(6)	C(4)-C(5)-C(6)	125.9(7)
Pt-C(6)-C(5)	73.3(6)	Pt-C(6)-C(7)	106.9(7)
C(5)-C(6)-C(7)	127.2(7)	C(6)-C(7)-C(8)	112.9(9)
C(1)-C(8)-C(7)	115.4(7)	Fe(1)-C(9)-O(9)	179.2(10)
Fe(1)-C(10)-O(10)	175.5(9)	Fe(1)-C(11)-O(11)	177.5(12)
Fe(2)-C(12)-O(12)	179.5(9)	Fe(2)-C(13)-O(13)	178.7(10)
Fe(2)-C(14)-O(14)	178.1(9)		

Table 30. X-ray Crystallographic Collection and Processing Data for $Fe_2(CO)_6(\mu_3\text{-}S)_2Pt(1,10\text{-phen})$

Space group	P 1
Cell constants	
a, Å	7.688 (1)
b, Å	11.118 (2)
c, Å	13.257 (2)
α, Å	70.26 (1)
β, Å	76.25 (1)
γ, Å	78.68 (1)
V, $Å^3$	1027.7 (3)
Molecular formula	$C_{18}H_8O_6N_2S_2Fe_2Pt$
fw	719.19
Formula units per cell(Z)	2
ρ, g cm^{-1}	2.324
Abs. coeff. (μ), cm^{-1}	87.67
Radiation (λ), Å	0.71073
Collection range, deg	$3^\circ \leq 2\theta \leq 50^\circ$
Independent data, $I > 3\sigma(I)$	3257
Total variables	280
R	0.0356
R_w	0.0381
Weights	$w = [\sigma^2(F_o)+0.00028F_o^2]^{-1}$

Table 31. Atomic Coordinates ($x10^4$) and Isotropic Thermal Parameters ($Å^2x10^3$) for $Fe_2(CO)_6(\mu_3\text{-}S)_2Pt(1,10\text{-phen})$

atom	x	y	z	u
Pt	2197(1)	1583(1)	1840(1)	33(1)*
Fe(1)	-188(1)	2444(1)	3901(1)	40(1)*
Fe(2)	2762(1)	3308(1)	3379(1)	41(1)*
S(1)	1025(3)	3496(2)	2137(2)	44(1)*
S(2)	2541(3)	1224(2)	3567(1)	41(1)*
N(1)	1726(7)	1926(5)	299(5)	38(2)*
C(2)	1095(11)	3035(7)	-383(6)	50(3)*
C(3)	785(12)	3084(9)	-1377(7)	62(4)*
C(4)	1101(11)	2039(9)	-1714(7)	59(4)*
C(4A)	1800(10)	855(8)	-1036(6)	49(3)*
C(5)	2225(12)	-339(10)	-1286(8)	64(4)*
C(6)	2933(12)	-1409(9)	-612(8)	63(4)*
C(6A)	3306(10)	-1440(7)	414(7)	50(3)*
C(7)	4071(11)	-2523(8)	1165(8)	60(4)*
C(8)	4357(11)	-2425(8)	2109(8)	61(4)*
C(9)	3872(10)	-1242(7)	2331(6)	47(3)*
N(10)	3133(8)	-212(5)	1649(5)	41(2)*
C(10A)	2856(9)	-290(7)	696(6)	41(3)*
C(10B)	2123(9)	846(7)	-29(6)	37(3)*
C(11)	-1793(11)	3802(8)	4000(7)	50(3)*
O(11)	-2820(9)	4685(6)	4045(6)	81(3)*
C(12)	-205(10)	1804(7)	5322(6)	45(3)*

Table 31. continued

O(12)	-168(8)	1411(6)	6236(4)	60(3)*
C(13)	-1736(11)	1492(7)	3789(6)	47(3)*
O(13)	-2751(8)	914(6)	3713(5)	65(3)*
C(14)	1812(11)	4830(8)	3557(6)	50(3)*
O(14)	1173(9)	5789(5)	3689(5)	69(3)*
C(15)	3599(11)	2778(8)	4627(7)	54(4)*
O(15)	4074(10)	2435(7)	5439(5)	80(3)*
C(16)	4791(13)	3696(8)	2432(7)	56(4)*
O(16)	6059(10)	4009(7)	1812(6)	83(3)*

* Equivalent isotropic U defined as one third of the trace of the orthogonalised U_{ij} tensor

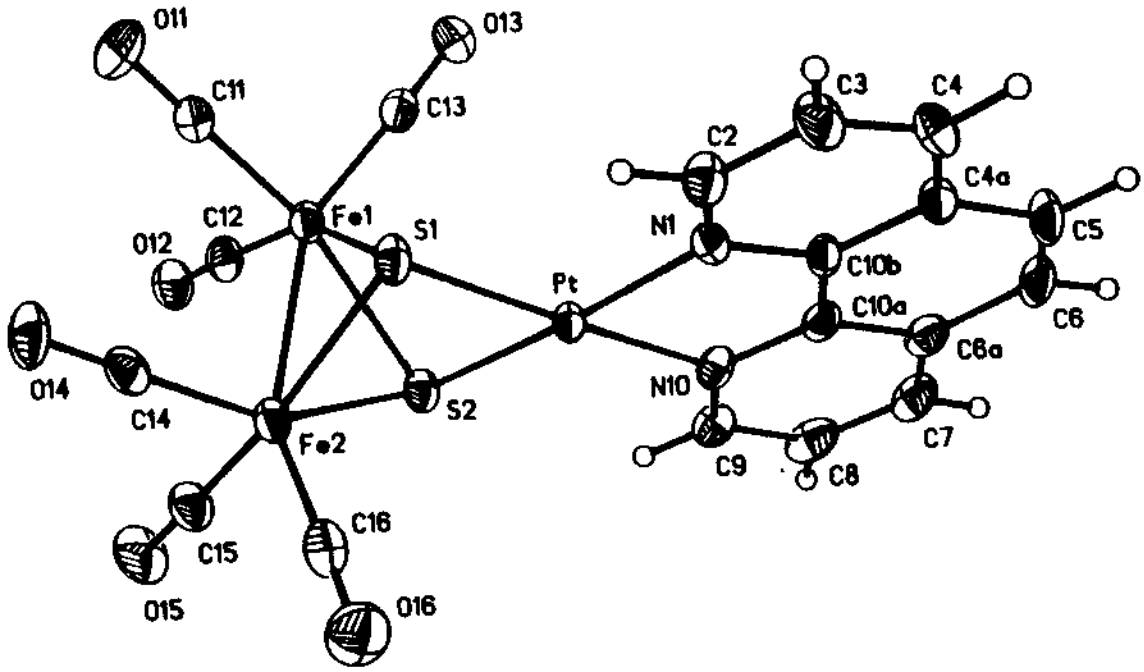

Figure 9. ORTEP diagram of $Fe_2(CO)_6(\mu_3\text{-}S)_2Pt(1,10\text{-phen})$ with the thermal ellipsoids drawn at the 30% probability level. H atoms are omitted for clarity. Structure determined by W. H. Watson and A. Nagl, Texas Christian University

Table 32. Bond Distances (Å) for $Fe_2(CO)_6(\mu_3\text{-}S)_2Pt(1,10\text{-phen})$

Pt-S(1)	2.266(2)	Pt-S(2)	2.258(2)
Pt-N(1)	2.056(6)	Pt-N(10)	2.064(6)
Fe(1)-Fe(2)	2.492(2)	Fe(1)-S(1)	2.292(2)
Fe(1)-S(2)	2.299(2)	Fe(1)-C(11)	1.773(8)
Fe(1)-C(12)	1.772(7)	Fe(1)-C(13)	1.802(10)
Fe(2)-S(2)	2.290(3)	Fe(2)-S(2)	2.281(2)
Fe(2)-C(14)	1.776(9)	Fe(2)-C(15)	1.787(9)
Fe(2)-C(16)	1.779(9)	N(1)-C(2)	1.339(9)
N(1)-C(10B)	1.366(10)	C(2)-C(3)	1.375(14)
C(3)-C(4)	1.341(15)	C(4)-C(4A)	1.408(11)
C(4A)-C(5)	1.434(15)	C(4A)-C(10B)	1.411(13)
C(5)-C(6)	1.330(12)	C(6)-C(6A)	1.445(15)
C(6A)-C(7)	1.407(11)	C(6A)-C(10A)	1.407(12)
C(7)-C(8)	1.364(16)	C(8)-C(9)	1.404(13)
C(9)-N(10)	1.319(9)	N(10)-C(10A)	1.363(11)
C(10A)-C(10B)	1.412(9)	C(11)-O(11)	1.142(10)
C(12)-O(12)	1.147(9)	C(13)-O(13)	1.144(12)
C(14)-O(14)	1.134(11)	C(15)-O(15)	1.137(12)
C(16)-O(16)	1.142(11)		

Table 33. Bond Angles (deg) for $Fe_2(CO)_6(\mu_3\text{-}S)_2Pt(1,10\text{-phen})$

S(1)-Pt-S(2)	77.4(1)	S(1)-Pt-N(1)	101.1(2)
S(2)-Pt-N(1)	176.7(2)	S(1)-Pt-N(10)	176.3(2)
S(2)-Pt-N(10)	101.0(2)	N(1)-Pt-N(10)	80.4(2)
Fe(2)-Fe(1)-S(1)	57.0(1)	Fe(2)-Fe(1)-S(2)	56.7(1)
S(1)-Fe(1)-S(2)	76.0(1)	Fe(2)-Fe(1)-C(11)	103.6(3)
S(1)-Fe(1)-C(11)	91.7(2)	S(2)-Fe(1)-C(11)	160.2(3)
Fe(2)-Fe(1)-C(12)	97.0(3)	S(1)-Fe(1)-C(12)	154.1(3)
S(2)-Fe(1)-C(12)	90.0(2)	C(11)-Fe(1)-C(12)	94.9(4)
Fe(2)-Fe(1)-C(13)	152.9(3)	S(1)-Fe(1)-C(13)	104.9(2)
S(2)-Fe(1)-C(13)	101.7(3)	C(11)-Fe(1)-C(13)	96.5(4)
C(12)-Fe(1)-C(13)	99.3(4)	Fe(1)-Fe(2)-S(1)	57.1(1)
Fe(1)-Fe(2)-S(2)	57.4(1)	S(1)-Fe(2)-S(2)	76.4(1)
Fe(1)-Fe(2)-C(14)	94.5(3)	S(1)-Fe(2)-C(14)	93.4(3)
S(2)-Fe(2)-C(14)	151.4(3)	Fe(1)-Fe(2)-C(15)	103.9(3)
S(1)-Fe(2)-C(15)	160.5(3)	S(2)-Fe(2)-C(15)	89.7(3)
C(14)-Fe(2)-C(15)	92.4(4)	Fe(1)-Fe(2)-C(16)	150.7(4)
S(1)-Fe(2)-C(16)	97.3(4)	S(2)-Fe(2)-C(16)	106.3(3)
C(14)-Fe(2)-C(16)	101.5(4)	C(15)-Fe(2)-C(16)	99.8(4)
Pt-S(1)-Fe(1)	90.3(1)	Pt-S(1)-Fe(2)	95.8(1)
Fe(1)-S(1)-Fe(2)	65.9(1)	Pt-S(2)-Fe(1)	90.3(1)
Pt-S(2)-Fe(2)	96.2(1)	Fe(1)-S(2)-Fe(2)	65.9(1)
Pt-N(1)-C(2)	128.5(6)	Pt-N(1)-C(10B)	112.8(4)
C(2)-N(1)-C(10B)	118.7(7)	N(1)-C(2)-C(3)	121.0(8)

Table 33. Continued

C(2)-C(3)-C(4)	122.2(8)	C(3)-C(4)-C(4A)	118.9(9)
C(4)-C(4A)-C(5)	125.5(9)	C(4)-C(4A)-C(10B)	117.3(9)
C(5)-C(4A)-C(10B)	117.3(7)	C(4A)-C(5)-C(6)	121.7(11)
C(5)-C(6)-C(6A)	122.1(10)	C(6)-C(6A)-C(7)	125.7(9)
C(6)-C(6A)-C(10A)	117.4(7)	C(7)-C(6A)-C(10A)	116.9(9)
C(6A)-C(7)-C(8)	120.0(9)	C(7)-C(8)-C(9)	119.7(7)
C(8)-C(9)-N(10)	121.7(9)	Pt-N(10)-C(9)	128.4(7)
Pt-N(10)-C(10A)	112.3(4)	C(9)-N(10)-C(10A)	119.3(7)
C(6A)-C(10A)-N(10)	122.3(6)	C(6A)-C(10A)-C(10B)	120.2(8)
N(10)-C(10A)-C(10B)	117.5(7)	N(1)-C(10B)-C(4A)	121.9(6)
N(1)-C(10B)-C(10A)	116.8(7)	C(4A)-C(10B)-C(10A)	21.3(8)
Fe(1)-C(11)-O(11)	178.8(7)	Fe(1)-C(12)-O(12)	177.7(8)
Fe(1)-C(13)-O(13)	178.3(7)	Fe(2)-C(14)-O(14)	178.4(6)
Fe(2)-C(15)-O(15)	177.7(8)	Fe(2)-C(16)-O(16)	176.6(8)

examined in THF. $[Et_3BH][Li]$ and $[(sec\text{-}Bu)_3BH][K]$ react with **3** at -78 °C to give the thermally unstable cluster $[FeCo_2(CO)_9(\mu_2\text{-}PPhH)^-]$, [**8**$^-$], as a result of hydride attack at the μ_3-phosphinidene capping ligand and heterolytic scission of a Co-P bond. At -90 °C, ^{13}C NMR analysis of [**8**$^-$] reveals that the $Co(CO)_3$ groups display a single CO resonance due to rapid threefold carbonyl scrambling, the $Fe(CO)_3$ group bound by the μ_2-phosphido ligand exhibits three resolvable carbonyl resonances, indicating hindered threefold carbonyl scrambling about the iron center. Reduction of **3** with MeLi is suggested to proceed at a cobalt-bound CO group, giving the acyl cluster $[FeCo_2(CO)_8\{C(O)Me\}(\mu_3\text{-}PPh)^-]$, [**9**$^-$]. IR analysis reveals a 51:49 mixture of solvent-separated and acyl oxygen-$[Li^+]$ contact ion pairs, respectively at -70 °C. Use of the Grignard reagents t-BuMgCl or MeMgBr gives the 49-electron cluster $[FeCo_2(CO)_9(\mu_3\text{-}PPh)^{-\bullet}]$, [**10**$^{-\bullet}$]. [MeO][Li] reacts with **3** at a cobalt-bound CO group at -78 °C to furnish the methoxycarbonyl cluster $[FeCo_2(CO)_8\{C(O)OMe\}(\mu_3\text{-}PPh)^-]$, [**11**$^-$], which is shown by IR analysis to exist exclusively as an ester oxygen-$[Li^+]$ contact ion pair. ^{31}P NMR analysis suggests that [**11**$^-$] rearanges to the μ_2-methoxyphosphido cluster $[FeCo_2(CO)_9(\mu_2\text{-}PPhOMe)^-]$, [**14**$^-$], at ambient temperature as the major product. Treatment of **3** with methanolic $[Et_4N][OH]$ in THF at -70 °C gives the corresponding methoxycarbonyl and hydroxycarbonyl clusters

in a 55:45 ratio, respectively, as determined by IR band-shape analysis. All the IR spectroscopic data are summarized in Table 34. The reactivity and stability of these new anionic clusters are discussed in next chapter.

Table 34. Infrared Spectral Data in the Carbonyl Region for **1** and Related Anionic Clusters.[a]

$FeCo_2(CO)_9(\mu_3\text{-}PPh)$[b]	2101(s), 2059(vs), 2048(vs), 1981(s), 1969(s)
$FeCo_2(CO)_9(\mu_3\text{-}PPh)$	2093(s), 2050(vs), 2038(vs), 2030(sh), 2014(m), 1966(m)
$[FeCo_2(CO)_9(\mu_2\text{-}PPhH)^-]$	2037(m), 2011(w), 1985(vs), 1967(m), 1955(s), 1944(m), 1930(sh), 1799(w, br)
$[FeCo_2(CO)_9(\mu_2\text{-}PPhH)^-]$[c]	2040(m), 1985(vs), 1956(sh), 1778(w, b), 1724(vw, b)
$[FeCo_2(CO)_8\{C(O)Me\}(\mu_3\text{-}PPh)^-]$	2043(m), 2032(w), 1976(vs), 1966(sh), 1949(m), 1920(b), 1793(w), 1648(w, acyl-SSIP), 1595(w, acyl-CIP)
$[FeCo_2(CO)_8\{C(O)Me\}(\mu_3\text{-}PPh)^-]$[d]	2041(m), 2032(w), 1978(vs), 1961(sh), 1949(m), 1920(b), 1793(w), 1648(w, acyl-SSIP)
$[FeCo_2(CO)_9(\mu_3\text{-}PPh)^{-\bullet}][Cp_2Co]$[e]	2038(m), 1986(vs), 1975(vs), 1946(m, sh), 1920 (m)
$[FeCo_2(CO)_9(\mu_3\text{-}PPh)^{-\bullet}][MgCl]$	2044(m), 1978(vs), 1973(s, sh), 1966(s, sh), 1905(w, br)
$[FeCo_2(CO)_9(\mu_3\text{-}PPh)^{-\bullet}][Cp_2Co]$	2044(m), 1976(vs), 1972(s, sh), 1966(s, sh), 1901(w, br)
$[FeCo_2(CO)_8\{C(O)OMe\}(\mu_3\text{-}PPh)^-][Li]$	2051(m), 2036(m), 1994(vs), 1977(vs), 1952(m), 1928(m), 1797(w, br), 1582(w, ester-CIP)

Table34 continued

$[FeCo_2(CO)_8\{C(O)OMe\}(\mu_3\text{-}PPh)^-]^d$	2046(m), 2036(m), 1990(vs), 1978(vs), 1952(m), 1927(m), 1627(m, ester-SSIP)

[a]All spectra were recorded in THF at -70 °C unless otherwise noted. [b]Recorded in cyclohexane at room temperature. See Ref. 4. [c]Recorded in CH_2Cl_2 at -70 °C. [d]~10 mol equiv of 12-crown-4 present. [e]Recorded in 1,2-dichloroethane at room temperature. See Ref. 5.

CHAPTER REFERENCES

1. (a) Richmond, M. G.; Kochi, J. K. Inorg. Chem. **1986**, 25, 656. (b) Richmond, M. G.; Kochi, J. K. Organometallics **1987**, 6, 254.

2. (a) Astruc, D. Angew. Chem., Int. Ed. Engl. **1988**, 27, 643. (b) Chanon, M. Acc. Chem. Res. **1987**, 20, 214. (c) Chanon, M.; Tobe, M. L. Angew Chem., Int. Ed. Engl. **1982**, 21, 1. (d) Bunnett, J. F. Acc. Chem. Res. **1978**, 11, 413. (e) Saveant, J. M.; Acc. Chem. Res. **1980**, 13, 323.

3. (a) Narayanan, B. A.; Amatore, C.; Kochi, J. K. Organometallics **1987**, 6, 129; **1986**, 5, 926; **1984**, 3, 802. (b) Narayanan, B. A.; Amatore, C.; Casey, C. P.; Kochi, J. K. J. Am. Chem. Soc. **1983**, 105, 6351. (c) See also: Summer, C. E.; Nelson, G. O. J. Am. Chem. Soc. **1984**, 106, 432.

4. (a) Richter, F.; Beurich, H.; Vahrenkamp, H. J. Organomet. Chem. **1979**, 166, C5. (b) Muller, M.; Vahrenkamp, H. Chem. Ber. **1983**, 116, 2311.

5. Honrath, U.; Vahrenkamp, H. Z. Naturforsch. **1984**, 39b, 555.

CHAPTER IV

DISCUSSION

A. Kinetics of Ligand Substitution of Tetracobalt Cluster by Phosphine and Phosphite Ligands

The reaction under consideration is the substitution of a ligand for CO on $Co_4(CO)_{10}(\mu_4\text{-}PPh)_2$, [1], (eq 6).

$$\underset{\mathbf{1}}{Co_4(CO)_{10}(\mu_4\text{-}PPh)_2} + L \rightarrow \underset{\mathbf{4a\text{-}h}}{Co_4(CO)_9(L)(\mu_4\text{-}PPh)_2} + CO \qquad (6)$$

L = a: $P(OMe)_3$, b: $P(OEt)_3$, c: PPh_2H, d: $P(O\text{-}i\text{-}Pr)_3$, e: $P(n\text{-}Bu)_3$, f: PPh_3, g: $P(i\text{-}Pr)_3$, h: PCy_3.

The ligands used were $P(OMe)_3$, $P(OEt)_3$, PPh_2H, $P(O\text{-}i\text{-}Pr)_3$, $P(n\text{-}Bu)_3$, PPh_3, $P(i\text{-}Pr)_3$, and PCy_3. By following the decrease in the absorbance of $Co_4(CO)_{10}(\mu_4\text{-}PPh)_2$ at 2040 cm^{-1}, good pseudo-first-order kinetic plots were obtained for each of the ligands and the rate constants, k_{obsd}, were obtained from the slope. A plot of k_{obsd} vs. ligand concentration was linear with a non-zero intercept. This kinetic behavior is consistent with the following two-term rate law:

$$\text{Rate} = k_{obsd}\,[\text{Cluster}] = (\,k_1 + k_2[L]\,)\,[\text{Cluster}] \qquad (7)$$

The values of k_1 and k_2 were determined from the intercept and slope, respectively. Very significant differences in the relative values of k_1 and k_2 exist for these reactions. The results reveal that the ligand-dependent process (k_2 term) contributes more than 90% of the total rate at 1 M phosphine/phosphite concentrations. Further support for this bimolecular reaction derives from the activation parameters given in Table 17. The moderately low values of $\Delta H^{\ddagger}$ and negative $\Delta S^{\ddagger}$ values are consistent with an associative reaction that involves ligand attack on the cobalt cluster **1**.[1] The data suggest that the reaction of ligand with the cobalt cluster **1** leads to an adduct with an expanded cluster polyhedron (Scheme 4). Implicit in this formulation is the required scission of a carbonyl-bridged Co-Co bond coupled with the conversion of the associated μ_2-bridging CO group into a terminal CO group. Application of Polyhedral Skeletal Electron Pair (PSEP) theory[2-4] predicts that the closo cluster **1** should transform to the corresponding phosphinated nido cluster upon associative ligand addition.[5,6] The stability of these clusters is anticipated to be short based on the crystallographic results of the related nido aminomethylbis(difluorophosphine)-bridged cluster $Co_4(CO)_3(\mu_4\text{-}PPh)_2[CH_3N(PF_2)_2]_4$.[7] There the noncarbonyl-bridged Co-Co bonds and the carbonyl-bridged Co-Co bond are 0.19 and 0.06 shorter, respectively, than the corresponding

Scheme 4

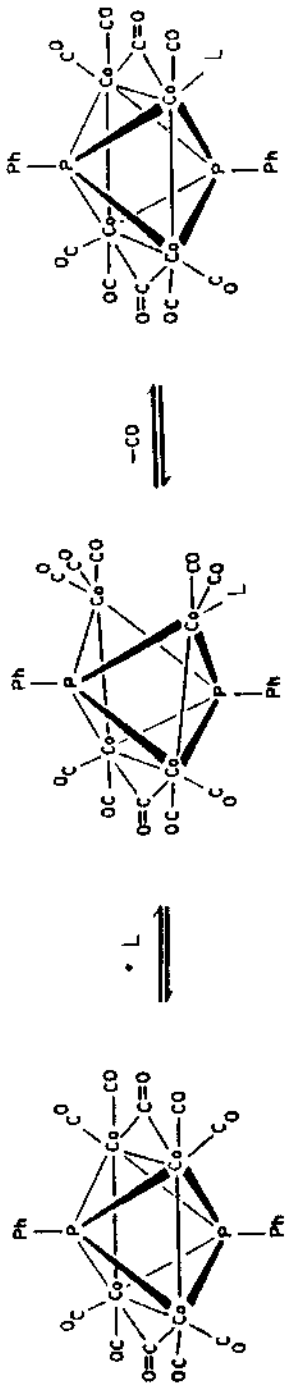

bonds in the closo parent cluster **1**.[8,9] Furthermore, the μ_4-P...μ_4-P nonbonded distance is reduced from 2.540(5) in **1** to 2.440(9) in $Co_4(CO)_3(\mu_4\text{-}PPh)_2[CH_3N(PF_2)_2]_4$[7] as the "optimum" Co-Co and Co-(μ_4)P distances and angels are perturbed upon adoption of the nido polyhedral structure. The observation of nido-$Co_4(CO)_3(\mu_4\text{-}PPh)_2[CH_3N(PF_2)_2]_4$ is possible due to the bridging nature of $CH_3N(PF_2)_2$ which promotes the stabilization of novel metal cluster polyhedra.[10] However, use of the monodentate ligand permits the formation of **4** upon CO loss and reformation of the Co-Co bond.

The minor unimolecular contribution to the rate law deserves special comment because the current studies provide additional evidence for a structural reorganization of cluster prior to phosphine capture. For large cone angle ligands ($\geq 145^\circ$), the majority of phosphine-independent substitution pathways involving metal clusters typically proceed via dissociative CO loss[11] (Scheme 5). The positive $\Delta S^\ddagger$ values obtained for the conversion of **1** → **4** using the ligands PPh_3, $P(i\text{-}Pr)_3$, and PCy_3 are consistent with a dissociative pathway. Further support for this dissociative pathway derives from the CO inhibition of **1** → **4f** (entry 11, 13, 15, 19; Table 7). However, for small cone angle ligands ($< 145^\circ$), the CO dissociation pathway is unlikely to be operative due to the negative $\Delta S^\ddagger$ values obtained for the conversion of **1** → **4** along with a lack of CO inhibition of

Scheme 5

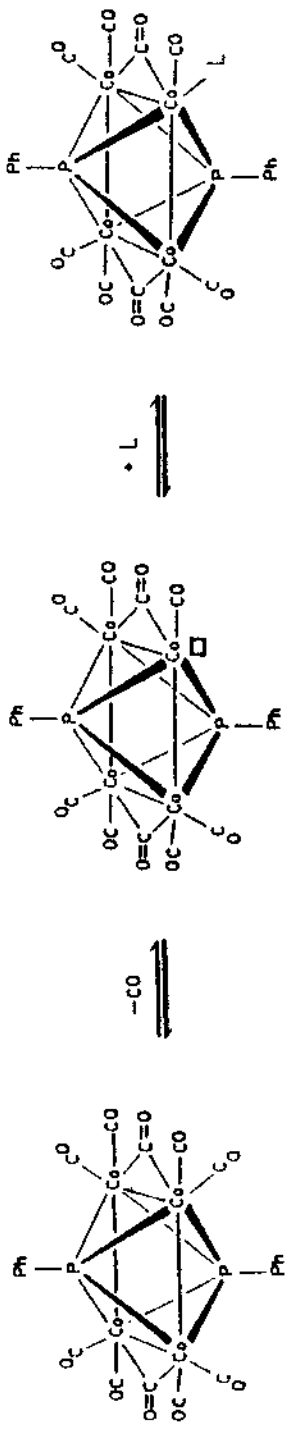

Scheme 6

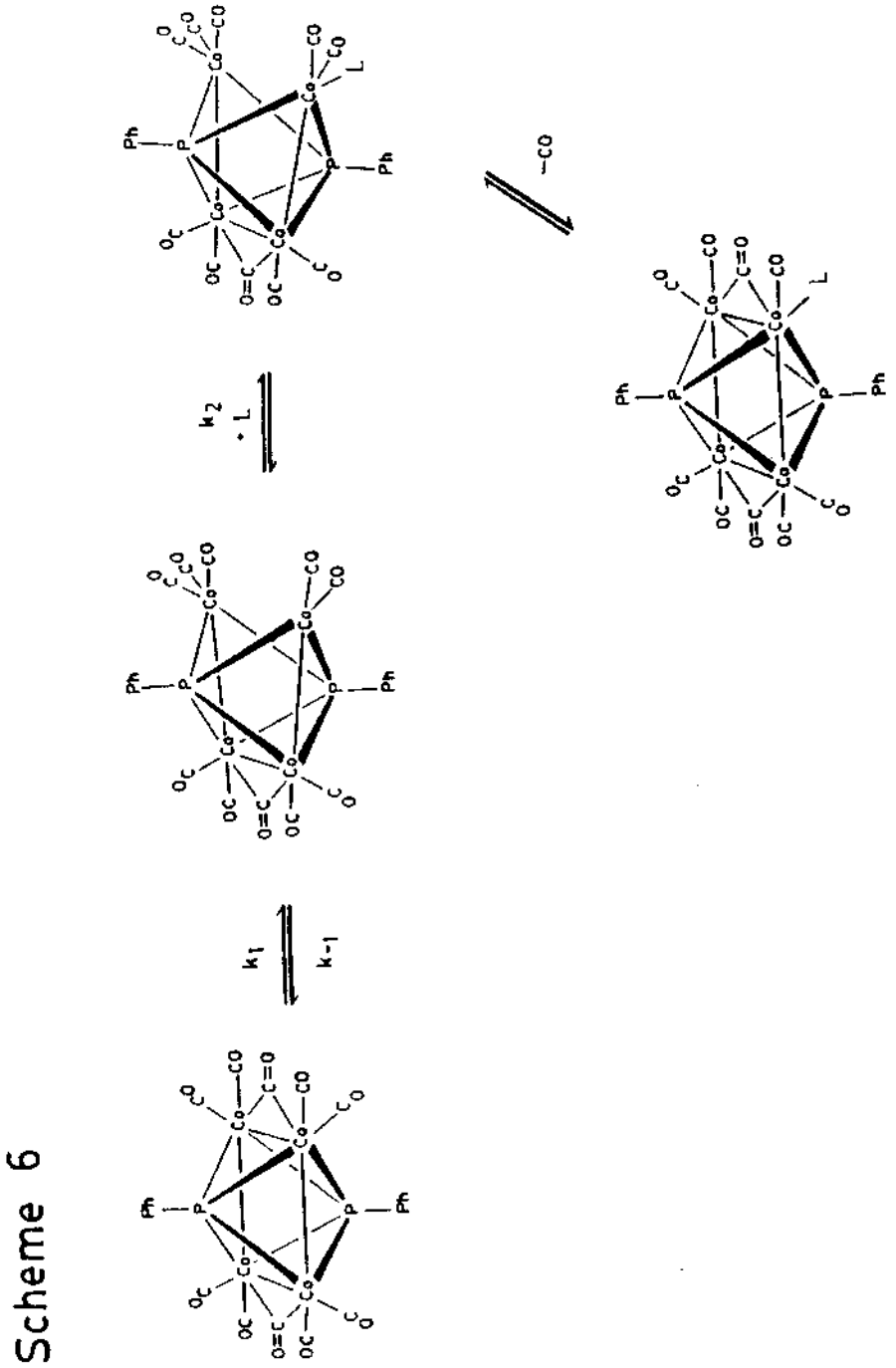

1 → **4b** (entry 7, table 5; entry 17, table 7), mandating a CO independent mechanism (Scheme 6). In this scheme $k_1 << k_{-1}$ and $k_{-1} << k_2$ is required for a reversible Co-Co bond scission process independent of saturation kinetics.[12,13]

The rearrangement in Scheme 6 may also be considered as a valence-tautomeric equilibrium which has been unequivocally demonstrated by Huttner and coworkers.[14,15] However, the observed activation entropies of these systems differ vastly from the tetrahedral clusters examined by Huttner. For example, the reversible scission of the Fe-Mn bond in $Cp(CO)_2MnFe_2(CO)_6(\mu_3\text{-}PPh)$ displays a positive activation entropy ascribed to the release of strain accompanying the formation of the intermediate edge-opened cluster. A four-vertex arachno cluster derived from a tetrahedran (Scheme 7).

Scheme 7

It is possible that an analogous valence tautomerism exists for the tetracobalt clusters **1**; however, with two

μ_4-phenylphosphinidene groups present it is not immediately clear that positive $\Delta S^{\ddagger}$ values should be expected.[16] Two μ_4-PPh groups are much more confining than the one μ_3-PPh group present in the Huttner clusters. Furthermore, if we consider the Co-Co bond scission in $Co_4(CO)_3(\mu_4\text{-}PPh)_2[CH_3N(PF_2)_2]_4$ (vide supra) as a rough indicator of the geometrical changes accompanying the cluster opening in Scheme 3, severe destabilizing structural perturbations are expected within the cluster core, coupled with an overall loss in the cluster's degrees of freedom. Such a rearrangement should, therefore, manifest itself in a negative $\Delta S^{\ddagger}$. Examples of unimolecular structural reorganizations displaying negative $\Delta S^{\ddagger}$ values are seen in the work of San Fillippo,[13] Marks,[17] Bryndza and Tam,[18] and Carpenter.[19]

B. X-Ray Crystallographic Structure of $Co_4(CO)_9(PCy_3)(\mu_4\text{-}PPh)_2$

The structure of $Co_4(CO)_9(PCy_3)(\mu_4\text{-}PPh)_2$ (Fig. 7) consists of four Co atoms in a planar, rectangular array and is capped by a pair of μ_4-phenylphosphinidene groups to give a closo octahedral core commonly observed in this genre of cluster. Asymmetric carbonyl-bridged and non-carbonyl-bridged Co-Co bonds are observed as a result of the destabilizing effect of the large PCy_3 ligand which possesses a cone angle of 170°.[20] At the site of PCy_3

substitution the carbonyl-bridged Co-Co bond length is 2.544 (2) Å while the non-carbonyl-bridged Co-Co bond is 2.806 (1) Å. These bond lengths are 0.018 (2) and 0.129 (1) Å longer than the opposite carbonyl-bridged and non-carbonyl-bridged Co-Co bonds, respectively. Similar bond length alterations have been observed in $Co_4(CO)_8(dmpe)(\mu_4\text{-}PPh)_2$[21] and $Co_4(CO)_8(Ph_2PCH{=}CHPPh_2)(\mu_4\text{-}PPh)_2$[22] and are attributed to unfavorable P-ligand/cluster interactions which are minimized through Co-Co bond lengthening.

Another indication of unfavorable intramolecular PCy_3/cluster interactions is seen in the disposition of the μ_4-phenylphosphinidene group that is <u>cis</u> to the PCy_3. The plane formed by the phenyl group bound to P(2) and the tetracobalt plane possesses a dihedral angle of 81.8(7)° which represents a tipping of 8.1(6)° between P(2)-C(20) and the normal to the tetracobalt plane. A near perpendicular relation of these planes is found in the parent cluster.[8,9] Furthermore, the twist angle between the μ_4-phenylphosphinidene groups is 77.3(8)°. The phenyl group associated with P(2) twists and tips from its preferred orientation (vide supra) as a result of close intramolecular contacts with the ancillary PCy_3 ligand.

The terminal Co-CO distances range from 1.763 (10) Å to 1.809 (11) Å while the bridging Co-CO distances are asymmetric, ranging from 1.906 (9) Å to 2.006 (9) Å. The remaining C-O, C-P, and C-C distances are unexceptional and

require no comment.

C. Synthesis of $Fe_2(CO)_6(\mu_3\text{-}S)_2Pt(L\frown L)$

A THF solution of $Fe_2(CO)_6(\mu\text{-}S)_2$, [**2**], was added 2 mol equiv of $[BEt_3H][Li]$ at -78 °C to produce the dianion $[Fe_2(CO)_6(\mu\text{-}S)_2]^{-2}$ in quantitative yield. When this dianion was treated with various $(L\frown L)PtCl_2$ (where L⁀L = 1,5-cod, bpy, 1,10-phen, diphos, dppf) in THF at -78 °C, no immediate reaction was observed. However, reaction did occur when reaction solution was allowed to warm to room temperature. The reaction is shown in equation 8. The isolated product yields range from 82-94%.

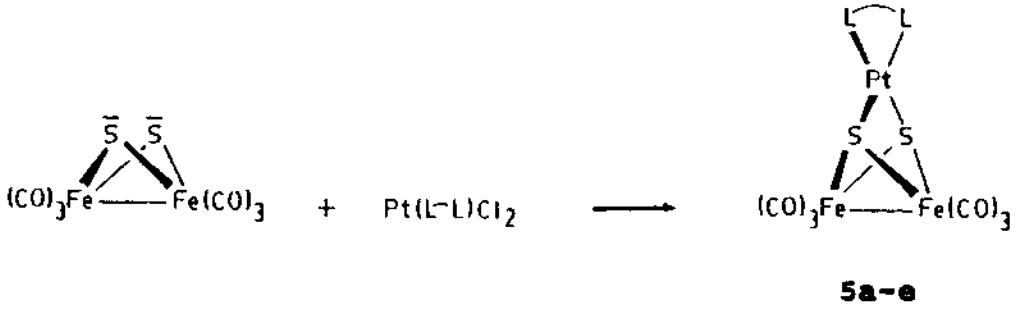

(8)

5a-e

L⁀L = a: 1,5-cod, b: bpy, c: 1,10-phen, d: diphos, e: dppf

The initial red colored solution of **2** becomes a deep red as the hydride is added and then dark emerald green when more than 1 molar equivalent of $[BEt_3H][Li]$ has been added. Addition of the second equivalent of the hydride produces no further color change. This supports a two-step sequence

where the first hydride adds to the disulfide linkage to give $[Fe_2(CO)_6(\mu_2\text{-}SH)(\mu_2\text{-}S^-)]$. Addition of the second equivalent of hydride serves to deprotonate the cluster thiol group and generate the desired dianion which exhibits a green color. Reaction of the green solution with various $(L\frown L)PtCl_2$ complexes causes a final color change back to red.

Polyhedral Skeletal Electron Pair (PSEP) Theory[2,3] predicts the formation of a nido cluster geometry when the products $Fe_2(CO)_6(\mu_3\text{-}S)_2Pt(L\frown L)$ are formmed. Most platinum complexes prefer a square planar geometry and are not predicted to adopt an arachno polyhedral geometry. However, further support for this arachno geometry derives from the X-ray results of $Fe_2(CO)_6(\mu_3\text{-}S)_2Pt(1,5\text{-cod})$ and $Fe_2(CO)_6(\mu_3\text{-}S)_2Pt(1,10\text{-phen})$.

D. Redox Reactivity of $Fe_2(CO)_6(\mu_3\text{-}S)2Pt(L\frown L)$

The reaction between $Fe_2(CO)_6(\mu_3\text{-}S)_2Pt(L\frown L)$, [**5**], ($L\frown L$ = 1,5-cod, bpy, 1,10-phen) and reducing agents was examined next. Treatment of **5a-c** in THF at -78 °C with 1.0 mol equiv of $[Et_3BH][Li]$ led to the generation of a new species in essentially quantitative yield determined by IR analysis. The low-temperature IR spectrum (-70 °C) exhibited carbonyl stretching bands that were shifted to lower frequency as relative to the parent cluster; these frequencies are listed in Table 24. Use of MeLi (1.0 mol equiv) also gave the same

IR spectrum. On the basis of the absence of a low frequency formyl (acyl) C-O stretching band between 1650-1500 cm^{-1},[23] a CO reduction pathway [i.e., Fe-CO → Fe-C(O)-H(Me)$^-$] can immediately be ruled out. The similarity of both IR spectra suggests that both reactions proceed by a single-electron transfer process to give the corresponding cluster radical anion $Fe_2(CO)_6(\mu_3\text{-}S)_2Pt(L\frown L)^{-\bullet}$ [**6**$^{-\bullet}$] as shown in Eqn 9.

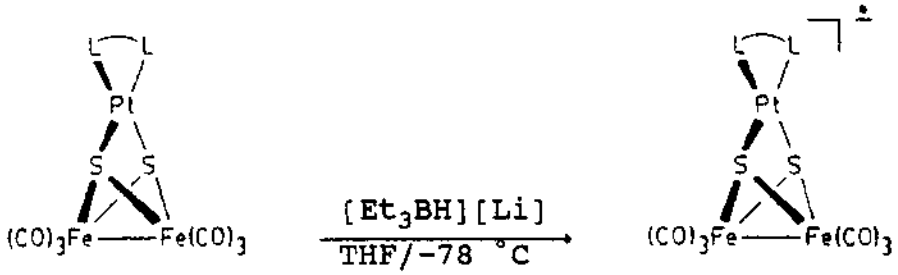

5a-c **[6a-c$^{-\bullet}$]** (9)

L⌢L = a: 1,5-cod, b: bpy, c: 1,10-phen

Figure 10 shows the low-temperature IR spectra of $Fe_2(CO)_6(\mu_3\text{-}S)_2Pt(1,5\text{-cod})$ and radical anion $Fe_2(CO)_6(\mu_3\text{-}S)_2Pt(1,5\text{-cod})^{-\bullet}$ obtained using $[Et_3BH][Li]$. Figure 11 shows the low-temperature IR spectra of $Fe_2(CO)_6(\mu_3\text{-}S)_2Pt(bpy)$ and radical anion $Fe_2(CO)_6(\mu_3\text{-}S)_2Pt(bpy)^{-\bullet}$ obtained using $[Et_3BH][Li]$. At no point in these reactions was any evidence obtained for the spectroscopic observation of reduction products derived from CO, μ_3-S, or direct metal (Fe or Pt) attack. Such intermediates could, however, serve as precursors to [**6**$^{-\bullet}$]. While hydrides and RLi reagents

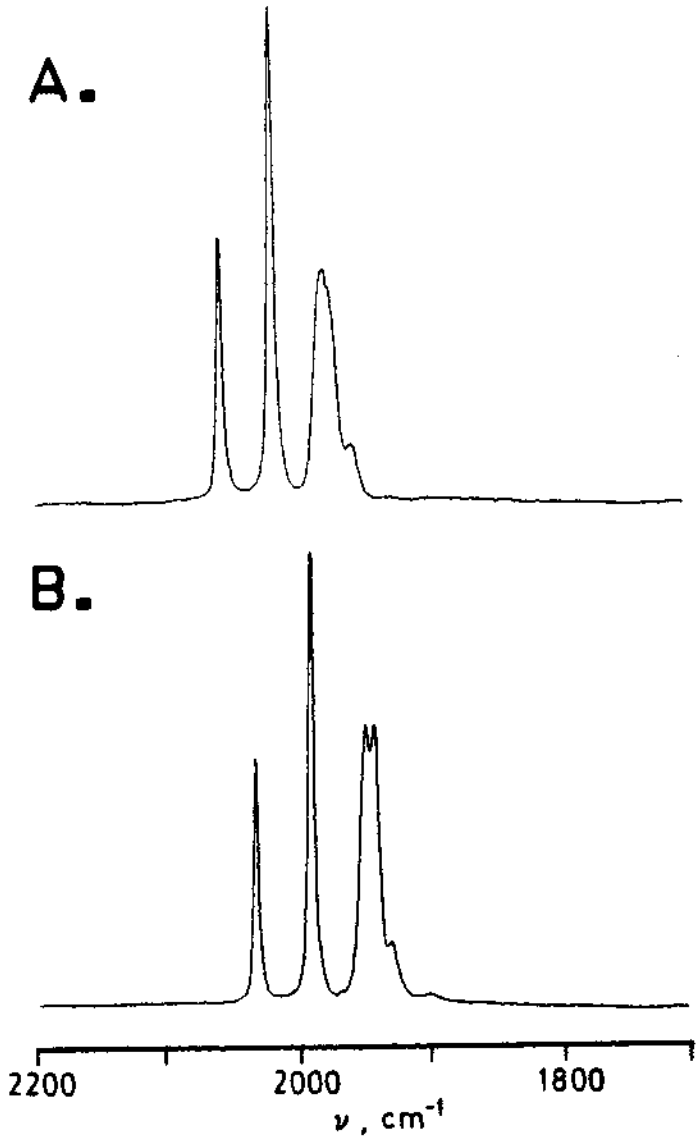

Figure 10. Infrared spectra of the carbonyl region for (a) $Fe_2(CO)_6(\mu_3\text{-}S)_2Pt(1,5\text{-cod})$ and (b) $[Fe_2(CO)_6(\mu_3\text{-}S)_2Pt(1,5\text{-cod})^{-\bullet}]$ at -70 °C in THF

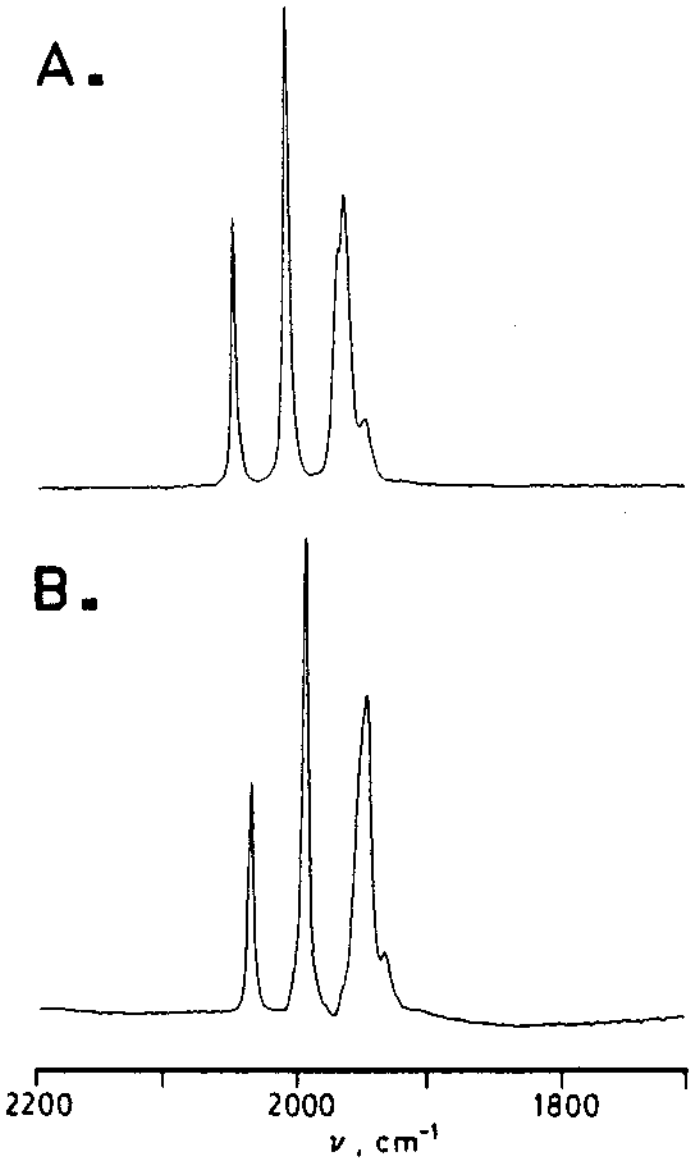

Figure 11. Infrared spectra of the carbonyl region for (a) $Fe_2(CO)_6(\mu_3\text{-}S)_2Pt(bpy)$ and (b) $[Fe_2(CO)_6(\mu_3\text{-}S)_2Pt(bpy)^{-\bullet}]$ at -70 °C in THF

typically function as two-electron reducing agents, there are ample literature precedents that these reagents function as single-electron reagents.[24] Moreover, similar reduction behavior has been observed with the known clusters $XCCo_3(CO)_9$ (where X = Ph, Me, Cl, and Br)[25] and $Fe_2(CO)_6(\mu_3\text{-}S)_2Cu(\eta\text{-}Cp^*)$.[26] Low-temperature IR studies (-78 °C) have shown that alkyl(aryl) lithiums and Grignard reagents react to give the known polynuclear radical anions.[27]

Confirmatory evidence for the existence of radical anion [**6**$^{-\bullet}$] derives from its independent generation using a known one-electron reducing agent. For example, the starting cluster **3** reacts with sodium naphthalide (1.0 mol equiv) in THF at -78 °C to give an IR spectrum identical to that obtained using [Li][Et_3BH] and MeLi. Figure 11 shows the low-temperature IR spectrum of radical anion [**6**$^{-\bullet}$] recorded using sodium naphthalide. The IR spectrum of radical anion [**6**$^{-\bullet}$] obtained from sodium naphthalide resembles that of starting cluster **5**, except for the expected low frequency shift in the CO bands of radical anion relative to the starting cluster. The spectral similarity between the starting cluster **5** and radical anion [**6**$^{-\bullet}$] indicates that radical anion [**6**$^{-\bullet}$] maintains an arachno polyhedron upon electron accession. This trend is well documented in other chemical and electrochemical reduction reactions involving closo and nido clusters.[27]

The frequencies of the CO bands in $Fe_2(CO)_6(\mu_3\text{-}S)_2Pt(1,5\text{-cod})^{-\bullet}$ are ~25 cm^{-1} lower in frequencies relative to the parent cluster. The frequencies of the CO bands in $Fe_2(CO)_6(\mu_3\text{-}S)_2Pt(bpy)^{-\bullet}$ and $Fe_2(CO)_6(\mu_3\text{-}S)_2Pt(1,10\text{-phen})^{-\bullet}$ are ~15 cm^{-1} lower in frequencies relative to the parent cluster. Interestingly enough, this same trend is also observed in the related paramagnetic arachno cluster $Fe_2(CO)_6(\mu_3\text{-}S)_2Cu(\eta\text{-}Cp^*)^{-\bullet}$.[26] Other well-documented examples of paramagnetic clusters reveal a ~60 cm^{-1} shift in the C-O stretching bands to lower frequencies relative to the neutral parent cluster.[28] The magnitude of the observed CO shift in the latter paramagnetic clusters is presumably a manifestation of complete electron delocalization over the polyhedral core, consistent with such clusters functioning as class III charge-transfer complexes.[29] Although the exact reason(s) why the CO bands of radical anion and the related arachno platinum analogues (vide supra) do not exhibit a 60 cm^{-1} low frequency shift is not known, it is likely that the odd electron is not completely delocalized over the two $Fe(CO)_3$ centers. Such a situation would minimize the amount of π^* backbonding available to the $Fe(CO)_3$ groups, resulting in only small CO frequency shifts. The extent of electron delocalization in this family of paramagnetic clusters is currently being examined using electrochemical and epr techniques.[30]

Radical anion [**6**$^{-\bullet}$] is thermally unstable. Upon warming to room temperature, radical anion [**6**$^{-\bullet}$] decomposes to form starting cluster with material loss. Using $[Cp_2Fe][BF_4]$ (1.1 equiv) Radical anion [**6**$^{-\bullet}$] may be oxidized to reform starting cluster in 88% yield and, thus, reinforcing the paramagnetic nature of radical anion.

The reaction between **5** (L⌒L = diphos, dppf) and reducing agents was also investigated. However, the corresponding radical anion was not observed, suggesting that the 0/-1 reduction couple occurs at a more negative potential than the non-phosphinated clusters.

5 (L⌒L = 1,5-cod, bpy, 1,10-phen, diphos, dppf) was also examined with oxidizing agents. Treatment of **5** in CH_2Cl_2 at -78 °C with 1.0 mol equiv of magic green led to the generation of a new species in essentially quantitative yield based on IR analysis. The low-temperature IR spectrum (-70 °C) exhibited the carbonyl stretching bands shifted to higher frequency; these carbonyl bands are listed in Table 25. Use of $Fe(1,10\text{-phen})_3^{3+}$ (1.0 mol equiv) in acetone solvent also gave a similar IR spectrum. Magic green and $Fe(1,10\text{-phen})_3^{3+}$ are known one-electron oxidizing agents.[31,32] Both reactions proceed by a single-electron transfer mechanism to give the corresponding cluster radical cation $Fe_2(CO)_6(\mu_3\text{-}S)_2Pt(L⌒L)^{+\bullet}$ [**7**$^{+\bullet}$] as shown in Eqn 10. Figure 12 shows the low-temperature IR spectra of neutral

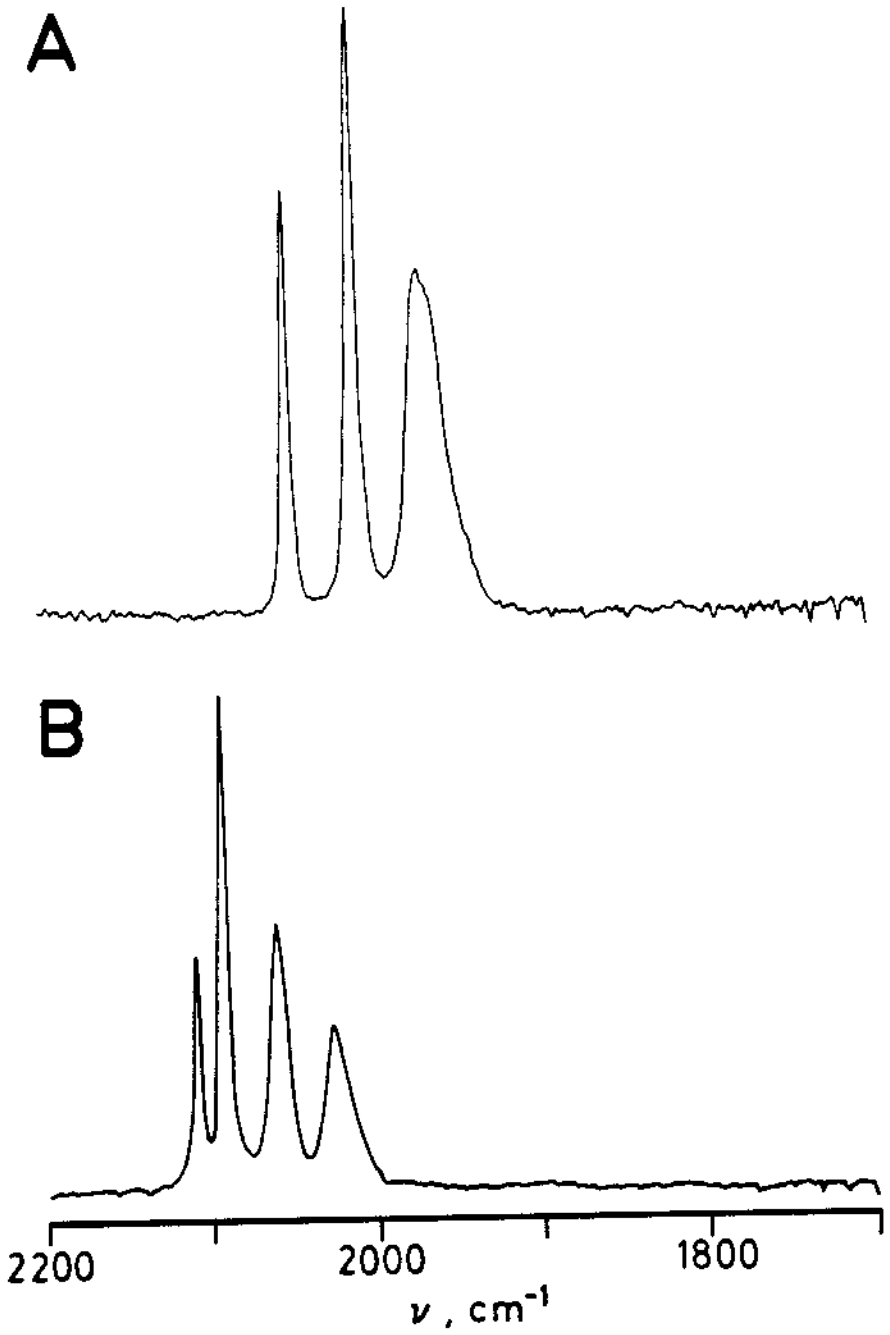

Figure 12. Infrared spectra of the carbonyl region for (a) $Fe_2(CO)_6(\mu_3\text{-}S)_2Pt(diphos)$ and (b) $[Fe_2(CO)_6(\mu_3\text{-}S)_2Pt(diphos)^{+2}]$ at -70 °C in CH_2Cl_2

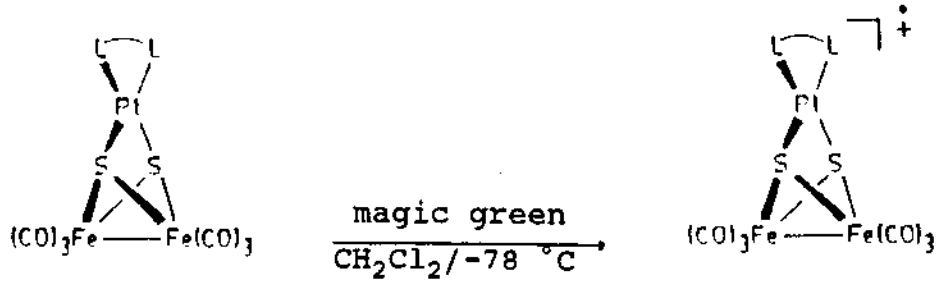

(10)

5a-e **[7a-e$^{+\bullet}$]**

L⌒L = a: 1,5-cod, b: bpy, c: 1,10-phen, d: diphos, e: dppf

$Fe_2(CO)_6(\mu_3\text{-}S)_2Pt$(diphos) and the radical cation $Fe_2(CO)_6(\mu_3\text{-}S)_2Pt(diphos)^{+\bullet}$, obtained using magic green. Slight difference in IR frequencies are observed for the radical cation depending on which solvent is used in the oxidation reaction. These small frequency differences are ascribed to a solvent effect. Upon oxidation, the neutral cluster's carbonyl bands shift ca. 80 ~ 100 cm^{-1} to higher frequencies (Table 25); this is expected due to the decrease in the ability of the metal to back donate electron density into the π^* orbitals of the CO ligands. A ~100 cm^{-1} high frequency shift in the C-O stretching bands of mononuclear cation radicals, relative to the neutral compounds, have been reported.[33]

All radical cations [7$^{+\bullet}$] are thermally unstable. Upon warming to room temperature, the radical cations [7$^{+\bullet}$] decompose to give small amount of starting cluster with

considerable material loss. The radical cations [$7^{+\bullet}$] may be reduced back to starting cluster using Cp_2Co (1.1 mol equiv) in 70% yield and, thus, reinforcing the paramagnetic nature of radical cation.

E. X-Ray Crystallographic Structure of $Fe_2(CO)_6(\mu_3\text{-}S)_2Pt(1,5\text{-cod})$

The structure of $Fe_2(CO)_6(\mu_3\text{-}S)_2Pt(1,5\text{-cod})$ (Fig. 9) was elucidated by single-crystal X-ray diffraction techniques. Final atomic coordinates and isotropic thermal parameters are given in Table 27. Bond lengths and angles are given in Tables 28 and 29. The metallic framework of this cluster is an isosceles triangle, the base of which is defined by a 2.501(2) Å Fe-Fe bonding edge and the two sides by the long nonbonding Fe•••Pt vectors. Each iron is pseudooctahedral, the coordination sphere being comprised of three carbonyls, two sulfur atoms, and one Fe-Fe bond. The platinum atom is in a square-planar environment containing cis sulfur atoms and the olefinic carbon atoms. One significant difference between $Fe_2(CO)_6(\mu_3\text{-}S)_2Pt(1,5\text{-cod})$ and $Fe_3(CO)_9(\mu_3\text{-}S)_2$[34], is that in the Fe_2Pt case, each sulfur atom functions as a formal three-electron donor to the mutually bonded iron atoms. A valence bond representation for $Fe_3(CO)_9(\mu_3\text{-}S)_2$, [**15**], however, suggests that 3 e^- donation by each S atom is directed to the pair of irons which are not mutually bonded, and furthermore, no reasonable structure can be drawn which involves a sulfur

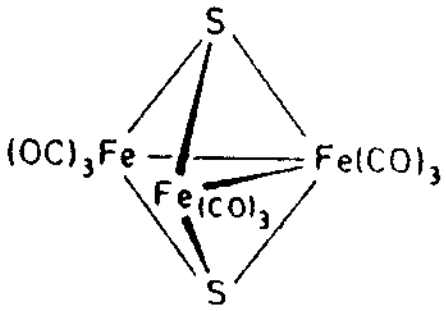

15

atom functioning as an electron-pair ($2e^-$) donor to the unique iron atom. There are no significant diferences observed between the apical and basal carbonyl bond lengths in $Fe_2(CO)_6(\mu_3\text{-}S)_2Pt(1,5\text{-cod})$. The mean Fe-C and C-O bond lengths for the six Fe-CO groups of 1.79 (1) Å and 1.14 (1) Å, respectively, are reasonably close to the mean Fe-C and C-O values of 1.78 (1) Å and 1.14 (1) Å, respectively, found for $Fe_2(CO)_6(\mu_3\text{-}S)_2$. All six Fe-C-O bond angles do not deviate significantly from linearity (within the range of 5°).

F. X-Ray Crystallographic Structure of $Fe_2(CO)_6(\mu_3\text{-}S)_2Pt(1,10\text{-phen})$

The structure of $Fe_2(CO)_6(\mu_3\text{-}S)_2Pt(1,10\text{-phen})$ (Fig. 10) was elucidated by single-crystal X-ray diffraction techniques. Final atomic coordinates and isotropic thermal parameters are given in Table 31. Bond lengths and angles are given in Tables 32 and 33. The metallic framework of

this cluster is similar as $Fe_2(CO)_6(\mu_3\text{-}S)_2Pt(1,5\text{-cod})$ except that the platinum atom is bonded to two nitrongen atoms. Fe-Fe bond distance is 2.492 (2) Å. The mean Fe-C and C-O bond lengths for the six Fe-CO groups of 1.78 (1) Å and 1.14 (1) Å, respectively, are close to the mean Fe-C and C-O values of $Fe_2(CO)_6(\mu_3\text{-}S)_2$ and $Fe_2(CO)_6(\mu_3\text{-}S)_2Pt(1,5\text{-cod})$. All six Fe-C-O bond angles do not deviate significantly from linearity (within the range of 3°).

G. Reactivity Studies of $FeCo_2(CO)_9(\mu_3\text{-}PPh)$

1. Reaction of $FeCo_2(CO)_9(\mu_3\text{-}PPh)$ with Hydrides

Treatment of a red-brown solution of $FeCo_2(CO)_9(\mu_3\text{-}PPh)$, **3**, in THF with 1.0 mol equiv of $[Et_3BH][Li]$ at -70 °C immediately affords a dark brown solution containing $[FeCo_2(CO)_9(\mu_2\text{-}PPhH)^-]$, [**8**$^-$], as the sole product based on *in situ* IR and NMR analyses. The low-temperature IR spectrum of [**8**$^-$] revealed carbonyl stretching bands at 2037(m), 2011(w), 1985(vs), 1967(m), 1955(s), 1944(m), 1930(sh), and 1799(w,br) cm^{-1} (see Figure 13a). These ν(CO) bands are shifted to lower frequency in comparison to the parent cluster, supporting the ascription of [**8**$^-$] as an anionic cluster. No formyl ν(CO) band was observed in the 1520-1630 cm^{-1} region of the IR spectrum,[23] which strongly suggests that hydride attack on a terminal CO group is an unimportant pathway. Use of $[(sec\text{-}Bu)_3BH][K]$ as the reducing agent yielded an IR spectrum that was identical to

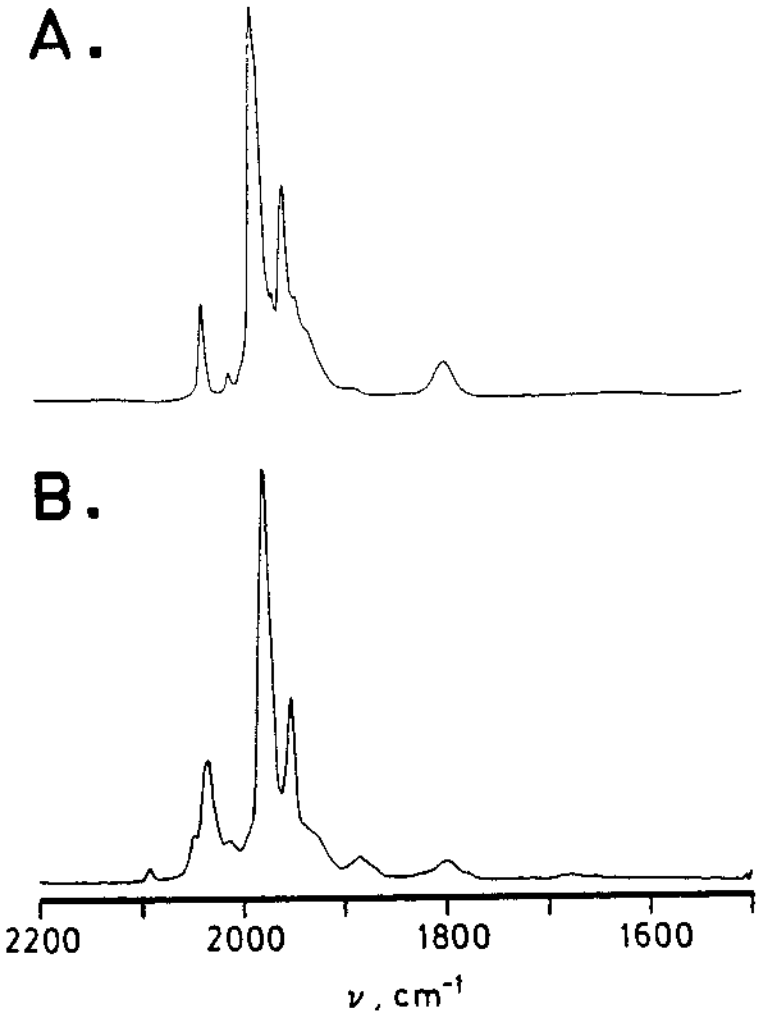

Figure 13. Infrared spectra of the carbonyl region for (a) $[FeCo_2(CO)_9(\mu_2\text{-}PPhH)^-]$ at -78 °C and (b) $[FeCo_2(CO)_9(\mu_2\text{-}PPhOMe)^-]$ at -5 °C. Both spectra were recorded in THF

that obtained with $[Et_3BH][Li]$. The IR spectral similarity of $[\mathbf{8}^-]$ using these two different trialkylborohydrides indicates that $[\mathbf{8}^-]$ exists as solvent-separated ion pair (SSIP), a feature easily confirmed through the addition of HMPA to a THF solution of $[\mathbf{8}^-]$.[35]

The unequivocal identity of $[\mathbf{8}^-]$ was ascertained by using low-temperature $^{31}P\{^1H\}$ NMR spectroscopy. The $^{31}P\{^1H\}$ resonance of **3** at -80 °C in THF/benzene-d_6 (5:1, v/v) appears as a singlet at δ 429.3, consistent with a μ_3-PPh group ligating the triangular face of the $FeCo_2$ cluster. This resonance is replaced by a singlet at δ 143.2 (d, J_{P-H} = 356 Hz) when treated with $[Et_3BH][Li]$. The observed ^{31}P doublet, which was obtained from a gated-decoupled spectrum, clearly establishes the attachment of the hydride at the μ_3-phosphinidene group in **3**, with further support derived from the high-field shift of the ^{31}P resonance that is typical for μ_2-phosphido moieties.[28d,36-39] Equation 11 depicts the proposed course of this reaction.

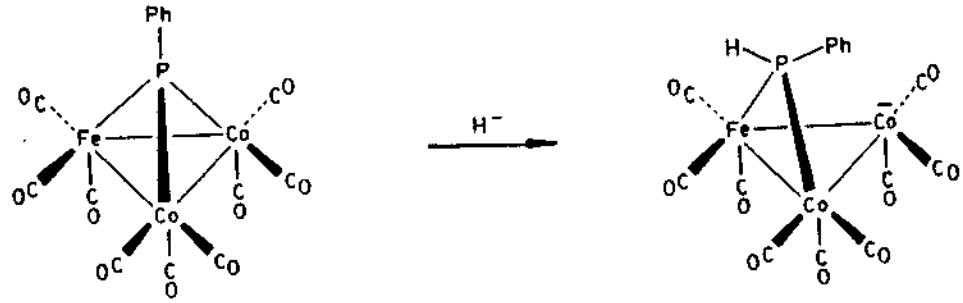

(11)

3 **8**$^-$

Hydride accession in **3** is depicted to occur anti with respect to the heterolytically cleaved Co-P bond. This stereochemistry is consistent with the course of hydride addition reported for the nido cluster $Fe_3(CO)_9(\mu_3\text{-}PPh)_2$.[28d] At low temperature hydride addition was shown to give $[Fe_3(CO)_9(\mu_3\text{-}PPh)(\mu_2\text{-}PPhH)^-]$, as a result of cleavage of the Fe_{basal}-P bond. These reactions bear resemblance to S_N2 reactions, where the entering and leaving groups are oriented anti or trans to each other. A formal inversion of the phosphorus center requires the phenyl group to adopt a position directly over the face of the cluster.[38h] It is now well documented that phosphido and phosphinidene tethering ligands are not, as a rule, chemically inert, especially under reducing conditions. In contrast to the many reports involving anion-induced cleavage of μ_2-phosphido-metal bonds,[37,38] compounds possessing μ_3-phosphinidene ligands have remained relatively unexplored. With the exception of two reports dealing with the transformation of a phosphinidene → phosphido linkage in homonuclear clusters,[28d,39] this study represents the first example of a hydride-induced μ_3-PPh → μ_2-PPhH conversion in a heterometallic cluster.

The slow exchange ^{13}C NMR spectrum of a ^{13}CO enriched sample of **3** (-80 °C; toluene-d_8) exhibits three carbonyl resonances at δ 218.7, 211.6, and 201.0 in an integral ratio of 1 : 2 : 6, respectively. Rapid threefold carbonyl

scrambling renders all the Co-CO groups equivalent and readily assignable to the highest-field resonance, while frozen Fe-CO motion allows for the observation of distinct axial and equatorial CO groups.[40] The $^{13}C\{^1H\}$ NMR spectrum of [**8**$^-$], prepared from ^{13}CO enriched **3**, reveals five carbonyl resonances at -90 °C in agreement with the proposed structure of [**8**$^-$]. Figure 14 shows the low-temperature ^{13}C NMR spectrum of [**8**$^-$]. The resonances at δ 208.6 and 221.8, both of which integrate for 3 CO groups, are assigned to the neutral and anionic $Co(CO)_3$ centers, respectively. Localized $Co(CO)_3$ rotation is rapid at both cobalt centers as observed in all structurally similar tetrahedrane clusters containing $Co(CO)_3$ vertices.[40,41] Two one carbon resonances at δ 214.0 and 215.8 derive from the unique equatorial CO groups of the $Fe(CO)_3$ moiety. No attempt has been made to specifically assign these resonances. The doublet resonance (1 CO) centered at δ 222.9 (J_{P-C} = 18.5 Hz) is ascribed to the axial Fe-CO group, on the basis of the near trans diaxial relationship that is expected for the μ_2-phosphido and axial Fe-CO groups.[28d]

2. Reaction of $FeCo_2(CO)_9(\mu_3\text{-}PPh)$ with MeLi

3 reacts with one equiv of MeLi in THF to give a black solution containing the acyl cluster [$FeCo_2(CO)_8\{C(O)Me\}(\mu_3\text{-}PPh)^-$], [**9**$^-$]. At -70 °C the IR spectrum of [**9**$^-$] displayed terminal ν(CO) bands at 2043(m), 2032(w), 1976(vs), 1966(sh), 1949(m), 1920(b), and 1793(w) cm^{-1} in addition two

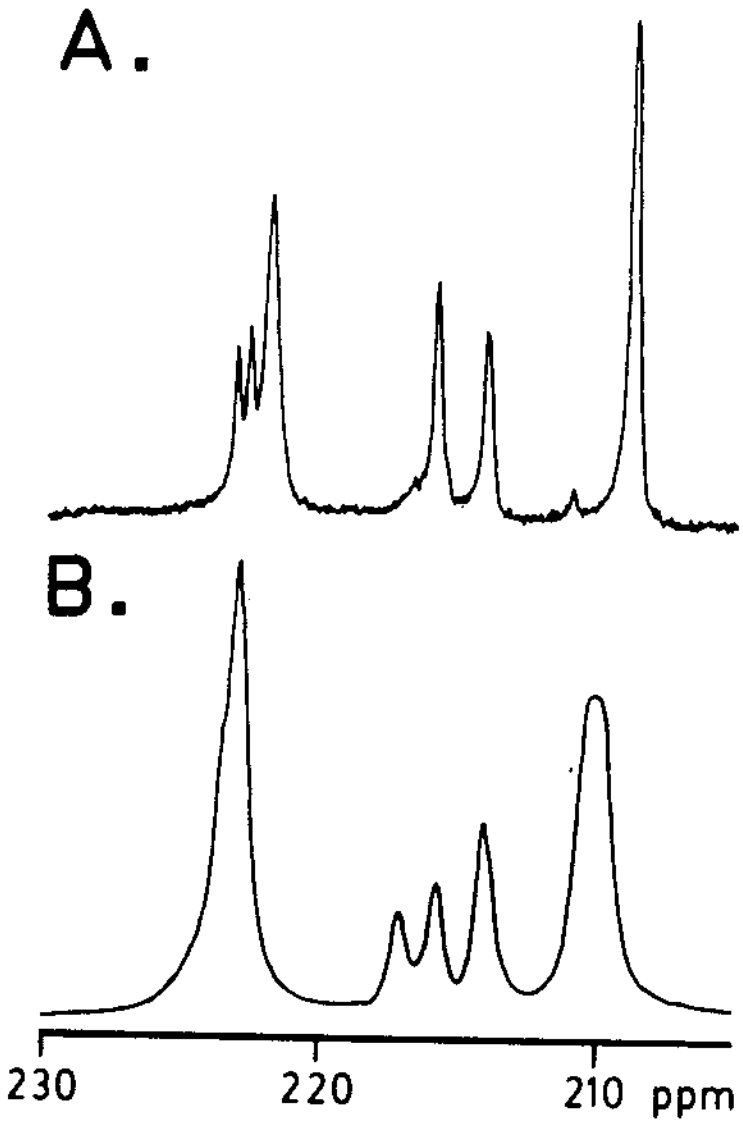

Figure 14. $^{13}C\{^{1}H\}$ NMR spectra of (a) $[FeCo_2(CO)_9(\mu_2\text{-}PPhH)^-]$ and (b) $[FeCo_2(CO)_8\{C(O)OMe\}(\mu_3\text{-}PPhH)^-]$. Both spectra were recorded in 2-MeTHF/benzene-d_6 (5:1) at -90 °C

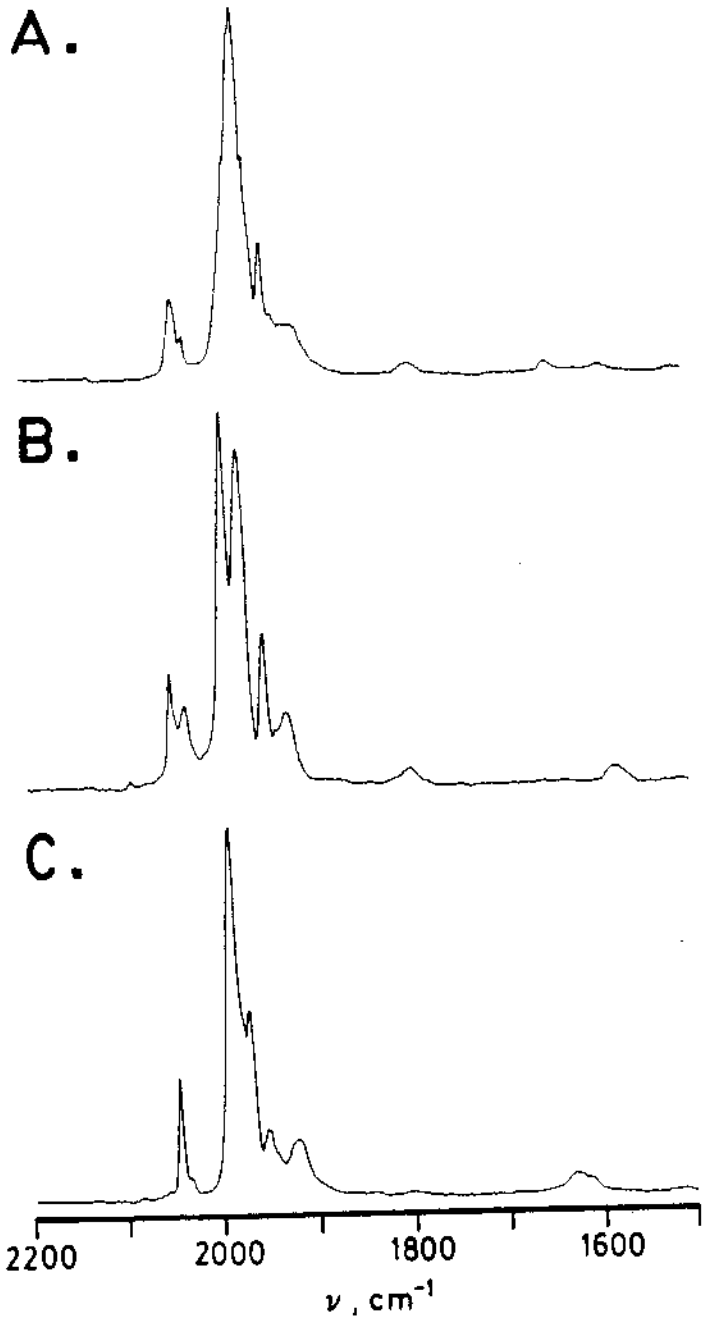

Figure 15. Infrared spectra of the carbonyl region for (a) $[FeCo_2(CO)_8\{C(O)Me\}(\mu_3\text{-}PPh)^-]$, (b) $[FeCo_2(CO)_8\{C(O)OMe\}(\mu_3\text{-}PPh)^-]$, and (c) $[FeCo_2(CO)_8(CO_2H)(\mu_3\text{-}PPh)^-]$. All spectra were recorded in THF at -70 °C

weak acyl ν(CO) bands at 1648 and 1595 cm^{-1} as shown in Figure 15a. The ratio of these acyl bands was determined via IR band-shape analysis which revealed a 51:49 ratio. When ~10 mol equiv of 12-crown-4 was added to [**9**$^-$] the latter acyl band disappeared completely while the former band grew in intensity. This behavior is indicative of an anionic metal-acyl moiety that exists as solvent-separated and acyl oxygen-[Li^+] contact ion pairs (CIP).[15,42,43] Disruption of the acyl oxygen-[Li^+] CIPs by 12-crown-4 is a well-established phenomenon that allows for the unambiguous assignment of both types of ion pairs present in solution.[28e] The observation of such ion pairs in polynuclear [**9**$^-$] is rare[44] in comparison to the many examples of ion pairing in mononuclear complexes.[35] Presumably, the dearth of data on cluster CIPs results from a greater electron delocalization of the anionic charge over the cluster's polyhedral core versus mononuclear complexes, which is in keeping with the electron reservoir properties of polynuclear clusters.[45] The IR data of the various clusters are summarized in Table 34.

A single broad $^{31}P\{^1H\}$ NMR resonance at δ 405.7 was observed for [**9**$^-$] at -78 °C, consistent with the presence of a μ_3-PPh group. In order to define the site of the acyl group, the $^{13}C\{^1H\}$ NMR spectrum of [**9**$^-$], prepared from ^{13}CO enriched **3** and MeLi, was examined. Unfortunately, the carbonyl resonances were extremely broad at -90 °C,

preventing a meaningful interpretation. This behavior most likely results from rapid carbonyl exchange about the cluster polyhedron, as has been observed with other $FeCo_2$ tetrahedrane clusters.[46] Support for this premise is found with the methoxycarbonyl cluster [**11**$^-$], which also displays very broad but discernable ^{13}C NMR resonances (vide infra).

At this time the site of the acyl moiety cannot unambiguously be assigned on the basis of the spectroscopic data. However, it is noted that the bicapped cluster $Fe_2Co_2(CO)_{11}(\mu_4\text{-PPh})_2$ has been shown to react with hydrides and MeLi, yielding anionic Co-CHO and Co-C(O)Me clusters, respectively.[47] This last report allows for the formulation of a cobalt-bound acyl group in **9**$^-$ as shown in Equation 12.[48]

(12)

3 **9**$^-$

3. Reaction of $FeCo_2(CO)_9(\mu_3\text{-PPh})$ with Grignard Reagents

When **3** (in THF) is treated with a slight excess of

t-BuMgCl at -78 °C a green solution is immediately obtained. IR analysis at -70 °C reveals the complete conversion to a compound with ν(CO) bands that are shifted to lower frequency relative to the parent cluster as shown in Table 34. The same product was also seen when MeMgBr (>3.5 mol equiv) was used, whereas no reaction was discerned at -78 °C when Me_3SiCH_2MgCl was used (5.0 mol equiv). Moreover, added $[CF_3SO_3][Li]$ or $[Ph_4B][Na]$ did not affect the course of this reaction. The lack of an observable acyl band(s) and the grossly different symmetry associated with the ν(CO) bands of this green material compared to the spectra of [**8**$^-$] and [**9**$^-$] argue against the attack of the Grignard reagent at the μ_3-PPh capping ligand or a terminal CO group. Since Grignard and organolithium reagents have been reported to function as single-electron transfer reagents in other organometallic complexes,[24a,26,49,50] $[FeCo_2(CO)_9(\mu_3\text{-}PPh)^{-\bullet}]$, [**10**$^{-\bullet}$], was independently synthesized from **3** and Cp_2Co and examined by IR analysis.[27] All of these IR spectra were identical within experimental error, which serves to establish the course of the reaction as shown in Equation 13. Samples containing [**10**$^{-\bullet}$] could also be oxidized back to **3** at -78 °C by using $[Cp_2Fe][BF_4]$, a reaction that supports the existence of the radical anion derived from **3**.

The reactivity described here may be contrasted with the isoelectronic and isolobal tricobalt clusters $Co_3(CO)_9(\mu_3\text{-}CR)$ (where R = H, Me, Ph, Cl, Br) which react

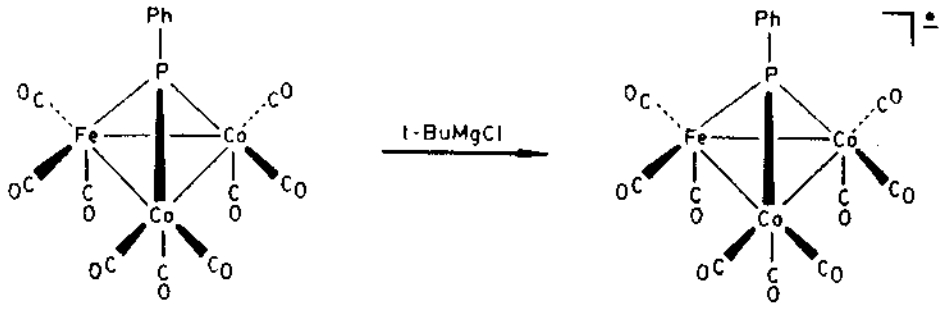

(13)

3 **$10^{-\bullet}$**

with MeLi at -78 °C to afford the corresponding radical anions [$RCCo_3(CO)_9^{-\bullet}$] without spectroscopically observable acyl clusters.[25] While the exact role played by the reducing agent and the initial cluster remains unknown at this time, subtle differences in these two variables are undoubtedly responsible for determining the preference for the $1e^-$ (set) or $2e^-$(polar) pathway.

The formation of [**$10^{-\bullet}$**] from **3** and t-BuMgCl (or MeMgBr) may be viewed as arising from either an outer- or inner-sphere electron-transfer mechanism.[29c,51] The latter manifold is favored, which presumably proceeds through the intimate complexation of **3** and RMgX in much the same fashion as reported for the reaction of ketones with Grignard reagents.[52] Here Grignard coordination at a carbonyl oxygen would be required prior to the formal electron-transfer step. Such a sequence is akin to the electron-transfer reactions reported for donor-acceptor complexes.[53]

Alternatively, if the acyl cluster $[FeCo_2(CO)_8\{C(O)R\}(\mu_3\text{-}PPh)^-]$ (where R = Me, t-Bu), formed by RMgX attack on a terminal CO group, underwent a homolytic C-C (acyl-R) bond cleavage, [**10**$^{-\bullet}$] and R• would be produced. Similar C-H formyl bond cleavages have been suggested as a route to paramagnetic clusters, provided that the accompanying R• (or H•) is efficiently extricated from the reaction by common radical deactivation steps.[28e,54,55] However, this pathway is considered unimportant given the characterization and stability (vide infra) of the acyl cluster [**9**$^-$]. Finally, the small scale of these reactions has prevented the characterization and assessment of the fate of the presumed organic radicals. Dimerization and/or hydrogen atom abstraction from the THF solvent represent the most likely consumption reactions for these radicals.[56]

4. Reaction of $FeCo_2(CO)_9(\mu_3\text{-}PPh)$ with [MeO][Li] and $[Et_4N][OH]$

The reaction of **3** in THF with one mol equiv of [MeO][Li] (1.3 M in MeOH) yields the purple methoxycarbonyl cluster $[FeCo_2(CO)_8\{C(O)OMe\}(\mu_3\text{-}PPh)^-]$, [**11**$^-$], in quantitative yield at -78 °C. Qualitatively, the low-temperature IR spectrum of [**11**$^-$] mirrors that of [**9**$^-$] as seen by the similar ν(CO) data in Table 1 and comparison of the IR spectra in Figures 15a and 15b. This suggests that methoxide attack occurs at a Co-CO group to give a cobalt

bound methoxycarbonyl moiety. Equation 14 illustrates the course of this reaction.

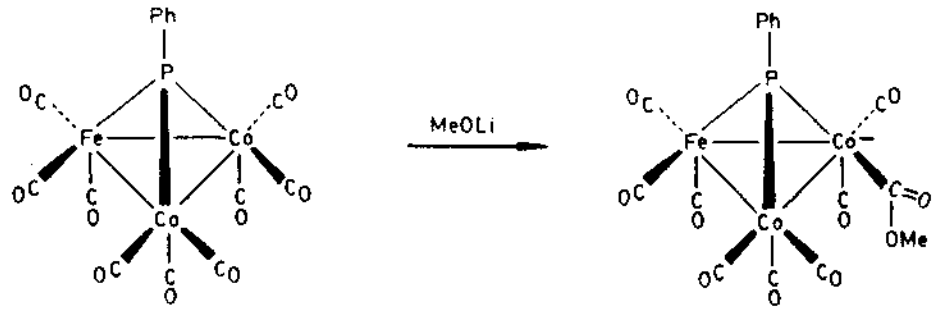

3 **11⁻** (14)

The observation of only one low-frequency ν(CO) band at 1582 cm^{-1} and its shift to 1627 cm^{-1} upon the addition of 12-crown-4 reveals that the initial cluster exists exclusively as a CIP within the limits of IR detection.[34,57] A significant contribution from the alkoxy-carbene resonance structure (shown below) is important in determining the ground-state structure of [**11**][Li]. Table 34 lists the frequency of the C-O stretching bands of [**11**][Li] and [**11⁻**].

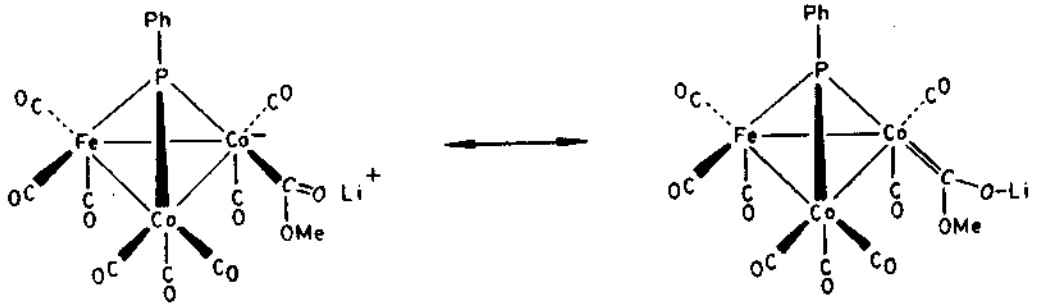

That [**11**][Li] exists entirely as a CIP reflects the fact that the methoxycarbonyl cluster is extremely electron rich and dissipates charge density by effectively competing with a THF solvent molecule in the ion pair equilibrium shown in Eq. 15.[58] At -70 °C, it is estimated that this

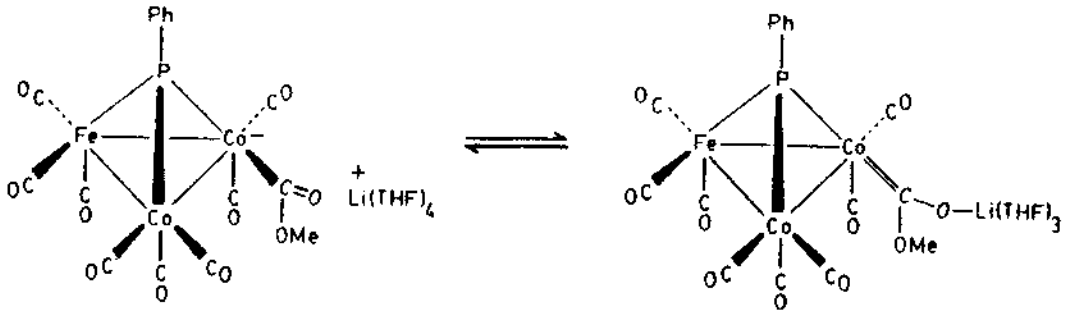

(15)

reaction has a $K_{eq} \geq 19$, which places an upper limit of SSIPs of [**11**$^-$] at 5 %. A clear degree of the electron richness in [**11**][Li] is also seen when these results are compared to those obtained from the corresponding tricobalt cluster $[Co_3(CO)_8\{C(O)OMe\}(\mu_3\text{-}CPh)^-]$, [**12**$^-$], prepared from $Co_3(CO)_9(\mu_3\text{-}CPh)$ and [MeO][Li]. At -70 °C, the methoxycarbonyl cluster [**12**$^-$] exists as an equilibrating mixture of solvent-separated (45%) and ester oxygen-[Li^+] contact ion pairs (55%).[50] The extent of ion pairing in these two structurally similar clusters is modulated by the μ_3-capping ligand. Here the enhanced electron donating ability of the μ_3-PPh group, relative to the weaker donating μ_3-CPh group, manifests itself in an increased concentration

of carbonyl oxygen-[Li^+] contact ion pairs. An analogous trend is also reflected by the location of highest frequency ν(CO) band of these anionic methoxycarbonyl clusters. This ν(CO) band has also been shown to function as a sensitive probe for the electron density associated with tetrahedrane clusters.[27c,59]

The identity of [**11**][Li] was further established by NMR spectroscopy. [**11**][Li] exhibited a single low-field ^{31}P resonance at δ 336.0, which is in keeping with the presence of a μ_3-PPh capping ligand. The $^{13}C\{^1H\}$ NMR spectrum of [**11**][Li] recorded at -90 °C (Figure 14b) provides the crucial evidence relating to the site of [MeO^-] attack in **3**. Despite the fact that the slow-exchange spectrum has not been fully reached, five broad carbonyl resonances were observed at δ 210.0, 214.0, 215.7, 217.1, and 222.9 with a relative integration ratio of nearly 3 : 1 : 1 : 1 : 3, respectively. The highest field resonance is readily assigned to the neutral $Co(CO)_3$ unit. As in the phosphido-bridged cluster [**8**$^-$], the equatorial carbonyls belonging to the $Fe(CO)_3$ moiety appear as distinct, one carbon resonances tentatively assigned as δ 214.0 and 215.7. The ester moiety accounts for the remaining one carbon at δ 217.5.[57] These last three assignments are by no means unequivocal; however, this uncertainty will not negate the premise of [MeO^-] attack at a terminal Co-CO group in **3**. The remaining resonance at δ 223.0 consists of a superposition of the

axial Fe-CO group and the two CO groups associated with the anionic ester-substituted cobalt center. Of the other possible structure alternatives, [MeO^-] attack at the μ_3-PPh group can be immediately ruled out when the IR data are considered (vide supra), while the existence of an anionic $Fe(CO)_2(CO_2Me)$ moiety is dismissed on the basis of the absence of two equivalent $Co(CO)_3$ groups.

The reaction between **3** and methanolic $[Et_4N][OH]$ was next examined as part of the group's interest in the generation of hydroxycarbonyl complexes.[60,61] When **3** in THF was treated with one mol equiv of $[Et_4N][OH]$ (1.3 M in MeOH) at -78 °C, immediate and quantitative conversion to [**11**$^-$] and the hydroxycarbonyl cluster [$FeCo_2(CO)_6(CO_2H)(\mu_3\text{-PPh})^-$], [**13**$^-$], was observed by IR analysis. The IR spectrum recorded at -70 °C revealed ν(CO) bands at 2046(s), 2036(w), 1990(vs), 1972(s), 1954(m), 1912(m), 1798(vw), 1626(w), and 1617(w) cm^{-1}. The IR spectrum is shown in Figure 15c. The terminal ν(CO) bands of this mixture are virtually identical with those given in Table 1 for the solvent-separated ions of [**11**$^-$]. This is the result expected for the superposition of the closely related derivatives. Disparate perturbations in the terminal C-O stretching bands of clusters [**11**$^-$] and [**13**$^-$] are not anticipated since the ester and acid functionalities possess similar electronic and steric properties. The ester C-O stretch at 1626 cm^{-1} is readily assigned to the solvent-separated ions of [**11**$^-$], on the

basis of its prior characterization (vide supra). Accordingly, the remaining low-frequency C-O stretch at 1617 cm^{-1} is attributed to the acid moiety of [**13**$^-$]. That the acid moiety is 9 cm^{-1} lower in energy than the ester group reflects the greater charge delocalization present in [**13**$^-$]. This phenomenon is directly attributable to the below carboxylate-like resonance structure.

The regioselectivity associated with this reaction is assumed to proceed through a kinetically controlled pathway involving [MeO^-] and [HO^-] attack at a terminal Co-CO group (see Eq. 14).[61]

The ratio of [**11**$^-$] to [**13**$^-$] at -70 °C was determined by measuring the area under the overlapping low-frequency ester and acid C-O stretching bands. IR band-shape analysis yielded a 55:45 ratio of [**11**$^-$] to [**13**$^-$]. This ratio is of interest when compared to the results obtained using other metal carbonyl complexes. For example, the mononuclear carbonyls $Fe(CO)_5$ and $Cr(CO)_6$ afford ester/acid ratios of

5:95[60] and 2:98[62] respectively, while the polynuclear clusters $Co_4(CO)_{10}(\mu_4\text{-PPh})_2$ and $Co_3(CO)_9(\mu_3\text{-CPh})$ give ester/acid ratios of 23:77[61] and 51:48,[50] respectively. While it appears that these results suggest that polynuclear complexes favor higher yields of the corresponding methoxycarbonyl clusters, additional examples are required before any generalizations can confidently be made. The subtle balance involving the nature of the initial carbonyl complex, gegencation, and anion solvation are but some of the factors that determine the observed ester/acid ratio.[60,61]

5. Reactivity and Stability Studies

All of the new mixed-metal anionic clusters were observed to be stable for a period of at least one week when maintained at -78 °C. Extensive cluster decomposition accompanied all reaction mixtures that were warmed to room temperature. Besides the presence of varying amounts of regenerated **3** (<20 %), the only other carbonyl containing material observed was $[Co(CO)_4^-]$.[63] Yields of $[Co(CO)_4^-]$ ranged from 16% to 37%, as determined by quantitative IR spectroscopy. No perceptible stabilization was noticed when clusters [**9**$^-$] and [**11**$^-$] were allowed to warm-up in the presence of 12-crown-4 or [PPN][Cl]. Variable-temperature IR studies revealed that [**9**$^-$] and [**11**$^-$] decomposed to $[Co(CO)_4^-]$ at rates virtually identical to solutions without

these additives. The relative instability of these mixed-metal anionic clusters may be contrasted to that of $[Co_3(CO)_9(\mu_3\text{-}CPh)^{-\bullet}]$. Enhanced cluster stabilization and retardation of electron-transfer processes have been reported for $[Co(CO)_9(\mu_3\text{-}CPh)^{-\bullet}]$ in the presence of nonspecific, charge-delocalized cations such as $[PPN^+]$ and $[Na(15\text{-crown-}5)^+]$.[64] However, recent reports have shown that in the case of $[Co_3(CO)_9(\mu_3\text{-}CMe)^{-\bullet}]$ decomposition is preceded by dissociative CO loss and that this destructive process is concentration dependent.[65] Finally, the growth of crystals suitable for X-ray diffraction analysis was thwarted due to poor crystal quality and competing cluster decomposition.

When monitored by IR spectroscopy, the decomposition of [**8**$^-$] and [**9**$^-$] was observed to occur without the spectroscopically observable intermediates. A different course of reaction was noted for [**11**$^-$]. Starting at -25 °C, the solution acquired a brown color and the ester ν(CO) band at 1582 cm $^{-1}$ and the terminal ν(CO) bands at 2051 and 1994 cm^{-1} diminished in intensity. This transformation is complete by ca. -5 °C and the resulting spectrum (Figure 1b) closely resembles that of [**8**$^-$]. Also evident in this warm-up process is the presence of a small amount of **3** and $[Co(CO)_4^-]$, which are estimated at <10 % yield. The similarity of the IR spectrum of [**8**$^-$] and [**11**$^-$] (recorded at -5 °C) strongly supports the ester → phosphido sequence

shown in Eq. 16.

^{31}P NMR spectroscopy has also provided complementary data for the reaction shown in Eq. 16. When [**11**$^-$] was briefly warmed to -25 °C and then cooled back down to

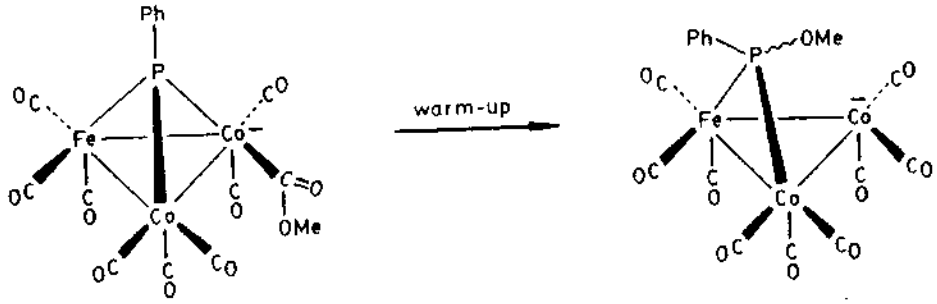

(16)

11$^-$ **14**$^-$

-78 °C,[21,22] ^{31}P NMR analysis revealed two major resonances at δ 336.0 and 320.0. The latter resonance is assigned to the methoxyphosphido cluster [$FeCo_2(CO)_9(\mu_2$-PPhOMe)$^-$], [**14**$^-$], while the former resonance belongs to [**11**$^-$]. The chemical shift ascribed to the proposed μ_2-PPhOMe group is slightly outside the range expected for a μ_2-phosphido group (δ 300-50),[35] however Bruce et al.[38] have also observed a similar low-field ^{31}P chemical shift for a μ_2-PPhOMe bridged ruthenium cluster (i.e., δ 297.2). A ^{31}P gated-decoupled NMR spectrum of a mixture containing [**11**$^-$] and [**14**$^-$] failed to reveal any ^1H-^{31}P coupling, presumably due to the broadness associated with these resonances. The stereochemistry associated with the μ_2-PPhOMe ligand in [**14**$^-$] is unknown at this time and no attempt has been made

to determine it.

An analogous reaction involving the transformation of the formyl complexes $[Fe_2(CO)_5\{C(O)H\}(\mu_2\text{-}PR_2)_2^-]$ (where R = Me, Ph) to the corresponding phosphido/phosphines $[Fe_2(CO)_6(\mu_2\text{-}PR_2)(PR_2H)^-]$ has been demonstrated by Wojcicki and coworkers.[36d,66] The observation of the methoxyphosphido cluster [**14**$^-$] from [**11**$^-$] upon warm-up illustrates the critical role played by the reaction temperature. At -78 °C, [**11**$^-$] is formed via a kinetically controlled reaction, while at higher temperature (> -20 °C) [**14**$^-$] is derived as a result of thermodynamic product control.

Anion functionalization using methyl triflate and trifluoroacetic acid was also examined in an attempt to further characterize these new clusters.[67] Unfortunately, no reaction was observed by IR spectroscopy when either [**8**$^-$] or [**9**$^-$] was treated with methyl triflate at -78 °C. Extensive polymerization accompanied all reactions upon warm-up. Solvent polymerization and the absence of cluster alkylation indicate the O-alkylation of THF is favored.[68] The unreactive nature of [**8**$^-$] toward electrophiles was also demonstrated by changing the reaction solvent to CH_2Cl_2. CH_2Cl_2 solutions of [**8**$^-$] at -78°C showed no noticeable reaction with methyl triflate (1-5 equiv) and trifluoroacetic acid (~5 equiv).[69] Warm-up of these solutions led to the regeneration of **3** in reduced yield (~20-50 %). It is possible that [**8**$^-$] functions as a

hydride-transfer agent much like that reported for metal formyls,[23] but this remains to be established. Finally, cluster [**12**][Li] regenerates **3** in quantitative yield at -78 °C when treated with trifluoroacetic acid (~5 equiv), consistent with the many reports of acid-promoted ester decomposition.[60,61,70]

CHAPTER REFERENCES

1. (a) Basolo, F.; Pearson, R. G. "Mechanisms of Inorganic Reactions", Wiley, New York, **1967**. (b) Atwood, J. D. "Inorganic and Organometallic Reaction Mechanisms", Brooks/Cole Monterey, CA, **1985**.

2. (a) Wade, K. Chem. Br. **1975**, 11, 177. (b) Wade, K. Adv. Inorg. Chem. Radiochem. **1976**, 18, 1. (c) Wade, K. in "Transition Metal Clusters", Johnson, B. F. G. Ed.; Wiley, New York, **1980**; Ch 3. (d) Mingos, D. M. P. Acc. Chem. Res. **1984**, 17, 311. (e) Mingos, D. M. P. Nature (London), Phys. Sci. **1972**, 236, 99.

3. Also see: (a) Teo, B. K. Inorg. Chem. **1984**, 23, 1251. (b) Teo, B. K.; Longoni, G.; Chung, F. R. K. Inorg. Chem. **1984**, 23, 1257. (c) Teo, B. K. Inorg. Chem. **1985**, 24, 115. (d) Mingos, D. M. P. Inorg. Chem. **1985**, 24, 114.

4. (a) Halet, J. F.; Hoffmann, R.; Saillard, J. Y. Inorg. Chem. **1985**, 24, 1695. (b) Ohst, H. H.; Kochi, J. K. Organometallics **1986**, 5, 1359.

5. Albers, M. O.; Robinson, D. J.; Coville, N. J. Coord. Chem. Rev. **1986**, 69, 127.

6. Also see: (a) Bor, G.; Dietler, H. K.; Pino, P.; Poë, A. J. J. Organomet. Chem. **1978**, 154, 301. (b) Darensbourg, D. J.; Zalewski, D. J. Inorg. Chem. **1984**, 23, 4382. (c) Vahrenkamp, H. Adv. Organomet. Chem. **1983**, 22, 169. (d) Lesch, D. A.; Rauchfuss, T. B. Organometallics **1982**, 1, 499. (e) Adams, R. D. Polyhedron **1985**, 4, 2003, and references therein. (f) Hieber, W.; Kruck, T. Chem. Ber. **1962**, 95, 2027. (g) Bogan, Jr. L. E.; Lesch, D. A.; Rauchfuss, T. B. J. Organomet. Chem. **1983**, 250, 429.

7. Richmond, M. G.; Kochi, J. K. Inorg. Chem. **1987**, 26, 541.

8. Ryan, R. C.; Pittman, Jr. C. U.; O'Connor, J. P.; Dahl, L. F. J. Organomet. Chem. **1980**, 193, 247.

9. Ryan, R. C.; Dahl, L. F. J. Am. Chem. Soc. **1975**, 97, 6904.

10. King, R. B. Acc. Chem. Res. **1980**, 13, 243.

11. Atwood, J. D.; Wovkulich, M. J.; Sonnenberger, D. C. Acc. Chem. Res. **1983**, 16, 350.

12. (a) Wax, M. J.; Bergman, R. G. J. Am. Chem. Soc. **1981**, 103, 7028. (b) Cotton, J. D.; Kimlin, H. A. J. Organomet. Chem. **1985**, 294, 213. (c) Bryndza, H. E.; Bergman, R. G. J. Am. Chem. Soc. **1979**, 101, 4766.

13. Sundararajan, G.; San Fillippo, Jr. J. Organometallics **1985**, 4, 606.

14. Schneider, J.; Minelli, M.; Huttner, G. J. Organomet. Chem. **1985**, 294, 75.

15. Huttner, G.; Knoll, K. Angew. Chem. Int. Ed. Engl. **1987**, 26, 743.

16. Also see: Laine, R. M. J. Mol. Catal. **1982**, 14, 137.

17. Grynkewich, G. W.; Marks, T. J. Inorg. Chem. **1976**, 15, 1307.

18. Bryndza, H. E.; Tam, W. Chem. Rev. **1988**, 88, 1163, and references therein.

19. (a) Whitman, D. W.; Carpenter, B. K. J. Am. Chem. Soc. **1982**, 104, 6473. (b) Carpenter, B. K. J. Am. Chem. Soc. **1983**, 105, 1700.

20. Tolman, C. A. Chem. Rev. **1977**, 77, 313.

21. Schulman, C. L.; Richmond, M. G.; Watson, W. H.; Nagl, A. J. Organomet. Chem. **1989**, 368, 367.

22. Richmond, M. G.; Kochi, J. K. Organometallics **1987**, 6, 254.

23. Gladysz, J. A. Adv. Organomet. Chem. **1982**, 20, 1.

24. (a) Bedard, R. L.; Dahl, L. F. J. Am. Chem. Soc. **1986**, 108, 5942. (b) Michaud, P.; Astruc, D.; Ammeter, J. H. J. Am. Chem. Soc. **1982**, 104, 3755. (c) Astruc, D. Acc. Chem. Res. **1986**, 12, 377. (d) Touchard, D.; Fillaut, J. L.; Khasnis, D. V.; Dixneuf, P. H.; Mealli, C.; Masi, D.; Toupet, L. Organometallics **1988**, 7, 67.

25. Hwang, S.; Richmond, M. G. Unpublished results.

26. Don, M. J.; Richmond, M. G. Inorg. Chim. Acta **1990**, 173, 61.

27. (a) Beurich, H.; Madach, T.; Richter, F.; Vahrenkamp, H. Angew. Chem. Int. Ed. Engl. **1979**, 18, 690. (b) Honrath, U.; Vahrenkamp, H. Z. Naturforsch. **1984**, 39B, 555. (c) Lindsay, P. N.; Peake, B. M.; Robinson, B. H.; Simpson, J.; Honrath, U.; Vahrenkamp, H.; Bond, A. M. Organometallics **1984**, 3, 413. (d) Bedard, R. L.; Roe, A. D.; Dahl, L. F. J. Am. Chem. Soc. **1986**, 108, 5924. (e) Jaeger, J. T.; Field, J. S.; Collison, D.; Speck, G. P.; Peake, B. M.; Hahnle, J.; Vahrenkamp, H. Organometallics **1988**, 7, 1753. (f) Geiger, W. E. Prog. Inorg. Chem. **1985**, 33, 275.

28. (a) Peake, B. M.; Robinson, B. H.; Simpson, J.; Watson, D. J. Inorg. Chem. **1977**, 16, 405. (b) Teo, B. K.; Hall, M.B.; Fenske, R. F.; Dahl, L. F. J. Organomet. Chem. **1974**, 70, 413. (c) Ohst, H. H.; Kochi, J. K. J. Am. Chem. Soc. **1986**, 108, 2897. (d) Ohst, H. H.; Kochi, J. K. Inorg. Chem. **1986**, 25, 2066. (e) Dumond, D. S.; Richmond, M. G. J. Am. Chem. Soc. **1988**, 110, 7548.

29. (a) Robin, M. D.; Day, P. Adv. Inorg. Chem. Radiochem. **1967**, 10, 248. (b) Cannon, R. D. Adv. Inorg. Chem. Radiochem. **1978**, 21, 179. (c) Taube, H. Angew. Chem. Int. Ed. Engl. **1984**, 23, 329.

30. Unpublished results. Geiger, Jr. W. E.

31. Davies, A. G.; Hay-Motherwell, R. S.; Evans, J. C.; Rowlands, C. C. J. Chem. Soc., Chem. Commun. **1986**, 20, 1513.

32 Peloso, A. J. Organomet. Chem. **1974**, 67, 423.

33. (a) Brisdon, B. J.; Enger, S. K.; Weaver, M. J.; Walton, R. A. Inorg. Chem. **1987**, 26, 3340. (b) Glyn, P.; George, M. W.; Hodges, P. M.; Turner, J. J. J. Chem. Soc., Chem. Commun. **1989**, 1655.

34. Dahl, L. F.; Sutton, P. W. Inorg. Chem. **1963**, 2, 1067.

35. Darensbourg, M. Y. Adv. Organomet. Chem. **1985**, 33, 221, and references therein.

36. (a) Carty, A. J.; MacLaughlin, S. A.; Nucciarone, D. in "Phosphorus-31 NMR Spectroscopy in Stereochemical Analysis", Verkade, J. G.; Quin, L. D., Eds.; VCH

Publishers: Deerfield Beach, FL; **1987**; Ch 16. (b) Garrou, P. E. Chem. Rev. **1981**, 81, 229. (c) Carty, A. J. Adv. Chem. Ser. **1982**, 196, 163.

37. (a) Yu, Y. F.; Gallucci, J.; Wojcicki, A. J. Am. Chem. Soc. **1983**, 105, 4826. (b) Yu, Y. F.; Gallucci, J.; Wojcicki, A. J. Chem. Soc., Chem. Commun. **1984**, 653. (c) Yu, Y. F.; Chau, C. N.; Wojcicki, A.; Calligaris, M.; Nardin, G.; Balducci, G. J. Am. Chem. Soc. **1984**, 106, 3704. (d) Shyu, S. G.; Wojcicki, A. Organometallics **1985**, 4, 1457. (e) Yu, Y. F.; Chau, C. N.; Wojcicki, A. Inorg. Chem. **1986**, 25, 4098. (f) Shyu, S. G.; Calligaris, M.; Nardin, G.; Wojcicki, A. J. Am. Chem. Soc. **1987**, 109, 3617.

38. See also: (a) Williams, G. D.; Geoffroy, G. L.; Whittle, R. R.; Rheingold, A. L. J. Am. Chem. Soc. **1985**, 107, 729. (b) Geoffroy, G. L.; Rosenberg, S.; Shulman, P. M.; Whittle, R. R. J. Am. Chem. Soc. **1984**, 106, 1519. (c) Rosenberg, S.; Whittle, R. R.; Geoffroy, G. L. J. Am. Chem. Soc. **1984**, 106, 5934. (d) Knoll, K.; Huttner, G.; Zsolnai, L.; Orama, O.; Wasiucionek, M. J. Organomet. Chem. **1986**, 310, 225. (e) Buchholz, D.; Huttner, G.; Zsolnai, L. J. Organomet. Chem. **1990**, 381, 97. (f) Buchholz, D.; Huttner, G.; Imhof, W. J. Organomet. Chem. **1990**, 391, 307. (g) Chau, C. N.; Yu, Y. F.; Wojcicki, A.; Calligaris, M.; Nardin, G.; Balducci, G. Organometallics **1987**, 6, 308. (h) Kyba, E. P.; Davis, R. E.; Clubb, C. N.; Liu, S. T.; Palacios, H. O. A.; McKennis, J. S. Organometallics **1986**, 5, 869.

39. Bruce, M. I.; Liddell, M. J.; Tiekink, E. R. T. J. Organomet. Chem. **1990**, 391, 81.

40. Aime, S.; Milone, L.; Rossetti, R.; Stanghellini, P. L. Inorg. Chim. Acta **1977**, 25, 103.

41. Gates, R. A.; D'Agostino, M. F.; Sutin, K. A.; McGlinchey, M. J.; Janik, T. S.; Churchill, M. R. Organometallics **1990**, 9, 20, and references therein.

42. Vahrenkamp, H. Phil. Trans. R. Soc. Lond. A **1982**, 308, 17.

43. (a) Ginsberg, R. E.; Berg, J. M.; Rothrock, R. K.; Collman, J. P.; Hodgson, K. O.; Dahl, L. F. J. Am. Chem. Soc. **1979**, 101, 7218. (b) Collman, J. P.; Rothrock, R. K.; Finke, R. G.; Moore, E. J.; Rose-Munch, F. Inorg. Chem. **1982**, 21, 146.

44. (a) Collman, J. P.; Finke, R. G.; Matlock, P. L.; Wahren, R.; Komoto, R. G.; Brauman, J. I. J. Am. Chem. Soc. **1978**, 100, 1119. (b) Chen, C. K.; Cheng, C. H. Inorg. Chem. **1983**, 22, 3378. (c) Schick, K. P.; Jones, N. L.; Sekula, P.; Boag, N. M.; Labinger, J. A.; Kaesz, H. D. Inorg. Chem. **1984**, 23, 2204. (d) Chen, C. K.; Cheng, C. H.; Hseu, T. H. Organometallics **1987**, 6, 868.

(e) Vandenberg, D. M.; Chin-Choy, T.; Ford, P. C. J. Organomet. Chem. **1989**, 366, 257.

45. Richmond, M. G.; Kochi, J. K. Inorg. Chem. **1986**, 25, 656, and references therein.

46. Epstein, R. A.; Withers, H. W.; Geoffroy, G. L. Inorg. Chem. **1979**, 18, 942.

47. Richmond, M. G.; Kochi, J. K. J. Organomet. Chem. **1987**, 323, 219.

48. An equatorially disposed acyl group has been invoked for convenience. The distinction between equatorial versus axial substitution is clouded due to the presumed presence of rapid, localized carbonyl scrambling at the anionic cobalt center.

49. (a) Aradi, A. A.; Grevels, F. W.; Kruger, C.; Raabe, E. Organometallics **1988**, 7, 812, and references therein.

50. Kochi, J. K. "Organometallic Mechanisms and Catalysis", Academic Press: New York; **1978**.

51. (a) Taube, H. J. Chem. Ed. **1968**, 45, 452. (b) Sutin, N. Acc. Chem. Res. **1982**, 15, 275. (c) Pross, A. Acc. Chem. Res. **1985**, 18, 212. (d) Marcus, R. A. Annu. Rev. Phys. Chem. **1964**, 15, 155. (e) Eberson, L. Adv. Phys. Org. Chem. **1982**, 18, 79. (f) See also: Purcell, K. F.; Kotz, J. C. "Inorganic Chemistry", Saunders, W. B. Co.: Philadelphia; **1977**; Ch 12.

52. (a) Ashby, E. C. Pure Appl. Chem. **1980**, 52, 545, and references therein. (b) Minisci, F.; Citterio, A. In "Advances in Free-Radical Chemistry", Williams, G. H., Ed.; Heyden: London, **1980**; pp. 125-126.

53. (a) Bockman, T. M.; Kochi, J. K. J. Am. Chem. Soc. **1989**, 111, 4669, and references therein. (b) Kochi, J. K. Angew. Chem., Int. Ed. Engl. **1988**, 27, 1227, and references therein.

54. Dumond, D. S.; Hwang, S.; Richmond, M. G. Inorg. Chim. Acta **1989**, 160, 135.

55. Narayanan, B. A.; Amatore, C.; Kochi, J. K. Organometallics **1986**, 5, 926; **1987**, 6, 129.

56. (a) Ingold, K. U. Pure Appl. Chem. **1984**, 56, 1767, and references therein. (b) Jordan, R. F. J. Chem. Ed. **1988**, 65, 285. (c) See also: Bates, R. B.; Kroposki, L. M.; Potter, D. E. J. Org. Chem. **1972**, 37, 560.

57. Ford, P. C.; Rokicki, A. Adv. Organomet. Chem. **1988**, 28, 139, and references therein.

58. (a) Darensbourg, M. Y.; Jimenez, P.; Sackett, J. R.; Hanckel, J. M.; Kump, R. L. J. Am. Chem. Soc. **1982**, 104, 1521. (b) Schaschel, E.; Day, M. C. J. Am. Chem. Soc. **1968**, 90, 503. (c) Hammonds, C. N.; Day, M. C. J. Phys. Chem. **1969**, 73, 1151. (d) Setzer, W. N.; Schleyer, P. v. R. Adv. Organomet. Chem. **1985**, 24, 353, and references therein.

59. Penfold, B. R.; Robinson, B. H. Acc. Chem. Res. **1973**, 6, 73.

60. Lee, S. W.; Tucker, W. D.; Richmond, M. G. Inorg. Chem. **1990**, 29, 3053.

61. Partin, J. A.; Richmond, M. G. J. Organomet. Chem. **1990**, 396, 339.

62. Partin, J. A.; Richmond, M. G., Unpublished results.

63. (a) Gladysz, J. A.; Williams, G. M.; Tam, W.; Johnson, D. L.; Parker, D. W.; Selover, J. C. Inorg. Chem. **1979**, 18, 553. (b) Edgell, W. F.; Hedge, S,; Barbatta, A. J. Am. Chem. Soc. **1978**, 100, 1406.

64. Kirk, C. M.; Peake, B. M.; Robinson, B. H.; Simpson, J. Aust. J. Chem. **1983**, 36, 441.

65. (a) Hinkelmann, K.; Mahlendorf, F.; Heinze, J.; Schacht, H. T.; Field, J. S.; Vahrenkamp, H. Angew. Chem., Int. Ed. Engl. **1987**, 26, 353. (b) Hinkelmann, K.; Heinze, J.; Schacht, H. T.; Field, J. S.; Vahrenkamp, H. J. Am. Chem. Soc. **1989**, 111, 5078.

66. See also: Wojcicki, A. in "Coordination Chemistry and Catalysis," Ziolkowski, J. J.; Ed.; World Scientific: New Jersey; **1988**; pp. 3-25.

67. For example, see: (a) Richmond, M. G.; Kochi, J. K. Organometallics **1987**, 6, 777, and references therein. (b) Jensen, C. M.; Knobler, C. B.; Kaesz, H. D. J. Am. Chem. Soc. **1984**, 106, 5926, and references therein. (c) Adams, R. D. Chem. Rev. **1989**, 89, 1703.

68. (a) Howells, R. D.; McCown, J. D. Chem. Rev. **1977**, 77, 69. (b) Matyjaszewski, K.; Penczeks, S. J. Polym. Sci. **1974**, 12, 1905. (c) Wu, T. K.; Pruckmayr, G. Macromolecules **1978**, 11, 77; 265. (d) Kobayaski, S.; Danda, H.; Saegusa, T. Macromolecules **1974**, 7, 415.

69. See also: Went, M. J.; Brock, C. P.; Shriver, D. F. Organometallics **1986**, 5, 755.

70. (a) Gross, D. C.; Ford, P. C. Inorg. Chem. **1982**, 21, 1702. (b) Chini, P.; Martinengo, S,; Giordano, G. Gazz. Chim. Ital. **1972**, 102, 330. (c) Katz, N. E.; Szalda, D. J.; Chou, M. H.; Creutz, C.; Sutin, N. J. Am. Chem. Soc. **1989**, 111, 6591. (d) Lilga, M. A.; Ibers, J. A. Organometallics **1985**, 4, 590.

BIBLIOGRAPHY

Abrahams, S. C. Acta Crystallogr. **1955**, 8, 661.

Ackermann, P. G.; Mayer, J. E. J. Chem. Phys. **1936**, 4, 377.

Adams, R. D. Chem. Rev. **1989**, 89, 1703.

Adams, R. D. Polyhedron **1985**, 4, 2003.

Adams, R. D.; Babin, J. E.; Tasi, M.; Wolfe, T. A. J. Am. Chem. Soc. **1988**, 110, 7093.

Ahmed, M. G.; Alder, R. W.; James, G. H.; Sinnott, M. L.; Whiting, M. C. J. Chem. Soc., Chem. Commun. **1968**, 1523.

Aime, S.; Milone, L.; Rossetti, R.; Stanghellini, P. L. Inorg. Chim. Acta **1977**, 25, 103.

Albers, M. O.; Robinson, D. J.; Coville, N. J. Coord. Chem. Rev. **1986**, 69, 127.

Albiez, T.; Powell, A. K.; Vahrenkamp, H. Chem. Ber. **1990**, 123, 667.

Angelici, R. Acc. Chem. Res. **1988**, 21, 387.

Aradi, A. A.; Grevels, F. W.; Kruger, C.; Raabe, E. Organometallics **1988**, 7, 812.

Ashby, E. C. Pure Appl. Chem. **1980**, 52, 545.

Astruc, D. Acc. Chem. Res. **1986**, 12, 377.

Astruc, D. Angew. Chem., Int. Ed. Engl. **1988**, 27, 643.

Astruc, D. Chem. Rev. **1988**, 88, 1189.

Atwood, J. D. "Inorganic and Organometallic Reaction Mechanisms", Brooks/Cole Monterey, CA, **1985**.

Atwood, J. D.; Wovkulich, M. J.; Sonnenberger, D. C. Acc. Chem. Res. **1983**, 16, 350.

Bartholomew, C. H.; Agrawal, P. K.; Katzer, J. R. Adv. Catal. **1982**, 31, 135.

Basolo, F. Inorg. Chim. Acta **1981**, 50, 65.

Basolo, F.; Pearson, R. G. "Mechanisms of Inorganic Reactions", Wiley, New York, **1967**.

Bates, R. B.; Kroposki, L. M.; Potter, D. E. J. Org. Chem. **1972**, 37, 560.

Bedard, R. L.; Dahl, L. F. J. Am. Chem. Soc. **1986**, 108, 5942.

Bedard, R. L.; Roe, A. D.; Dahl, L. F. J. Am. Chem. Soc. **1986**, 108, 5924.

Bergersen, F. J.; Postgate, J. R. "A Century of Nitrogen Fixation Research", The royal Society, London, **1987**.

Beurich, H.; Madach, T.; Richter, F.; Vahrenkamp, H. Angew. Chem. Int. Ed. Engl. **1979**, 18, 690.

Bianco, V. D.; Doronzo, S. Inorg. Synth. **1976**, 13, 161.

Bockman, T. M.; Kochi, J. K. J. Am. Chem. Soc. **1989**, 111, 4669.

Bogan, Jr. L. E.; Lesch, D. A.; Rauchfuss, T. B. J. Organomet. Chem. **1983**, 250, 429.

Bor, G.; Dietler, H. K.; Pino, P.; Poë, A. J. J. Organomet. Chem. **1978**, 154, 301.

Bricker, J. C.; Nagel, C. C.; Bhattacharyya, A. A. J. Am. Chem. Soc. **1985**, 107, 377.

Bricker, J. C.; Nagel, C. C.; Shore, S. G. J. Am. Chem. Soc. **1982**, 104, 1444.

Brisdon, B. J.; Enger, S. K.; Weaver, M. J.; Walton, R. A. Inorg. Chem. **1987**, 26, 3340.

Browning, C. S.; Farrar, D. H.; Gukathasan, R. R.; Morris, S. A. Organometallics, **1985**, 4, 1750.

Bruce, M. I.; Liddell, M. J.; Tiekink, E. R. T. J. Organomet. Chem. **1990**, 391, 81.

Bryndza, H. E.; Bergman, R. G. J. Am. Chem. Soc. **1979**, 101, 4766.

Bryndza, H. E.; Tam, W. Chem. Rev. **1988**, 88, 1163.

Buchholz, D.; Huttner, G.; Imhof, W. J. Organomet. Chem. **1990**, 391, 307.

Buchholz, D.; Huttner, G.; Zsolnai, L. J. Organomet. Chem. **1990**, 381, 97.

Bullock, R. M.; Casey, C. P. Acc. Chem. Res. **1987**, 20, 167.

Bunnett, J. F. Acc. Chem. Res. **1978**, 11, 413.

Burdett, J. K. J. Chem. Soc. Dalton Trans. **1977**, 423.

Burgess, B. K. Chem. Rev. **1990**, 90, 1377.

Candlin, J. P.; Shortland, A. C. J. Organomet. Chem. **1969**, 16, 289.

Cannon, R. D. Adv. Inorg. Chem. Radiochem. **1978**, 21, 179.

Carpenter, B. K. J. Am. Chem. Soc. **1983**, 105, 1700.

Carty, A. J. Adv. Chem. Ser. **1982**, 196, 163.

Carty, A. J.; MacLaughlin, S. A.; Nucciarone, D. in "Phosphorus-31 NMR Spectroscopy in Stereochemical Analysis", Verkade, J. G.; Quin, L. D., Eds.; VCH Publishers: Deerfield Beach, FL; **1987**; Ch 16.

Chanon, M. Acc. Chem. Res. **1987**, 20, 214.

Chanon, M.; Tobe, M. L. Angew Chem., Int. Ed. Engl. **1982**, 21, 1.

Chau, C. N.; Yu, Y. F.; Wojcicki, A.; Calligaris, M.; Nardin, G.; Balducci, G. Organometallics **1987**, 6, 308.

Chen, C. K.; Cheng, C. H. Inorg. Chem. **1983**, 22, 3378.

Chen, C. K.; Cheng, C. H.; Hseu, T. H. Organometallics **1987**, 6, 868.

Chini, P.; Martinengo, S,; Giordano, G. Gazz. Chim. Ital. **1972**, 102, 330.

Collman, J. P.; Finke, R. G.; Matlock, P. L.; Wahren, R.; Komoto, R. G.; Brauman, J. I. J. Am. Chem. Soc. **1978**, 100, 1119.

Collman, J. P.; Rothrock, R. K.; Finke, R. G.; Moore, E. J.; Rose-Munch, F. Inorg. Chem. **1982**, 21, 146.

Cotton, J. D.; Kimlin, H. A. J. Organomet. Chem. **1985**, 294, 213.

Coucouvanis, D. Acc. Chem. Res. **1981**, 14, 201.

Dahl, L. F.; Martell, C.; Wampler, D. L. J. Am. Chem. Soc. **1961**, 83, 1761.

Dahl, L. F.; Sutton, P. W. Inorg. Chem. **1963**, 2, 1067.

Dahlinger, K.; Poë, A. J.; Sayal, P. K.; Sekhar, V. C. J. Chem. Soc., Dalton Trans. **1986**, 2145.

Darensbourg, D. J. in "The Chemistry of Metal Cluster Complexes," Shriver, D. F.; Kaesz, H. D.; Adams, R. D., Eds.; VCH Publishers; New York; **1990**; Ch 4.

Darensbourg, D. J.; Baldwin-Zuschke, B. J. J. Am. Chem. Soc. **1982**, 104, 3906.

Darensbourg, D. J.; Peterson, B. S.; Schmidt, Jr. R. E. Organometallics **1982**, 1, 306.

Darensbourg, D. J.; Zalewski, D. J. Inorg. Chem. **1984**, 23, 4382.

Darensbourg, M. Y. Adv. Organomet. Chem. **1985**, 33, 221.

Darensbourg, M. Y.; Jimenez, P.; Sackett, J. R.; Hanckel, J. M.; Kump, R. L. J. Am. Chem. Soc. **1982**, 104, 1521.

Davies, A. G.; Hay-Motherwell, R. S.; Evans, J. C.; Rowlands, C. C. J. Chem. Soc., Chem. Commun. **1986**, 20, 1513.

Day, V. W.; Lesch, D. A.; Rauchfuss, T. B. J. Am. Chem. Soc. **1982**, 104, 1290.

DeSimone, R. E.; Drago, R. S. J. Am. Chem. Soc. **1970**, 92, 2343.

Doi, Y.; Koshizuka, K.; Keii, T. Inorg. Chem. **1982**, 21, 2732.

Doi, Y.; Tamura, S.; Koshizuka, K. Inorg. Chim. Acta **1982**, 65, L63.

Doi, Y.; Tamura, S.; Koshizuka, K. J. Mol. Catal. **1983**, 19, 213.

Don, M. J.; Richmond, M. G. Inorg. Chim. Acta **1990**, 173, 61.

Don, M. J.; Richmond, M. G.; Watson, W. H.; Nagl, A. Acta Cryst. **1991**, C47, 93.

Drenth, W.; Kwart, H. "Kinetics Applied to Organic Reactions", Marcel Dekker: New York, **1980**.

Drew, D.; Doyle, J. R. Inorg. Synth. **1973**, 13, 48.

Dumond, D. S.; Hwang, S.; Richmond, M. G. Inorg. Chim. Acta **1989**, 160, 135.

Dumond, D. S.; Richmond, M. G. J. Am. Chem. Soc. **1988**, 110, 7548.

Eberson, L. Adv. Phys. Org. Chem. **1982**, 18, 79.

Edgell, W. F.; Hedge, S,; Barbatta, A. J. Am. Chem. Soc. **1978**, 100, 1406.

Eisch, J. J.; King, R. B. "Organometallic Syntheses", Academic Press: New York, **1965**, pp. 70-71.

Epstein, R. A.; Withers, H. W.; Geoffroy, G. L. Inorg. Chem. **1979**, 18, 942.

Fieser, L. F.; Fieser, M. "Reagents for Organic Synthesis", Wiley: New York, **1967**, Vol 1.

Ford, P. C.; Rokicki, A. Adv. Organomet. Chem. **1988**, 28, 139.

Friend, C. M.; Roberts, J. T. Acc. Chem. Res. **1988**, 21, 394.

Gansow, O. A.; Burke, A. R.; LaMar, G. N. J. Chem. Soc., Chem. Commun. **1972**, 456.

Garrou, P. E. Chem. Rev. **1981**, 81, 229.

Gates, B. C.; Guczi, L.; Knozinger, H., Eds.; "Metal Clusters in Catalysis", Elsevier: New York, **1986**.

Gates, R. A.; D'Agostino, M. F.; Sutin, K. A.; McGlinchey, M. J.; Janik, T. S.; Churchill, M. R. Organometallics **1990**, 9, 20.

Geiger, W. E. Prog. Inorg. Chem. **1985**, 33, 275.

Geoffroy, G. L. Acc. Chem. Res. **1980**, 13, 469.

Geoffroy, G. L.; Rosenberg, S.; Shulman, P. M.; Whittle, R. R. J. Am. Chem. Soc. **1984**, 106, 1519.

Ginsberg, R. E.; Berg, J. M.; Rothrock, R. K.; Collman, J. P.; Hodgson, K. O.; Dahl, L. F. J. Am. Chem. Soc. **1979**, 101, 7218.

Gladfelter, W. L.; Geoffroy, G. L. Adv. Organomet. Chem. **1980**, 18, 207.

Gladysz, J. A. Adv. Organomet. Chem. **1982**, 20, 1.

Gladysz, J. A.; Williams, G. M.; Tam, W.; Johnson, D. L.; Parker, D. W.; Selover, J. C. Inorg. Chem. **1979**, 18, 553.

Glyn, P.; George, M. W.; Hodges, P. M.; Turner, J. J. J. Chem. Soc., Chem. Commun. **1989**, 1655.

Gordon, A. J.; Ford, R. A. "The Chemist's Companion. A Handbook of Practical Data, Techniques, and References", Wiley: New york, **1976**.

Graff, J. L.; Wrighton, M. S. J. Am. Chem. Soc. **1980**, 102, 2123.

Gross, D. C.; Ford, P. C. Inorg. Chem. **1982**, 21, 1702.

Grynkewich, G. W.; Marks, T. J. Inorg. Chem. **1976**, 15, 1307.

Gusbeth, P.; Vahrenkamp, H. Chem. Ber. **1985**, 118, 1758.

Halet, J. F.; Hoffmann, R.; Saillard, J. Y. Inorg. Chem. **1985**, 24, 1695.

Hammonds, C. N.; Day, M. C. J. Phys. Chem. **1969**, 73, 1151.

Hegedus, L. L.; McCabe, R. W. "Catalyst poisoning", Marcel Decker, Ed.; New York, **1984**.

Hendrickson, D. N.; Sohn, Y. S.; Gray, H. B. Inorg. Chem. **1971**, 10, 1559.

Hieber, W.; Gruber, J. Z. Anorg. Allg. Chem. **1958**, 296, 91.

Hieber, W.; Kruck, T. Chem. Ber. **1962**, 95, 2027.

Hieber, W.; Zeidler, A. Z. Anorg. Allg. Chem. **1964**, 329, 92.

Hinkelmann, K.; Heinze, J.; Schacht, H. T.; Field, J. S.; Vahrenkamp, H. J. Am. Chem. Soc. **1989**, 111, 5078.

Hinkelmann, K.; Mahlendorf, F.; Heinze, J.; Schacht, H. T.; Field, J. S.; Vahrenkamp, H. Angew. Chem., Int. Ed. Engl. **1987**, 26, 353.

Hoffmann, R. "Solids and Surfaces: A Chemist's View of Bonding in Extended Structures", VCH Publishers: New York, **1988**.

Holm, R. H. Chem. Soc. Rev. **1981**, 10, 455.

Honrath, U.; Vahrenkamp, H. Z. Naturforsch. **1984**, 39b, 555.

Howells, R. D.; McCown, J. D. Chem. Rev. **1977**, 77, 69.

Hughes, M. N., Ed.; "The Inorganic Chemistry of Biological Process", Wiley: New York, **1984**.

Huttner, G.; Knoll, K. Angew. Chem., Int. Ed. Engl. **1987**, 26, 743.

Huttner, G,; Schneider, J.; Muller, H. D.; Mohr, G.; von Seyerl, J.; Wohlfahrt, L. Angew. Chem., Int. Ed. Engl. **1979**, 18, 76.

Ingold, K. U. Pure Appl. Chem. **1984**, 56, 1767.

Jacobson, A. J.; Chianelli, R. R.; Rich, S. M.; Whittingham, M. S. Mater Res. Bull. **1979**, 14, 1437.

Jacobson, A. J.; Whittingham, M. S.; Rich, S. M. J. Electrochem Soc. **1979**, 126, 891.

Jaeger, J. T.; Aime, S.; Vahrenkamp, H. Organometallics **1986**, 5, 245.

Jaeger, J. T.; Field, J. S.; Collison, D.; Speck, G. P.; Peake, B. M.; Hahnle, J.; Vahrenkamp, H. Organometallics **1988**, 7, 1753.

Jensen, C. M.; Knobler, C. B.; Kaesz, H. D. J. Am. Chem. Soc. **1984**, 106, 5926.

John, G. R.; Johnson, B. F. G.; Lewis, J.; Mann, A. L. J. Organomet. Chem. **1979**, 171, C9.

Jordan, R. F. J. Chem. Ed. **1988**, 65, 285.

Kaesz, H. D.; Knobler, C. B.; Andrews, M. A.; van Buskirk, G.; Szostak, R.; Strouse, C. E.; Lin, Y. C.; Mayr, A. Pure Appl. Chem. **1982**, 54, 131.

Karel, K. J.; Norton, J. R. J. Am. Chem. Soc. **1974**, 96, 6812.

Katz, N. E.; Szalda, D. J.; Chou, M. H.; Creutz, C.; Sutin, N. J. Am. Chem. Soc. **1989**, 111, 6591.

King, R. B. Acc. Chem. Res. **1980**, 13, 243.

Kirk, C. M.; Peake, B. M.; Robinson, B. H.; Simpson, J. Aust. J. Chem. **1983**, 36, 441.

Knoll, K.; Huttner, G.; Zsolnai, L.; Orama, O.; Wasiucionek, M. J. Organomet. Chem. **1986**, 310, 225.

Knox, S. A. R. Pure Appl. Chem. **1984**, 56, 81.

Kobayaski, S.; Danda, H.; Saegusa, T. Macromolecules **1974**, 7, 415.

Kochi, J. K. Angew. Chem., Int. Ed. Engl. **1988**, 27, 1227.

Kochi, J. K. J. Organomet. Chem. **1986**, 300, 139.

Kochi, J. K. "Organometallic Mechanisms and Catalysis", Academic Press: New York; **1978**.

Kofron, W. G.; Backlawski, L. M. J. Org. Chem. **1976**, 41, 1879.

Kubiak, C. P.; Schneemeyer, L. F.; Wrighton, M. S. J. Am. Chem. Soc. 1980, 102, 6898.

Kuivila, H. G.; Beumel Jr, O. F. J. Am. Chem. Soc. **1961**, 83, 1246.

Kyba, E. P.; Davis, R. E.; Clubb, C. N.; Liu, S. T.; Palacios, H. O. A.; McKennis, J. S. Organometallics **1986**, 5, 869.

Laine, R. M. J. Mol. Catal. **1982**, 14, 137.

Langford, C. H.; Gray, H. B. in "Ligand Substitution Processes", New York: Benjamin, **1965**.

Lausarot, P. M.; Vaglio, G. A.; Valle, M. Inorg Chim. Acta **1977**, 25, L107.

Lausarot, P. M.; Vaglio, G. A.; Valle, M. Inorg. Chim. Acta **1979**, 36, 213.

Lee, S. W.; Tucker, W. D.; Richmond, M. G. Inorg. Chem. **1990**, 29, 3053.

Lesch, D. A.; Rauchfuss, T. B. Inorg. Chem. **1983**, 22, 1854.

Lesch, D. A.; Rauchfuss, T. B. Organometallics **1982**, 1, 499.

Lilga, M. A.; Ibers, J. A. Organometallics **1985**, 4, 590.

Christou, G. Acc. Chem. Res. **1989**, 22, 328.

Lindsay, P. N.; Peake, B. M.; Robinson, B. H.; Simpson, J.; Honrath, U.; Vahrenkamp, H.; Bond, A. M. Organometallics **1984**, 3, 413.

Lippard, S. J. Angew. Chem., Int. Ed. Engl. **1988**, 27, 344.

Marcus, R. A. Annu. Rev. Phys. Chem. **1964**, 15, 155.

Mason, R.; Mingos, D. M. P. J. Organomet. Chem. **1973**, 50, 53.

Matyjaszewski, K.; Penczeks, S. J. Polym. Sci. **1974**, 12, 1905.

Michaud, P.; Astruc, D.; Ammeter, J. H. J. Am. Chem. Soc. **1982**, 104, 3755.

Mingos, D. M. P. Acc. Chem. Res. **1984**, 17, 311.

Mingos, D. M. P. Chem. Soc. Rev. **1986**, 15, 31.

Mingos, D. M. P. Nature (London), Phys. Sci. **1972**, 236, 99.

Mingos, D. M. P. Inorg. Chem. **1985**, 24, 114.

Minisci, F.; Citterio, A. in "Advances in Free-Radical Chemistry", Williams, G. H., Ed.; Heyden: London, **1980**; pp. 125-126.

Morris, R. J.; Girolami, G. S. Inorg. Chem. **1990**, 29, 4167.

Moskovits, M. Acc. Chem. Res. **1979**, 12, 229.

Moskovits, M., Ed.; "Metal Clusters", Wiley: New York, **1986**.

Muetterties, E. A. Science (Washington, D. C.) **1977**, 196, 839.

Muetterties, E. A.; Rhodin, T. N.; Band, E.; Brucker, C. F.; Pretzer, W. R. Chem. Rev. **1979**, 79, 91.

Muller, M.; Vahrenkamp, H. Chem. Ber. **1983**, 116, 2311.

Narayanan, B. A.; Amatore, C.; Casey, C. P.; Kochi, J. K. J. Am. Chem. Soc. **1983**, 105, 6351.

Narayanan, B. A.; Amatore, C.; Kochi, J. K. Organometallics **1984**, 3, 802.

Narayanan, B. A.; Amatore, C.; Kochi, J. K. Organometallics **1986**, 5, 926.

Narayanan, B. A.; Amatore, C.; Kochi, J. K. Organometallics **1987**, 6, 129.

Nomyia, K.; Suzuki, H. J. Organomet. Chem. **1979**, 168, 115.

Ohst, H. H.; Kochi, J. K. Inorg. Chem. **1986**, 25, 2066.

Ohst, H. H.; Kochi, J. K. J. Am. Chem. Soc. **1986**, 108, 2897.

Ohst, H. H.; Kochi, J. K. Organometallics **1986**, 5, 1359.

Orme-Johnson, W. H. Annu. Rev. Biophys. Biophys. Chem. **1985**, 14, 419.

Orpen, A. G. J. Chem. Soc., Chem. Commun. **1985**, 1310.

Partin, J. A.; Richmond, M. G. J. Organomet. Chem. **1990**, 396, 339.

Peake, B. M.; Robinson, B. H.; Simpson, J.; Watson, D. J. Inorg. Chem. **1977**, 16, 405.

Peloso, A. J. Organomet. Chem. **1974**, 67, 423.

Penfold, B. R.; Robinson, B. H. Acc. Chem. Res. **1973**, 6, 73.

Pittman, Jr. C. U.; Richmond, M. G.; Wilemon, G. M.; Absi-Halabi, M. in "Catalysis of Organic Reactions", Kosak, J. R., Ed.; Marcel Dekker: New York, **1984**, Ch. 5.

Pittman, Jr. C. U.; Ryan, R. C. Chem. Technol. **1978**, 8, 170.

Pittman, Jr. C. U.; Wilemon, G. M.; Wilson, W. D.; Ryan, R. C. Angew. Chem., Int. Ed. Engl. **1980**, 19, 478.

Planalp, R. P.; Vahrenkamp, H. Organometallics **1987**, 6, 492.

Poë, A. J.; Sekhar, V. C. Inorg Chem. **1985**, 24, 4376.

Poë, A. J.; Twigg, M. V. Inorg. Chem. **1974**, 13, 2982.

Pross, A. Acc. Chem. Res. **1985**, 18, 212.

Purcell, K. F.; Kotz, J. C. "Inorganic Chemistry", Saunders, W. B. Co.: Philadelphia; **1977**; Ch 12.

Qudar, J. J. Catal. Rev. Sci. Eng. **1980**, 22, 171.

Richmond, M. G.; Absi-Halabi, M.; Pittman, Jr. C. U. J. Mol. Catal. **1984**, 22, 367.

Richmond, M. G.; Kochi, J. K. Inorg. Chem. **1986**, 25, 656.

Richmond, M. G.; Kochi, J. K. Inorg. Chem. **1986**, 25, 1334.

Richmond, M. G.; Kochi, J. K. Inorg. Chem. **1987**, 26, 541.

Richmond, M. G.; Kochi, J. K. Inorg. Chim. Acta **1987**, 126, 83.

Richmond, M. G.; Kochi, J. K. J. Organomet. Chem. **1987**, 323, 219.

Richmond, M. G.; Kochi, J. K. Organometallics **1987**, 6, 254.

Richmond, M. G.; Kochi, J. K. Organometallics **1987**, 6, 777.

Richter, F.; Beurich, H.; Vahrenkamp, H. J. Organomet. Chem. **1979**, 166, C5.

Roberts, D. A.; Geoffroy, G. L. in "Comprehensive Organometallic Chemistry," Wilkinson, G.; Stone, F. G. A.; Abels, E. W., Eds.; Pergamon Press: Oxford; U. K.; **1982**; Ch 40.

Robin, M. D.; Day, P. Adv. Inorg. Chem. Radiochem. **1967**, 10, 248.

Rosenberg, S.; Whittle, R. R.; Geoffroy, G. L. J. Am. Chem. Soc. **1984**, 106, 5934.

Rossetti, R.; Gervasio, G.; Stanghellini, P. L. Inorg. Chim. Acta. **1979**, 35, 73.

Ryan, R. C.; Dahl, L. F. J. Am. Chem. Soc. **1975**, 97, 6904.

Ryan, R. C.; Pittman, Jr. C. U.; O'Connor, J. P. J. Am. Chem. Soc. **1977**, 99, 1986.

Ryan, R. C.; Pittman, Jr. C. U.; O'Connor, J. P.; Dahl, L. F. J. Organomat. Chem. **1980**, 193, 247.

Saillard, J. Y.; Hoffmann, R. J. Am. Chem. Soc. **1984**, 106, 2006.

Sappa, E.; Tiripicchio, A.; Braunstein, P. Coord. Chem. Rev. **1985**, 65, 219.

Sappa, E.; Tiripicchio, A.; Carty, A. J.; Toogood, G. E. Prog. Inorg. Chem. **1987**, 35, 437.

Saveant, J. M.; Acc. Chem. Res. **1980**, 13, 323.

Schaschel, E.; Day, M. C. J. Am. Chem. Soc. **1968**, 90, 503.

Schick, K. P.; Jones, N. L.; Sekula, P.; Boag, N. M.; Labinger, J. A.; Kaesz, H. D. Inorg. Chem. **1984**, 23, 2204.

Schmidt, W; Steckhan, E. Chem. Ber. **1980**, 113, 577.

Schneider, J.; Minelli, M.; Huttner, G. J. Organomet. Chem. **1985**, 294, 75.

Schulman, C. L.; Richmond, M. G.; Watson, W. H.; Nagl, A. J. Organomet. Chem. **1989**, 368, 367.

Schuman, S. C.; Shalit, H. Catal. Rev. **1970**, 4, 245.

Setzer, W. N.; Schleyer, P. V. R. Adv. Organomet. Chem. **1985**, 24, 353.

Seyferth, D.; Henderson, R. S.; Gallagher, M. K. Organometallics **1989**, 8, 119.

Seyferth, D.; Henderson, R. S,; Song, L. C. Organometallics **1982**, 1, 125.

Shen, J. -K.; Shi, Y. -L.; Gao, Y. -C.; Shi, Q. -Z.; Basolo, F. J. Am. Chem. Soc. **1988**, 110, 2414.

Shriver, D. F. "The Manipulation of Air-Sensitive Compounds", McGraw-Hill: New York, **1969**.

Shriver, D. F.; Sailor, M. J. Acc. Chem. Res. **1988**, 21, 374.

Shyu, S. G.; Calligaris, M.; Nardin, G.; Wojcicki, A. J. Am. Chem. Soc. **1987**, 109, 3617.

Shyu, S. G.; Wojcicki, A. Organometallics **1985**, 4, 1457.

Sonnenberger, D.; Atwood, J. D. Inorg. Chem. **1981**, 20, 3243.

Spiro, T. G., Ed; Molydenum Enzymes Wiley-Interscience : New York, **1986**.

Stephan, D. W. Coord. Chem. Rev. **1989**, 95, 41.

Summer, C. E.; Nelson, G. O. J. Am. Chem. Soc. **1984**, 106, 432.

Summerville, R. H.; Hoffmann, R. J. Am. Chem. Soc. **1976**, 98, 7240.

Sundararajan, G.; San Fillippo, Jr. J. Organometallics **1985**, 4, 606.

Sutin, N. Acc. Chem. Res. **1982**, 15, 275.

Taube, D. J.; Ford, P. C. Organometallics **1986**, 5, 99.

Taube, H. Angew. Chem. Int. Ed. Engl. **1984**, 23, 329.

Taube, H. J. Chem. Ed. **1968**, 45, 452.

Teo, B. K. Inorg. Chem. **1984**, 23, 1251.

Teo, B. K. Inorg. Chem. **1985**, 24, 115.

Teo, B. K.; Hall, M. B.; Fenske, R. G.; Dahl, L. F. Inorg. Chem. **1975**, 14, 3103.

Teo, B. K.; Hall, M. B.; Fenske, R. G.; Dahl, L. F. J. Organomet. Chem. **1974**, 70, 413.

Teo, B. K.; Longoni, G.; Chung, F. R. K. Inorg. Chem. **1984**, 23, 1257.

Tolman, C. A. Chem. Rev. **1977**, 77, 313.

Touchard, D.; Fillaut, J. L.; Khasnis, D. V.; Dixneuf, P. H.; Mealli, C.; Masi, D.; Toupet, L. Organometallics **1988**, 7, 67.

Vahrenkamp, H. Adv. Organomet. Chem. **1983**, 22, 169.

Vahrenkamp, H. J. Organomet. Chem. **1989**, 370, 65.

Vahrenkamp, H. Phil. Trans. R. Soc. Lond. A **1982**, 308, 17.

Vandenberg, D. M.; Chin-Choy, T.; Ford, P. C. J. Organomet. Chem. **1989**, 366, 257.

Vargas, M. D.; Nicholls, J. N. Adv. Inorg. Chem. Radiochem. **1986**, 30, 123.

Wade, K. Adv. Inorg. Chem. Radiochem. **1976**, 18, 1.

Wade, K. Chem. Br. **1975**, 11, 177.

Wade, K. in "Transition Metal Clusters", Johnson B. F. G., Ed.; Wiley, New York, **1980**; Ch 3.

Wakatsuki, Y.; Yamazaki, H. J. Organomet. Chem. **1988**, 347, 151.

Watt, G. W.; Cuddeback, J. E. J. Inorg. Nucl. Chem. **1971**, 33, 259.

Wax, M. J.; Bergman, R. G. J. Am. Chem. Soc. **1981**, 103, 7028.

Wei, C. H.; Dahl, L. F. Inorg. Chem. **1965**, 4, 1.

Weisser, O.; Landa, S. "Sulfide Catalysis, Their Properties and Applications", Pergamon Press; New York, **1973**.

Went, M. J.; Brock, C. P.; Shriver, D. F. Organometallics **1986**, 5, 755.

Whangbo, M. H.; Hoffmann, R. J. Am. Chem. Soc. **1978**, 100, 6093.

Wheeler, R. A.; Hoffmann, R. J. Am. Chem. Soc. **1988**, 110, 7315.

Wheeler, R. A.; Piela, L.; Hoffmann, R. J. Am. Chem. Soc. **1988**, 110, 7302.

Whitesides, G. M.; Goach, J. F.; Stedronsky, E. R. J. Am. Chem. Soc. **1972**, 94, 5258.

Whitman, D. W.; Carpenter, B. K. J. Am. Chem. Soc. **1982**, 104, 6473.

Williams, G. D.; Geoffroy, G. L.; Whittle, R. R.; Rheingold, A. L. J. Am. Chem. Soc. **1985**, 107, 729.

Withers, H. P.; Seyferth, D. Inorg. Chem. **1983**, 22, 2931.

Wojcicki, A. in "Coordination Chemistry and Catalysis," Ziolkowski, J. J., Ed.; World Scientific: New Jersey; **1988**; pp. 3-25.

Wu, T. K.; Pruckmayr, G. Macromolecules **1978**, 11, 77; 265.

Xiao, S. -X.; Trogler, W. C.; Ellis, D. E.; Berkovitch-Yellin, Z. J. Am. Chem. Soc. **1983**, 105, 7033.

Yu, Y. F.; Chau, C. N.; Wojcicki, A. Inorg. Chem. **1986**, 25, 4098.

Yu, Y. F.; Chau, C. N.; Wojcicki, A.; Calligaris, M.; Nardin, G.; Balducci, G. J. Am. Chem. Soc. **1984**, 106, 3704.

Yu, Y. F.; Gallucci, J.; Wojcicki, A. J. Am. Chem. Soc. **1983**, 105, 4826.

Yu, Y. F.; Gallucci, J.; Wojcicki, A. J. Chem. Soc., Chem. Commun. **1984**, 653.

Zheng, C.; Apeloig, Y.; Hoffmann, R. J. Am. Chem. Soc. **1988**, 110, 749.

Zimmerman, R.; Munch, E.; Brill, W.J.; Shah, V.K.;Henzl, M.T.; Rawlings, J.; Orme-Johnson, W.H. Biochim. Biophys. Acta **1978**, 537, 185.

Zonnevylle, M. C.; Silvestre, J.; Hoffmann, R. J. Am. Chem. Soc. **1986**, 108, 1509.